Structural Determinants for Histone and Inhibitor Recognition by the Bromodomain Protein 4

Inaugural-Dissertation

to obtain the academic degree

Doctor rerum naturalium

(Dr. rer. nat.)

Submitted to the Department of Biology, Chemistry and Pharmacy

of Freie Universität Berlin

by

MARIE JUNG

from Mulhouse

2015

Die vorliegende Arbeit wurde im Zeitraum von März 2012 bis Januar 2015 in der Onkologie-Chromatin Modulation & Oncogenomics Abteilung der Bayer Pharma AG in Berlin unter der Leitung von Herrn Dr. hab. Bernard Haendler angefertigt.

1. Gutachter **Dr. hab. Bernard Haendler**

Bayer Pharma AG
Global Drug Discovery - TRG Oncology/GT
Chromatin Modulation & OncoGenomics
Müllerstr. 178, S109-4-416B
13353 Berlin
Tel. +49 30 468 12669
E-Mail: bernard.haendler@bayer.com

2. Gutachter **Prof. Dr. Petra Knaus**

Institut für Chemie und Biochemie – Biochemie
Freie Universität Berlin
Thielallee 63
14195 Berlin
Tel.: +49 30 838 52935
knaus@chemie.fu-berlin.de

Tag der Disputation: 5. Oktober 2015

Acknowledgements

First of all, I would like to thank Dr. Bernard Haendler for giving me the opportunity to complete my Ph.D. thesis in his group and introducing me to an extremely interesting and promising therapeutic research field. I am also very grateful to Dr. Amaury Fernández-Montalván for teaching me a multitude of technologies and for our numerous interesting discussions. Both gave me the tools, constructive criticism and support to make my work feasible.

I would like to thank Prof. Dr. Petra Knaus from the Freie Universität Berlin for evaluating this work.

Furthermore, I want to express my thanks to the members of the chromatin modulation group, for their assistance, the pleasant working climate, the supportive discussions as well as the nice little chats and laughter.

For their nice help I also want to say thanks to the colleagues from the Screening and Protein Technologies departments.

Many thanks to all the Ph.D. students and postdoctoral fellows at Bayer Healthcare for great scientific discussions, inspiration and friendship.

Additionally, I am thankful to all my other dearest friends in Berlin and all over the world whose name list would blast this acknowledgement page and who all know who they are. I would also like to offer my special thanks to my relatives for their support throughout my studies. Last but not least I am very grateful to have Nicolas by my side.

Table of contents

1. Introduction

1.1. Chromatin organization and epigenetics

1.1.1. The chromatin

Walther Flemming first referred to chromatin as the darkly staining (from Greek 'Khroma' for "color") nuclear material (Flemming 1882). The function of the DNA in the nucleus remained unknown until the mid-twentieth century, when the work of Alfred Hershey and Martha Chase on phage T2 demonstrated that genetic material was made up of DNA. The double helix structure of the DNA was finally proposed by Watson and Crick in their landmark publication (Watson and Crick 1953) which ultimately earned them the Nobel prize in physiology and medicine in 1962. In eukaryotic cells the 2m long, negatively charged DNA located in the nucleus is folded and wrapped around basic proteins to form a complex called chromatin.

1.1.2. The nucleosome

At the first level of organization, 147 base pairs of tight superhelical DNA (~1.7 turns) are wrapped around a disc-shaped protein assembly of eight histone molecules, two copies each of H2A, H2B, H3, and H4, to form the nucleosome core particle (Kornberg 1974). Most chromatin is further condensed by winding in a polynucleosome fiber, which may be stabilized through the binding of histone H1 to each nucleosome and to the linker DNA (Phillips and Johns 1965) (Fig. 1.1 A.).

While initially thought to be an inert structure involved in packaging DNA into the confines of the nucleus, chromatin was later demonstrated to possess a more dynamic organization. Indeed modulation of the structure of the chromatin fiber is critical for the regulation of gene expression since it determines the accessibility and the sequential recruitment of regulatory factors to the underlying DNA (Khorasanizadeh 2004). Hence, various chromatin structures are commonly divided into euchromatin and heterochromatin (Fig. 1.1 B.). Euchromatin corresponds in general to genome regions that possess actively transcribed genes (or potentially active ones) and that are decondensed during interphase. By contrast, heterochromatin refers to the transcriptionally inactive and highly condensed regions of the genome (Quina, Buschbeck et al. 2006).

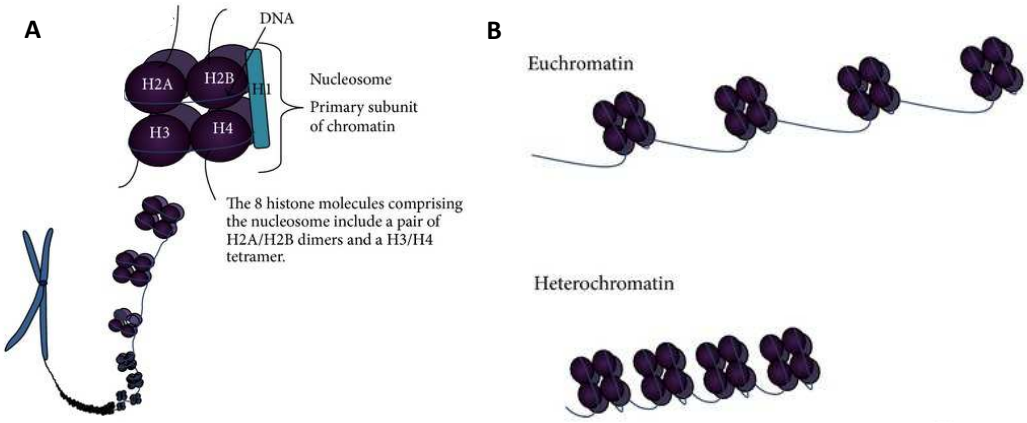

Figure 1.1 Chromatin compaction into nucleosomes.
A. The nucleosome core structure
B. The euchromatin/heterochromatin distinction
Adapted from (Conway O'Brien, Prideaux et al. 2014)

1.1.3. The epigenetic landscape

Genetics, the study of genes and heredity, can only partially explain the diversity within a species or an organism. Indeed, most cells present in an individual are strictly composed of identical DNA sequence. In 1942 Conrad Waddington, who was both a geneticist and a developmental biologist, used the phrase "epigenetic landscape" (Fig. 1.2) to describe how genes might interact with their surroundings to produce a phenotype. The term “epigenetics” was coined to mean the study of the causal mechanisms of development which bring the phenotype into being (Waddington 1942).

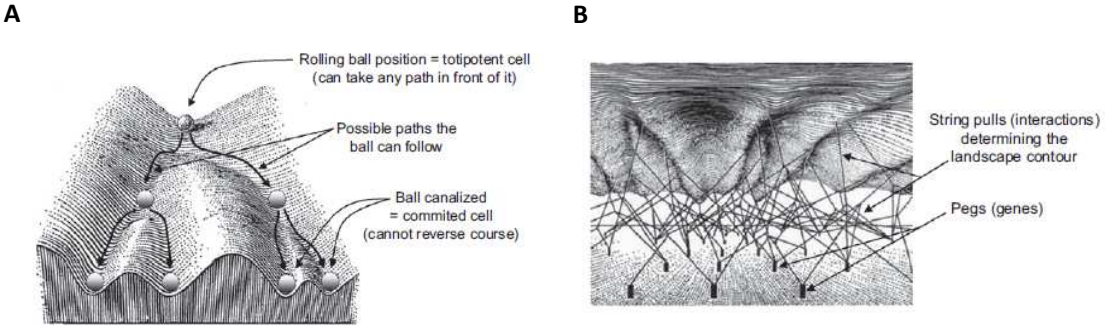

Figure 1.2 Epigenetic landscape and its genetic control as envisioned by Waddington.
A. Epigenetic landscape in the process of cellular decision making during development. The undulating surface leading to many lower-elevation endpoints, each endpoint corresponds to a specific developmental endpoint, such as differentiation of a specific tissue type. At various endpoints the cell (represented by a ball) can take specific permitted trajectories leading to different outcomes.
B. Genetic interactions in determining the shape of the epigenetic landscape. In the depiction, a sheet of fabric (the landscape) is connected by strings (interactions) to the pegs (genes). The pegs themselves are also linked to each other by strings, which represent the interactions among genes making up the landscape. The pegs (genes), through their string-pulls (interactions) among themselves as well as with the fabric, confer a specific stable contour to the fabric. Adapted from (Waddington 1957, Choudhuri 2011).

Epigenetics, in the broad sense is a bridge between genotype and phenotype that changes the final outcome of a locus or chromosome (Goldberg, Allis et al. 2007). Since 2008, a consensus definition of

the epigenetic trait, "stably heritable phenotype resulting from changes in a chromosome without alterations in the DNA sequence", was made (Berger, Kouzarides et al. 2009). These epigenetic modifications that occur outside the DNA sequence control gene expression or function (Berger, Kouzarides et al. 2009). The molecular foundation of the epigenetic concept is comprised of several highly interconnected pathways: DNA methylation, histone composition and post-translational modifications, and RNA-based mechanisms through noncoding RNAs (ncRNA) (Fig. 1.3).

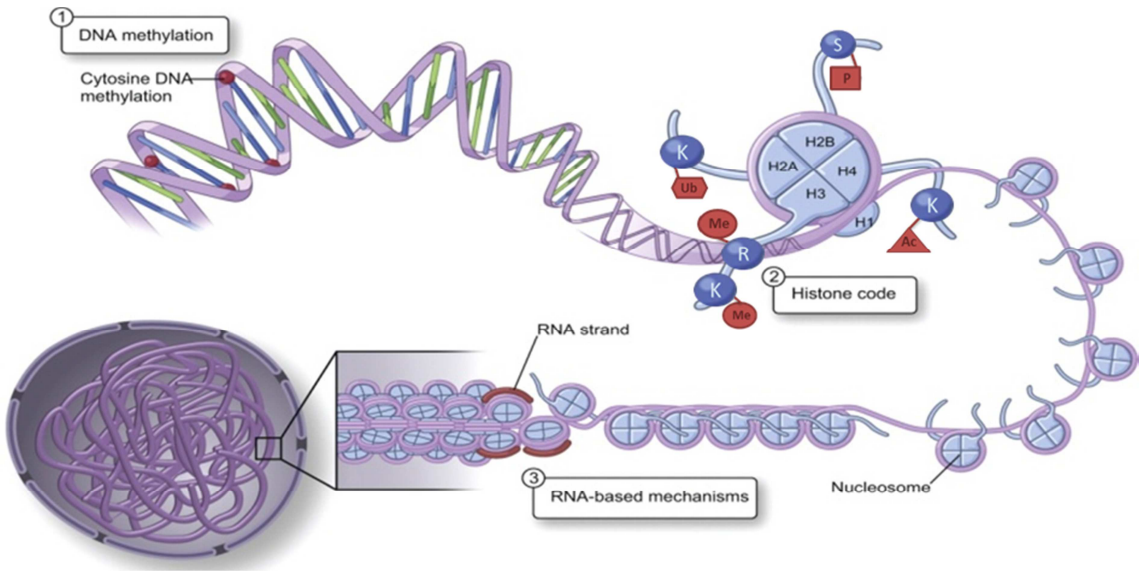

Figure 1.3 Three fundamental mechanisms of epigenetic gene regulation.
1) Cytosine residues within DNA can be methylated, 2) histone proteins can vary and be modified. Me = methylation, Ac = acetylation, P = phosphorylation, Ub = ubiquitination, 3) RNA-based mechanisms.
Adapted from (Yan, Matouk et al. 2010).

Gene expression is tightly controlled by chromatin structure that is dynamically regulated by chromatin modifications. Changes in epigenetic information are either stable or flexible depending on a large number of cellular factors, reflecting a physiological or pathological condition and the adaptability of the cell to its environment.

1.1.3.1. DNA methylation

DNA methylation is a common modification in genomes and is a stable epigenetic mark transmitted through DNA replication and cell division (Bird 2002). This covalent binding of a methyl group occurs almost exclusively at cytosines that are immediately followed by a guanine, forming so-called CpG (cytosine-phosphate-guanine) dinucleotides. Methylation of C is typically associated with the upstream region of gene sequences where CpG dinucleotides are particularly dense. Hypermethylation of gene promoters which have high levels of CpG sites, known as CpG islands, leads to gene inactivation, while their hypomethylation is associated with the transcriptional activation of surrounding genes (Bird 1986). DNA methylation established during development and

early postnatal life plays critical roles to regulate cell- and tissue-specific gene expression and genomic imprinting, a phenomenon in which the expression of a gene allele depends on its parent of origin (Reik, Dean et al. 2001, Bird 2002). Enzymes called DNMTs (DNA methyltransferases) add this methyl group to the cytosine (Fig. 1.4). *De novo* DNA methylation is catalyzed by DNMT 3A and 3B, whereas DNA methylation is maintained after the replication of the DNA by DNMT1, which methylates hemi-methylated DNA (Reik, Dean et al. 2001). Once established, DNA methylation is essentially maintained throughout life; however, a gradual hypomethylation occurs during aging, and has been linked with some types of cancer (van Otterdijk, Mathers et al. 2013).

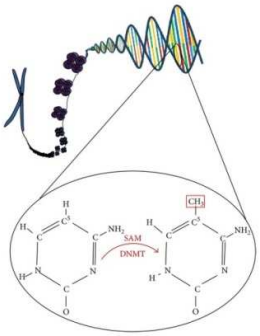

Figure 1.4 DNA methylation.
The addition of a methyl group from S-adenosylmethionine (SAM) to the 5-methylcytosine is catalyzed by DNA methyltransferase (DNMT) (Conway O'Brien, Prideaux et al. 2014).

More recently 5-hydroxymethylcytosine (5hmC) was revealed to be another prominent cytosine modification resulting of 5-methylcytosine oxidation by the enzymes of the ten eleven translocation (TET) family. 5hmC is thought to serve as an intermediate in the reaction of DNA demethylation or to act as a signal for chromatin factors (Tahiliani, Koh et al. 2009).

1.1.3.2. Histone variants and modifications

Substitutions of the individual components of the histone core with structurally distinct histone variants and covalent modifications alter the local fabric of the chromatin fiber (Volle and Dalal 2014).

The flexible N-terminal tails of the core histones protrude out of the nucleosome and are subject to various post-translational modifications (PTMs), including methylation, acetylation, phosphorylation, ubiquitination and sumoylation (Fig. 1.5 A.). Histone PTMs have different outcomes (Fig. 1.5 B.) and contribute to the control of gene expression by influencing chromatin compaction or signaling to other protein complexes.

A

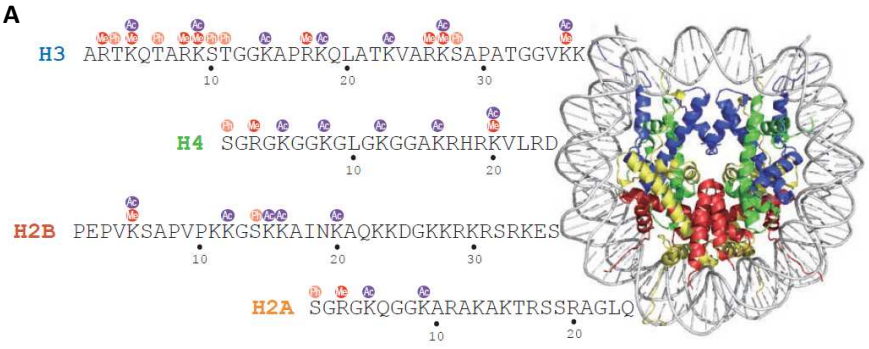

B

Histone	Modification	Effect
H1	Phosphorylation	Chromatin condensation; gene-specific activation and repression
	Ubiquitination	Transcriptional activation
H2A	Acetylation	*Tetrahymena* survival
	Ubiquitination	Elusive
H2B	Ubiquitination	Prerequisite of H3 methylation
	Phosphorylation	Chromatin condensation
	Acetylation	Chromatin remodelling
	Methylation	Chromatin stabilisation
	ADP-ribosylation	Elusive
H3	Methylation (H3-K4, R17)	Transcriptional activation
	Methylation (H3-K9, K79)	Transcriptional repression
	Acetylation	Transcriptional activation
	Phosphorylation	Chromatin condensation; transcriptional activation
	Ubiquitination	Nucleosome loosening
H4	Acetylation	Transcriptional activation
	Methylation (H4-K20)	Transcriptional repression
	Methylation (H4-R3)	Transcriptional activation

Figure 1.5 Histone modifications and their effects.
A. Nucleosome structure and histone N-terminal modifications. Me = methylation, Ac = acetylation, P = phosphorylation, Ub = ubiquitination (Horikoshi 2013).
B. Effects of the singular histone modifications described. In addition, there is interdependency and cross-talk between the different histone modifications that can alter their individual effects (He and Lehming 2003).

1.1.3.2.1. Histone variants

Canonical histones (H2A, H2B, H3, and H4) are deposited in a replication-coupled manner to package the newly replicated genome. In contrast, histone variants are expressed throughout the cell cycle and replace canonical histones or take their place when nucleosomes are evicted. Histone variants have distinct amino acid sequences that can influence both the physical properties of the nucleosome and nucleosome dynamics (Weber and Henikoff 2014). Recent advances have highlighted the influence of histone variants on cellular functions including transcription regulation (Jin, Zang et al. 2009), DNA damage repair (Xu, Ayrapetov et al. 2012), and disease (Dardenne, Pierredon et al. 2012).

Some PTMs are more prevalent on particular variants (Loyola, Bonaldi et al. 2006), thus the histone variants, whose expression is cell cycle regulated, are a critical component of the picture (Gurard-Levin and Almouzni 2014). Indeed the placement of variants can potentiate the action of enzymes, such as SUV39h1 (suppressor of variegation 3-9 homolog 1), an H3K9 methyltransferase (Rea, Eisenhaber et al. 2000) inducing more H3K9me1 on H3.1 compared to H3.3 (Loyola, Bonaldi et al. 2006).

In Drosophila, the histone H2A variant, H2Av, is required for euchromatic silencing and heterochromatin formation. In addition, acetylation of H4K12 is induced subsequent to H2Av replacement and before H3K9 methylation (Swaminathan, Baxter et al. 2005).

Notably, it is important to consider instances where histones do not have the capacity to bear the same modifications either due to mutations (Schwartzentruber, Korshunov et al. 2012) or the presence of variants, such as the centromeric H3 variant CenH3 (also known as CENP-A) (Muller and Almouzni 2014), which lack the target residue and how this can impact chromatin integrity (Gurard-Levin and Almouzni 2014).

The epigenetic influence of histones mediated by selective deposition of histone variants that can potentially affect the combination of PTMs can lead to functional changes that are important determinants of eukaryotic gene regulation.

1.1.3.2.2. Histone methylation

Histone methylation can be grouped into two major families, lysine methylation and arginine methylation. Lysines can be monomethylated, dimethylated or trimethylated on their ε-amine group by histone lysine methyltransferases (HKMTs), arginines can be monomethylated, symmetrically dimethylated or asymmetrically dimethylated on their guanidinyl group by protein arginine methyltransferases (PRMTs) (Marmorstein and Trievel 2009, Li, Luo et al. 2012). Histidines have been reported to be monomethylated but this methylation appears to be rare and has not been further characterized (Greer and Shi 2012). Since 2004, a large number of enzymes have been discovered with the ability to demethylate methylated histone lysine residues. The histone lysine demethylases (HKDMs) discovered thus far are defined into two families: lysine-specific demethylase (LSD) proteins and Jumonji domain (JMJD) containing (JMJC) proteins (Li, Luo et al. 2012).

Histone methylation has a dual impact on transcriptional activity and is associated with both actively transcribed and silenced genes depending on the specific contexts where the methylation mark is located (Peters and Schubeler 2005, Klose and Zhang 2007).

Small domains including the chromo, tudor, PWWP modules and PHD finger contained in diverse protein recognize histone methylation marks (Yun, Wu et al. 2011).

1.1.3.2.3. Histone acetylation

Histone acetylation was first discovered by Allfrey et al. in 1964 (Allfrey, Faulkner et al. 1964). The N-acetylation of lysine residues (Kac) on histone tails was associated with transcriptional activation. Each acetylation step removes a positive charge from the histone protein and thereby reduces the electrostatic interactions of acetylated core histones with the negatively charged DNA backbone, destabilizing the nucleosome (Ganesan, Nolan et al. 2009). Hence, histone acetylation generally results in a more open chromatin structure correlating with activation of gene transcription, whereas

deacetylation leads to compact chromatin structures and gene repression (Johnson and Turner 1999, Jenuwein and Allis 2001, Schreiber and Bernstein 2002).

Post-translational acetylation of N-terminal histone lysine residues is catalyzed by histone acetyltransferases (HATs). The level of histone acetylation is highly controlled and balanced by the activity of histone deacetylases (HDACs), the counterplayer of HATs, which catalyze the hydrolytic removal of acetyl groups (Fig. 1.6).

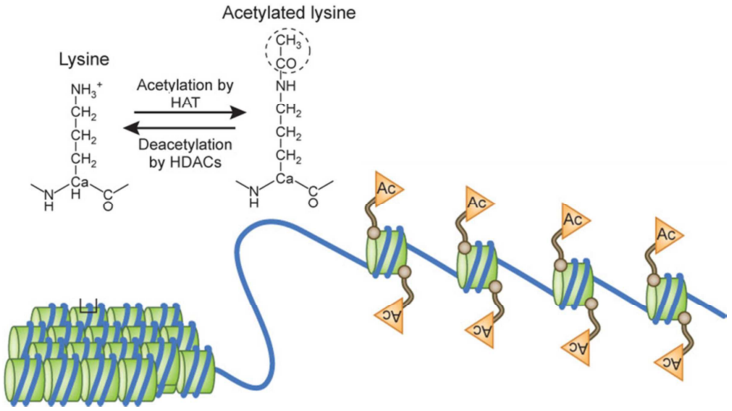

Figure 1.6 Histone Lysine acetylation.
Histone acetyltransferases (HATs) and histone deacetylases (HDACs) are two opposing classes of enzymes, which tightly control the equilibrium of histone acetylation and chromatin condensation. Ac, acetyl group. Adapted from (Korzus 2010).

Mammalian cells contain at least 17 HATs and 18 HDACs which individually can be responsible for acetylation and deacetylation of various substrates (Gong and Miller 2013). HATs are diverse and fall into several families including GNAT (ex. GCN5), MYST (ex. TIP60) and the "orphan" family (ex. p300) (Lee and Workman 2007). Mammalian HDACs are divided into 4 classes (Yang and Seto 2008, Gong and Miller 2013). Class I HDACs (HDAC 1-3, 8) are nuclear and ubiquitously expressed in all cells. Class II HDACs (HDAC 4-7, 9 and 10) are cell-type specific and are expressed mostly in the cytoplasm but can become nuclear upon various stimuli. Class III HDACs are the NAD-dependent sirtuins (SIRT1-7) where SIRT1, 6 and 7 are nuclear, SIRT2 is mainly cytoplasmic and SIRT 3-5 are mitochondrial (Feldman, Dittenhafer-Reed et al. 2012). Class IV contains only one member, HDAC11, which is mainly expressed in the nucleus in a cell-type specific manner. HDACs are sometimes referred to as lysine deacetylases rather than HDACs because of the many nonhistone targets they can use as substrates.

Importantly, acetylated histones constitute specific binding sites recognized by bromodomain (BD)-containing proteins (Filippakopoulos, Qi et al. 2010). Together, these effects enable access of the transcription machinery to the underlying chromatin, thereby enhancing gene expression at specific genes or over vast regions of the genome. The dynamic equilibrium between HATs and HDACs is crucial for normal cell proliferation, growth as well as differentiation, and represents a key mechanism of gene regulation.

1.1.3.2.4. Histone phosphorylation, ubiquitination, sumoylation

Histone phosphorylation, like histone acetylation, is most commonly associated with transcriptional activation (Loury and Sassone-Corsi 2003), presumably because it creates a repulsive force between the negative charges of phospho-histones and DNA that decondenses the chromatin and increases its accessibility to the transcriptional machinery. Histone phosphorylation provides a functional link between chromatin remodeling and intracellular signaling pathways, both of which involve protein kinases and phosphatases.

Protein ubiquitination (also called ubiquitylation) is most commonly associated with the marking of proteins for degradation by the proteasome, but has also been found to occur on histone tails. The ubiquitination of histone tails by attachment of the ubiquityl moiety plays critical roles in many processes in the nucleus, including transcription, maintenance of chromatin structure, and DNA repair (He and Lehming 2003, Shilatifard 2006, Cao and Yan 2012).

Finally, histone sumoylation is the least understood posttranslational histone modification. In yeast, it occurs on all four core histones and negatively regulates transcription, possibly by interfering with histone acetylation and ubiquitination (Shiio and Eisenman 2003). Its role in mammals has not been established yet.

1.1.3.2.5. The histone code: writers, erasers and readers

Histone modifications do not occur in isolation, but rather in a combinatorial manner. Widespread interplays between different histone PTM marks have been found and histone modification patterns have been proposed to function as a set of regulatory "codes" which are referred to as "histone code" (Strahl and Allis 2000). The repertoire of DNA and histone modifications is controlled by specific enzymes. These enzymes operate both independently and in synergy to establish the "histone code". This highly dynamic and flexible chromatin marking determines the pattern of gene expression in response to given external stimuli in combination with chromatin-associated proteins (Jenuwein and Allis 2001, Turner 2002).

The chemical modifications are added to the chromatin by so called "writers" and removed by "erasers". Writer enzymes include histone acetyltransferases, histone methyltransferases and kinases. Eraser enzymes include histone deacetylases, demethylases and phosphatases (Fig. 1.7).

This epigenetic code can be interpreted by "reader" proteins. Readers of epigenetic marks are structurally diverse proteins each possessing one or more evolutionarily conserved effector modules, which recognize covalent modifications of histone proteins or DNA (Filippakopoulos, Qi et al. 2010). Reader proteins include modules such as bromodomains (BDs), chromodomains, plant homeodomains (PHDs), tudor domains, and PWWP (Pro-Trp-Trp-Pro) domains (Fig. 1.6.). For

instance, HATs deposit acetylation marks on lysine residues, which are 'read' by BD modules and removed by HDACs (Filippakopoulos and Knapp 2014). Readers of histone marks often serve as platforms for the recruitment of a number of partners, thus forming large complexes with various cellular functions (Yun, Wu et al. 2011, Musselman, Lalonde et al. 2012). The interactions between reader proteins and histone marks are very specific and are further influenced by neighboring histone modifications, hence the concept of a histone code (Jenuwein and Allis 2001).

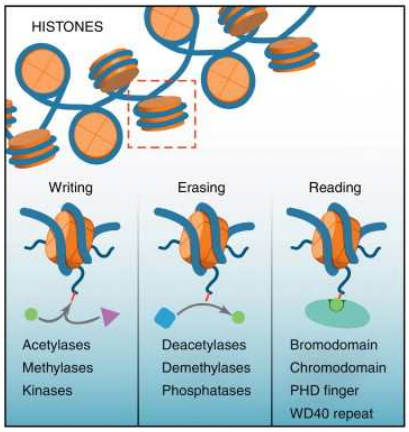

Figure 1.7 Histone writers, erasers and readers.
'Writers' introduce histone marks, 'erasers' take them out and 'readers' can recognize a particular form of histone modification (Prinjha, Witherington et al. 2012).

1.1.3.3. Non-coding RNAs

While less than 2% of the total genomic sequence encodes for proteins, at least 90% of the genome is actively transcribed into ncRNA (Qi and Du 2013). ncRNAs represent a heterogeneous group of RNAs that are generally classified based on their lengths.

Several types of small (<50 base pairs) and mid-size (<200 base pairs) ncRNAs have been described. Small ncRNAs include PIWI-interacting RNAs, transcription initiation RNAs and the microRNAS (miRNAs) (Schaukowitch and Kim 2014). The miRNAs are the best-studied group (Costa 2007). Base pairing between miRNA and mRNA leads to translational repression or mRNA degradation (Pillai, Bhattacharyya et al. 2007). miRNAs regulate a wide variety of complex cellular processes, including gene silencing, gene transcription, DNA imprinting, DNA demethylation, chromatin structure dynamics, and RNA interference (Costa 2005).

Mid-size ncRNAs include small nucleolar RNAs, promoter upstream transcripts, transcription start sites (TSS)-associated RNAs and promoter-associated small RNAs (Schaukowitch and Kim 2014).

Long ncRNAs (lncRNAs >200 base pairs), include circular RNAs, transcribed ultra-conserved regions, and large intergenic ncRNAs . Unlike the miRNAs, lncRNAs bind to other protein complexes and form a secondary structure (Wapinski and Chang 2011). Like the miRNAs, lncRNAs have been implicated in a variety of gene regulatory roles, including chromosome dosage compensation, genomic imprinting,

epigenetic regulation, cell cycle control, nuclear and cytoplasmic trafficking, transcription, translation, splicing, and cell differentiation, among others (Wapinski and Chang 2011).

Dysregulation of ncRNAs, including the miRNAs and lncRNAs in particular, is a critical factor in the pathobiology of several cancer types (Lee, Murphy et al. 2014).

1.1.3.4. Epigenetic treatments

Deregulation of epigenetic control has been associated with different human diseases, including cancer (Baylin and Jones 2011). In sharp contrast to irreversible genomic mutations that inactivate tumor suppressor genes or activate oncogenes in cancer, epigenetic modifications can potentially be reversed. Thus, the dynamism of the epigenome may allow the correction of aberrant epigenetic profiles by therapeutic manipulation using small molecule drugs (Simo-Riudalbas and Esteller 2014). Epigenetic therapies targeting two different chromatin regulators have already been approved by the Food and Drug Administration (FDA). This is the case for 5-azacytidine (Vidaza, Cellgene) and 5-aza-2'-deoxycytidine (Decitabine, Dacogen, Eisai), nucleoside analogues that irreversibly inhibit the DNA methyltransferases DNMT1 and DNMT3B, and which are currently used as first-line treatment for patients with myelodysplastic syndrome (Table 1.1) (Wells, Leber et al. 2014). Not only drugs targeting epigenetic writers are used in clinics at present, but also drugs against epigenetic erasers. The first compound found to inhibit HDACs was the natural product, trichostatin A (TSA) (Yoshida, Kijima et al. 1990) but its numerous side effects excluded this molecule from clinical trials. Vorinostat (Zolinza, Merck) and romidepsin (Istodax, Cellgene) are inhibitors of HDACs with an improved therapeutic window approved for the treatment of refractory cutaneous T-cell lymphoma (Table 1.1) (Khan and La Thangue 2012).

Table 1.1 Current epigenetic drugs targeting writers and erasers approved by the FDA or ongoing clinical trials.

category		target	compound	Indication	Status
Inhibitors of epigenetic writers	DNMT inhibitors	DNMT1 DNMT3B	Azacitidine (Vidaza)	Myelodysplastic Syndrome	**approved 2004**
		DNMT1 DNMT3B	Decitabine (Dacogen)	Myelodysplastic Syndrome	**approved 2006**
	HMT inhibitors	DOT1L	EPZ-5676	Hematological malignancies	Clinical trial (NCT01684150)
		EZH2	EPZ-6438	Advanced solid tumors, B-cell lymphoma	Clinical trial (NCT01897571)
			GSK-2816126	Relapsed or refractory Diffuse Large B Cell and Transformed Follicular Lymphoma	Clinical trial (NCT02082977)

category		target	compound	Indication	Status
Inhibitors of epigenetic erasers	Histone demethylase inhibitors	LSD1	ORY-1001	Relapsed or refractory acute leukemia	Clinical trial (ECT2013-002447-29)
			GSK-2879552	AML Relapsed or refractory Small Cell Lung Carcinoma	Clinical trial (NCT02177812 NCT02034123)
	HDAC inhibitors	panHDAC	Vorinostat (Zolinza)	Cutaneous T-cell Lymphoma	**approved 2006**
		panHDAC	Romidepsin (Istodax)	Cutaneous T-cell Lymphoma	**approved 2009**
		panHDAC	Panobinostat	Hematological malignancies, solid tumors	Clinical trial (NCT01321346)
		panHDAC	Belinostat	Ovary, colon, hematological malignancies	Clinical trial (NCT01686165)
		panHDAC	Pracinostat	Colorectal, MDS	Clinical trial (NCT01873703)
		panHDAC	Quisinostat	Advanced solid tumors, cutaneous T-cell lymphoma	Clinical trial (NCT01486277)
		Class I HDAC	CHR-3996	Refractory solid tumors	Clinical trial (NCT00697879)
		panHDAC	Phenylacetate	Brain tumor	Clinical trial (NCT00003241)
		panHDAC	Phenylbutirate	Advanced colorectal cancer	Clinical trial (NCT00002796)
		panHDAC	Valproic acid	Leukemia, solid tumors	Clinical trial (NCT00075010)
		Class I HDAC	Entinostat	Refractory advanced non-small cell lung cancer	Clinical trial (NCT00602030)
		Class I HDAC	Mocetinostat	Hematological malignancies, advanced solid tumors	Clinical trial (NCT02236195 NCT02282358)

category		target	compound	Indication	Status
Inhibitors of epigenetic erasers	HDAC inhibitors	Class I HDAC	CS055	Advanced non-small cell lung cancer	NCT01836679

Aberrant activity of HMTs due to chromosomal translocation, amplification, deletion, overexpression or silencing of their corresponding genes, has been discovered in cancer (Ryan and Bernstein 2012). Inhibitors targeting DOT1L, a key H3K79 methyltransferase recruited to unusual localizations in the development of MLL rearranged leukemia, or enhancer of zeste homologue 2 (EZH2), the catalytic component of the polycomb repressive complex (PRC2) responsible for H3K27 methylation and overexpressed or mutated in many cancers (Takawa, Masuda et al. 2011), are currently being tested in clinical trials by Epizyme and GlaxoSmithKline (Table 1.1).

The histone demethylase LSD1 (KDM1A) presents high-level expression in many cancer types and could be an important therapeutic target (Kahl, Gullotti et al. 2006, Hayami, Kelly et al. 2011, Kauffman, Robinson et al. 2011). Two LSD1 inhibitors are examined in clinical trials for the treatment of relapsed or refractory acute leukemia.

Using HDAC inhibition to reverse epigenetic aberrancies in cancer cells is a powerful approach for the treatment of several tumor types. A new generation of compounds derived from TSA and vorinostat like panobinostat, belinostat, givinostat, pracinostat and quisinostat are under clinical investigation. Phenylacetate, phenylbutyrate and valproic acid have weaker HDAC inhibitory effects than romidepsin or vorinostat, but their well-characterized kinetic properties and side-effect profiles have led to their investigation as anti-cancer agents in combination with other drugs (Fredly, Gjertsen et al. 2013, Simo-Riudalbas and Esteller 2014). Entinostat, mocetinostat, and CS055 represent a next-generation class of HDAC inhibitors with selectivity for class I HDACs (Bressi, Jennings et al. 2010). Although HDAC inhibitors were initially tested in clinical trials as single therapeutic agents, the tendency to use them in combination with other anti-cancer drugs is increasing (Simo-Riudalbas and Esteller 2014). For example in hematological malignancies, HDACs are aberrantly recruited to nuclear protein complexes and for this reason DNMT inhibitor treatment is now combined with HDAC inhibition (Khan and La Thangue 2012).

Although most efforts have concentrated on the various families of enzymes that contribute to writing and erasing processes, emerging data underline the therapeutic potential of inhibitors of reader proteins (Prinjha, Witherington et al. 2012). Especially with regard to the readers of acetylation marks, which are collectively named the bromodomains, the recent identification of specific small molecule inhibitors has opened the door for the development of new therapies against hematological and possibly solid malignancies.

1.2. The bromodomain family: Readers of acetylation

Histone acetylation affects a number of lysine residues in all histones and serves as a docking site for epigenetic readers containing the evolutionarily highly conserved bromodomain module (Zeng and Zhou 2002). The name of these reader domains comes from the Drosophila protein 'Brahma', which was the first bromodomain-containing protein identified (Tamkun, Deuring et al. 1992). BDs are found in several chromatin-associated proteins. In humans, a total of 61 evolutionarily conserved bromodomains have been identified in 46 different proteins, divided into eight families based on sequence alignment (Fig. 1.8 A.) (Chen, Yik et al. 2014).

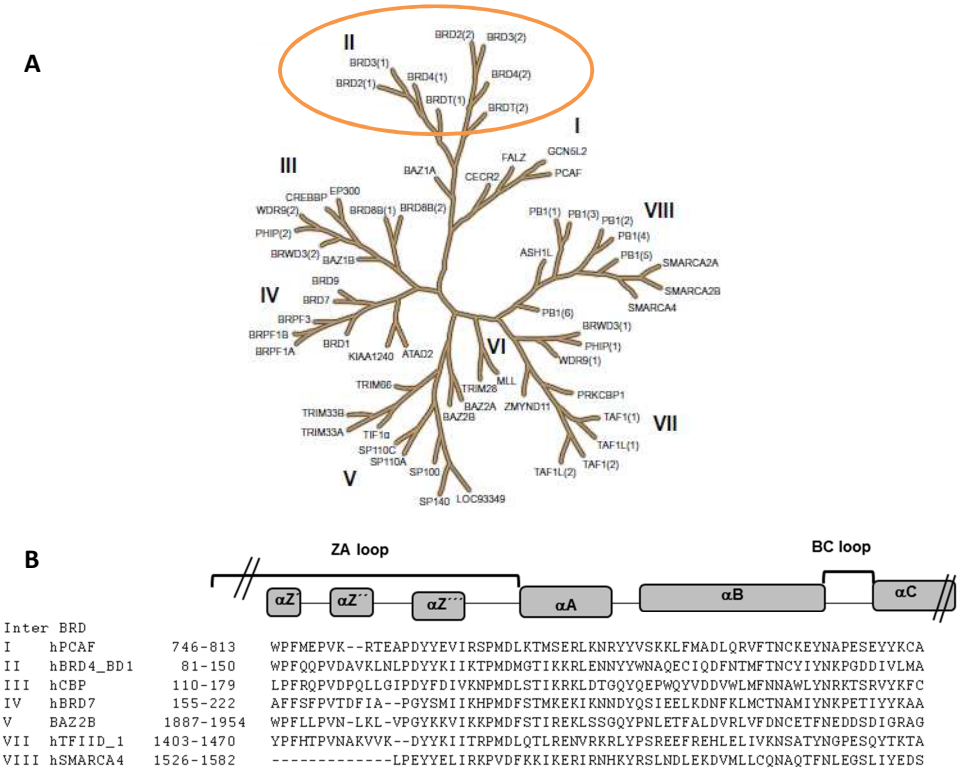

Figure 1.8 The bromodomain family.
A. Phylogenetic tree based on sequence alignments of predicted bromodomains. For proteins with multiple BDs, the domains have been numbered starting from the N-terminus and the number is shown in parentheses. The BET subfamily is highlighted in orange. Adapted from (Muller, Filippakopoulos et al. 2011). B. Alignment of representative members of the different bromodomain subfamilies. No member of subfamily VI is shown due to the low sequence conservation in the compared region. Secondary structure elements (α-helices) of human BRD4 are displayed above the sequence alignment. Adapted from (Jung, Philpott et al. 2014).

Despite large sequence variations, all bromodomain modules share a conserved fold comprising a left-handed bundle of four α helices (αZ, αA, αB, αC), linked by diverse loop regions (ZA and BC loops) that contribute to substrate specificity (Fig. 1.8 B.) (Filippakopoulos, Qi et al. 2010). Structural data have established that acetylated lysine is recognized in a central hydrophobic pocket, where it is anchored to a conserved asparagine residue (Dhalluin, Carlson et al. 1999).

Following the recognition of discrete patterns of acetylation marks together with neighboring amino acids, bromodomain-containing proteins engage in a variety of cellular functions. Bromodomain proteins include:

- **HATs and HAT-associated proteins** such as P300/CBP-associated factor (PCAF; also known as KAT2B) (Yang, Ogryzko et al. 1996)
- **The Bromo and Extra Terminal (BET) family of proteins** (Dey, Ellenberg et al. 2000).
- **ATP-dependent chromatin remodelling complexes** such as bromodomain adjacent to zinc finger domain protein 1B (BAZ1B; also known as Williams syndrome transcription factor)(Cavellan, Asp et al. 2006)
- **Helicases** such as SWI/SNF-related matrix-associated actin-dependent regulators of chromatin subfamily A (SMARCAs) (Trotter and Archer 2008)
- **Transcriptional co-activators** such as tripartite motif-containing proteins (TRIMs) and TBP-associated factors (TAFs) (Venturini, You et al. 1999)
- **Transcriptional mediators** such as TAF1 (Jacobson, Ladurner et al. 2000)
- **Histone methyltransferases** such as ASH1L and mixed lineage leukemia protein (MLL) (Gregory, Vakoc et al. 2007, Malik and Bhaumik 2010)
- **Nuclear scaffolding proteins** such as polybromo 1 (PB1) (Mohrmann, Langenberg et al. 2004)

1.2.1. The BET subfamily

The BET proteins belong to the subfamily II of BRDs. They derive their name from the presence of two related tandem bromodomains (BD1 and BD2) and of a unique extra-terminal region in the C-terminal moiety (Gallenkamp, Gelato et al. 2014). They are highly conserved and form a distinct subfamily with similar hydrophobic binding pockets (Florence and Faller 2001, Vidler, Brown et al. 2012). The original members of this subclass include the Drosophila gene female sterile homeotic (fsh; (Haynes, Mozer et al. 1989), the yeast S. cerevisiae gene bromodomain factor 1 (BDF1), and the human gene RING3 (Really Interesting New Gene 3; BRD2) (Florence and Faller 2001).

The four BET proteins described in vertebrates, BRD2, BRD3, BRD4 and BRDT, are ubiquitously expressed with the exception of BRDT, for which expression is restricted to the male germ line. BET proteins are found in the cell nucleus where they bind via their two bromodomains to acetylated proteins, including histones H3 and H4. Only BRD2 and BRD4 remain bound to chromatin during mitosis, a property that suggests that they contribute to epigenetic inheritance (Dey, Chitsaz et al. 2003, Kanno, Kanno et al. 2004). BET proteins have important differences in their binding preferences to acetylated histone motifs (Filippakopoulos, Picaud et al. 2012) but also unique functions. Nevertheless, there is more similarity among BD1 (or BD2) regions within the BET family than between the respective BD1 and BD2 of individual BET proteins.

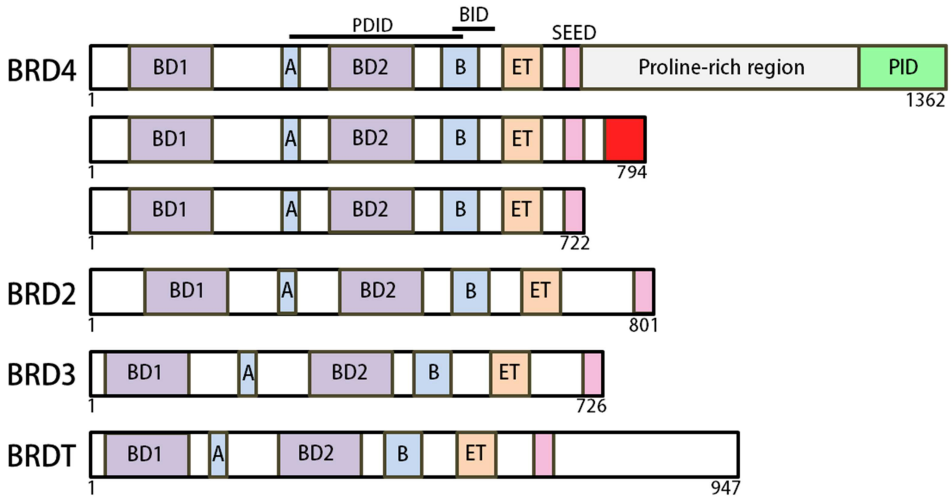

Figure 1.9 Domain organization of the human BET protein family.
Colored boxes delineate the conserved domains BD1, BD2, ET, motif A, motif B, the Ser/Glu/Asp-rich (SEED) and the PID regions. The conserved PDID and BID regions are overlined. The specific C-terminal region of BRD4 isoform 2 is highlighted in red. For BRD2, BRD3 and BRDT only the main isoform is shown.

Knockout mice deficient in individual BET family members have highlighted the relevance of these proteins for development and survival. Thus, Brd4 and Brd2 mutant mice die at early post-implantation and E11.5 stages, respectively (Houzelstein, Bullock et al. 2002, Shang, Wang et al. 2009). In vivo mutational analyses of Brd4 (Houzelstein, Bullock et al. 2002) and Brdt (Shang, Nickerson et al. 2007) in the mouse model have revealed that these genes are essential for embryonic development and spermatogenesis, respectively.

1.2.1.1. BRDT

The testis-specific BRDT is involved in the chromatin remodeling that takes place during spermiogenesis (Pivot-Pajot, Caron et al. 2003, Dhar, Thota et al. 2012). It controls meiotic divisions and post-meiotic repackaging of the genome (Gaucher, Boussouar et al. 2012). In addition, BRDT regulates spermatogenic gene expression by activating or repressing a number of essential genes. Selective deletion of the Brdt(BD1)-encoding region is sufficient to confer sterility in homozygous hypomorphic male mice (Shang, Nickerson et al. 2007). Beside the regulation of transcription, BRDT plays an additional role in mRNA alternative splicing (Berkovits, Wang et al. 2012, Berkovits and Wolgemuth 2013). Structural studies of murine Brdt have demonstrated that Brdt(BD1) binds to a diacetylated histone 4 peptide (H4K5acK8ac) in part through the conserved asparagine (Moriniere, Rousseaux et al. 2009). Additionally, Brdt I114 mutation (Moriniere, Rousseaux et al. 2009) and the triple mutant modified at positions P50, F51 and V55 (which correspond to I112, P48, F49 and V53 in human BRDT) or at the equivalent positions in BD2 lose their binding to the H4 N-terminal tail (Pivot-Pajot, Caron et al. 2003). It has been speculated that BET inhibitors with selectivity for BRDT may be used for male contraception (Matzuk, McKeown et al. 2012).

1.2.1.2. BRD2

The first described mammalian BET gene, BRD2 (RING3), was identified over two decades ago as a mitogen-activated nuclear kinase (Beck, Hanson et al. 1992). BRD2 binds to acetylated H4 (Kanno, Kanno et al. 2004) and H2A.Z (Draker, Ng et al. 2012). Surface plasmon resonance (SPR) reveals that BRD2 BD1 residues including Y113, N156 and D160 are essential for binding to a mono-acetylated H4 peptide (Umehara, Nakamura et al. 2010). This was confirmed for Y113 and its BD2 counterpart in living cells (Ito, Umehara et al. 2011), and by immunoprecipitation (Kanno, Kanno et al. 2004). Moreover BRD2 has intrinsic histone chaperone activity (LeRoy, Rickards et al. 2008) allowing the transfer of histones to a DNA molecule.

Transgenic mice that overexpress Brd2 in the lymphoid compartment develop lymphoma and leukemia (Greenwald, Tumang et al. 2004).

Nuclear BRD2 interacts with E2F transcription factors to form complexes with other proteins components of TAFIID such as Snf2, Baf155, HDAC11, CAF1b and NAP1L3, (Denis, McComb et al. 2006). BRD2 can also interact with components of the SWI/SNF complexes (Denis, McComb et al. 2006) regulating the selectivity of NF-κB (nuclear factor kappa-light-chain-enhancer of activated B cells) for its target genes (Dawson, Prinjha et al. 2011). Recent siRNA studies in melanoma cell lines indicate that BRD2 is the main BET protein involved in regulation of NF-κB and that BET inhibitor treatment causes transcriptional downregulation of the NF-κB subunit p105/p50 (Gallagher, Mijatov et al. 2014). An implication in the inflammatory response of macrophages via direct binding to regulatory regions of cytokine genes has furthermore been evidenced (Belkina, Nikolajczyk et al. 2013).

BRD2 was also linked to epigenetically deregulated expression of genes involved in energy metabolism. Reduced expression of Brd2 in mice produces a distinct hypomorphic phenotype with extreme obesity and hyperinsulinemia, but enhanced glucose tolerance and low blood glucose (Wang, Liu et al. 2010).

BRD2 was also involved in juvenile myoclonic epilepsy, however, another study did not show a link between BRD2 and photosensitive epilepsy (Yavuz, Ozdemir et al. 2012).

1.2.1.3. BRD3

No Brd3-deficient mice have been reported but an important role in erythroid maturation has been shown (Lamonica, Deng et al. 2011). BRD3 interacts with acetylated GATA1, a transcription factor with an essential role in hematopoiesis. A detailed analysis of BRD3's interaction with acetylated GATA1 has been reported (Gamsjaeger, Webb et al. 2011). Binding of BRD3 to GATA1 is observed both at active and inactive gene regions, and is independent of the acetylation status of histones. Mutation of several hydrophobic residues has strong effects whereas, interestingly, mutation of the

conserved N116 residue which forms the important hydrogen bond with the acetyl group of histone peptides has little impact on binding, suggesting that, at least in this particular case, alternative recognition mechanisms are possible.

BRD3 is implicated in the transcription elongation process by association with the PAF1 complex (Dawson, Prinjha et al. 2011).

Recently, BRD3 and BRD4 were shown to interact with WHSC1, a HMT that methylates histone H3K36. WHSC1 is recruited to the ERα (estrogen receptor alpha gene) by the BET proteins BRD3 and BRD4, and facilitates ERα gene expression (Feng, Zhang et al. 2014).

1.2.1.4. BRD4

BRD4 is the best studied member of the BET family. It was originally named MCAP (Mitotic Chromosome-Associated Protein) and described as a nuclear factor (Dey, Ellenberg et al. 2000). Expression of BRD4 was linked to cell division, as it is induced by growth stimulation and repressed by growth inhibition. The most notable feature of BRD4 is its association with euchromatin, also during mitosis, at a time when the majority of nuclear regulatory factors are released into the cytoplasm. Analysis of knockout mice indicates that Brd4 is essential for embryonic development. Fibroblasts derived from Brd4-deficient animals proliferate more slowly than control ones. Embryos of mice nullizygous for Brd4 die shortly after implantation and heterozygous animals have growth defects, before and after birth, implicating this protein in several essential physiological processes (Houzelstein, Bullock et al. 2002).

The BRD4 gene encodes three splice isoforms: one long isoform of 1362 residues, and two shorter isoforms (722 and 794 residues) that differ by a unique 75-residue coding exon at the C terminus (Floyd, Pacold et al. 2013) (Fig. 1.8). The long isoform contains a unique C-terminal positive transcription elongation factor b (P-TEFb) interacting domain (PID). The BRD4 short isoform is a nuclear membrane-associated protein, while the long isoform is associated with the nuclear matrix. Despite possessing identical bromodomains, the BRD4 short isoform possesses expanded histone binding affinity in comparison to the long isoform (Alsarraj, Faraji et al. 2013). Recently, a 794 amino acid-long short isoform containing a unique 75-residue coding exon was found to be involved in the signaling response to DNA damage (Floyd, Pacold et al. 2013).

1.2.1.4.1. BRD4 bromodomains

The structures of BRD4 BD1 (aa 58-169) and BD2 (aa 349-461) exhibit the classical bromodomain fold that consists of four α-helices (Z, A, B, C) and two interconnecting loops (ZA and BC) at the distal site to the domain N and C terminus (Dhalluin, Carlson et al. 1999). The four helices form a left-handed -helical bundle that composes the hydrophobic core of the domain while the two loops form a deep

cleft that composes a recognition site for the binding to acetylated lysines within histone tail sequences (Vollmuth, Blankenfeldt et al. 2009).

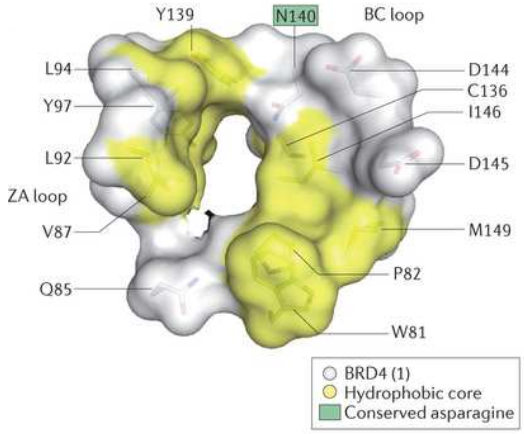

Figure 1.10 The BRD4 BD1 binding pocket.
The hydrophobic nature of the acetyl-lysine binding site stems from the aromatic and hydrophobic residues that line the central acetyl-lysine-binding cavity, shown here on BRD4(1) (PDB ID: 3UVW) (Filippakopoulos and Knapp 2014).

The interaction between bromodomains and acetyl-lysine is essential for cellular function. Cocrystal structures of BRD4 bromodomains and bound histone-derived peptides reveal that the acetyl-lysine side chain is anchored by a hydrogen bond formed with a conserved asparagine (e.g. N140 in BRD4 BD1) located in the BC loop and also found in other bromodomains (Owen, Ornaghi et al. 2000, Umehara, Nakamura et al. 2010). In BRD4 BD2 this asparagine is also essential for NF-κB-K310(ac) binding (Zhang, Liu et al. 2012). Additional amino acids in the ZA loop and in the αB and αC regions are essential for acetyl-lysine recognition (Filippakopoulos, Qi et al. 2010) and several water molecules are found at the bottom of the bromodomain pocket (Vollmuth, Blankenfeldt et al. 2009). X-ray structures solved in the presence of BET inhibitors such as JQ1 or I-BET762 show that these compounds effectively mimic the acetyl-lysine moiety (Filippakopoulos, Qi et al. 2010, Nicodeme, Jeffrey et al. 2010).

The static overview provided by crystal structure can be complemented by mutational analysis to unravel the precise contributions of the residues. Only a few such studies have been performed on BRD4. The first reported BRD4 mutants focused on the equivalent Y139 and Y432, or Y139 and V439 residues in BRD4 BD1 and BD2, respectively. These mutants have increased mobility and impaired interaction with acetylated chromatin in comparison to the wild-type form (Dey, Chitsaz et al. 2003). Mutating N140 and N433 in BRD4 BD1 and BD2, respectively, abolishes the binding to di-acetylated H4 peptides in a SPOT assay as well as in isothermal calorimetry (ITC), confirming the importance of the hydrogen bond formed by the highly conserved asparagine residue (Filippakopoulos, Picaud et al. 2012). N140 and the neighboring Y139 in BRD4 BD1, as well as the equivalent positions in BD2, are also important for the interaction with acetylated RelA (Zou, Huang et al. 2013). Recently, the

binding to histone peptide arrays of whole lysates from cells transiently transfected with tagged mutated BRD4 long and short isoforms was analyzed. Y139A substitution in BD1 did not significantly affect binding in either isoform compared to wild-type constructs, whereas introduction of Y433A into BD2 did not alter BRD4 long isoform binding but eliminated all but the H4K5/K8 diacetylated peptide binding in the BRD4 short isoform. The double point mutation Y139A/Y433A completely eliminated histone binding for both isoforms (Alsarraj, Faraji et al. 2013).

1.2.1.4.2. BRD4 interaction with histones

BRD4 bromodomains constitute a deep, hydrophobic substrate-binding pocket (Dhalluin, Carlson et al. 1999) which binds to acetylated histones H3 and H4 tails and plays an essential role in maintaining chromatin architecture (Wang, Li et al. 2012). Published affinities of BRD4 substrate interactions are usually weak and have been determined by a variety of different biophysical techniques employing various lengths for the studied peptidic substrates. Methods used for substrate identification comprise pull-down experiments, peptide arrays (SPOT), Nuclear Magnetic Resonance (NMR) and affinity quantification by biophysical techniques such as isothermal titration calorimetry (ITC), fluorescent polarization (FP) spectroscopy, and Surface Plasmon Resonance (SPR) (Table 1.2) (Filippakopoulos and Knapp 2012).

Table 1.2 Studied BRD4-histone tail interactions.
Adapted from (Filippakopoulos and Knapp 2012)

Bromodomain	Acetylated tail	Affinity (µM)	Method	Reference
BRD4 (BD1+BD2)	H4K5/8/12/16	2.7 ± 0.2	ITC	(Filippakopoulos, Picaud et al. 2012)
BRD4 (BD1)	H3K9	301 ± 40.9	ITC	(Filippakopoulos, Picaud et al. 2012)
	H3K9/14	Not quantified	NMR	(Liu, Wang et al. 2008)
	H4K5	810 ± 57	NMR	
	H4K8	84.7 ± 8.2	ITC	(Filippakopoulos, Picaud et al. 2012)
	H4K12	650 ± 11	NMR	(Liu, Wang et al. 2008)
	H4K5/8	6.8 ± 0.1	ITC	(Filippakopoulos, Picaud et al. 2012)
	H4K5/12	Not quantified	NMR	(Liu, Wang et al. 2008)
	H4K8/12	27.4 ± 0.9	ITC	(Filippakopoulos, Picaud et al. 2012)
	H4K12/16	46.1 ± 0.9	ITC	
	H4K12/16/20	20.4 ± 0.8	ITC	
	H4K5/8/12/16	2.8 ± 0.2	ITC	
BRD4 (BD2)	H3K14	260 ± 32.2	ITC	(Filippakopoulos, Picaud et al. 2012)
	H3K9/14	Not quantified	NMR	(Liu, Wang et al. 2008)
	H4K5	1000 ± 126	NMR	
		60.2 ± 2.5	ITC	(Filippakopoulos, Picaud et al. 2012)

Bromodomain	Acetylated tail	Affinity (µM)	Method	Reference
BRD4 (BD2)	H4K12	1350 ± 78	NMR	(Liu, Wang et al. 2008)
	H4K5/12	Not quantified	NMR	(Liu, Wang et al. 2008)
	H4K31	170 ± 10.1	ITC	(Filippakopoulos, Picaud et al. 2012)
	H4K5/8	63.3 ± 2.3	ITC	
	H4K8/12	20.4 ± 0.8	ITC	
	H4K12/16	49.3 ± 1.1	ITC	
	H4K12/16/20	22.7 ± 0.8	ITC	
	H4K5/8/12/16	26.6 ± 0.1	ITC	

Both BRD4 bromodomains exhibit affinity for histone H4 peptides with single or multiple acetylations although the N-terminal domain seems to bind with higher affinity than the C-terminal one. Furthermore, closely spaced multiple acetylation sites increase affinity of the histone tail for the BET proteins suggesting a cooperative role of neighboring sites for substrate binding (Filippakopoulos, Picaud et al. 2012).

1.2.1.4.3. BRD4 implication in transcription

Genome-wide studies indicate that BRD4 binding correlates with gene expression and that beside promoter regions, intergenic and intragenic regions are also recognized (Zhang, Prakash et al. 2012).
One of the multiple processes by which BRD4 regulates transcription is through modulation of RNA-Pol II activity. Unlike the other BET proteins, BRD4 contains a unique PID domain at its extreme C-terminus for interacting with P-TEFb (Bisgrove, Mahmoudi et al. 2007). BRD4 and hexamethylene bisacetamide (HMBA) inducible protein 1 (HEXIM1) are two opposing regulators of P-TEFb. P-TEFb is sequestered into the 7SK/HEXIM1 snRNP, where P-TEFb's kinase activity is inhibited by HEXIM1 in a 7SK-dependent manner (Diribarne and Bensaude 2009). At the start of the transcription cycle, RNA-Pol II with the hypophosphorylated CTD is assembled into the preinitiation complex (PIC) at the promoter. After RNA-Pol II recruitment to a gene promoter, Transcription factor II (TFIIH) phosphorylates serine 5 of the heptapeptide repeats in the CTD of RNA-Pol II, resulting in initial synthesis of short RNA species. However, shortly after initiation, the progression of Pol II is stalled by the concerted actions of two negative elongation factors, the DRB Sensitivity Inducing Factor (DSIF) and the Negative elongation factor (NELF). This checkpoint facilitates the recruitment of enzymes that ensure proper capping of the nascent pre-mRNAs. To overcome this checkpoint P-TEFb is recruited by BRD4 through its direct interaction with the acetylated cyclin T1, and phosphorylates DISF, NELF, and the Pol II CTD repeats at the Ser2 positions. These phosphorylation events promote the dissociation of NELF and convert DSIF into a positive elongation factor, thereby allowing Pol II to

engage in productive elongation to produce full-length transcripts (Zhou and Yik 2006, Chen, Yik et al. 2014) (Fig. 1.11).

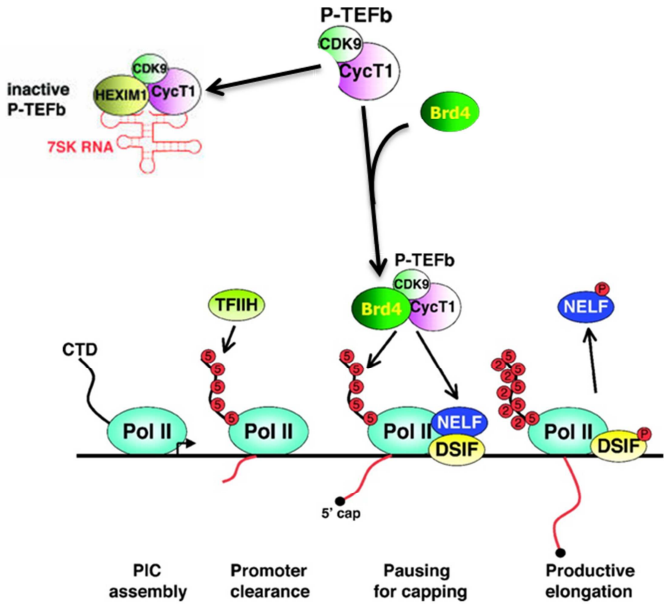

Figure 1.11 Regulation of P-TEFb activity by its negative regulator HEXIM1 and positive regulator BRD4. Adapted from (Zhou and Yik 2006, Chen, Yik et al. 2014)

An additional association between BRD4 BD2 and the P-TEFb subunit acetylated cyclin T1 was reported (Schroder, Cho et al. 2012). Importantly, only full-length BRD4 is found in the active P-TEFb complex, whereas the shorter splice variant can be present in the inactive complex, together with HEXIM1 and the 7SK RNA. HDAC and BET inhibition increase the mRNA and protein levels of HEXIM1 (Bartholomeeusen, Xiang et al. 2012). Furthermore a direct phosphorylation of RNA Pol II by BRD4 at the Ser2 residue during transcription initiation and transition to elongation has also been described (Devaiah, Lewis et al. 2012).

Stalling of RNA Pol II downstream of the start site represents an important regulation step in gene transcription but BRD4 also forms recruitment platforms for various transcription regulators affecting a large number of genes, many of which are involved in cell proliferation and apoptosis (Kwak and Lis 2013). BRD4 and Mediator were found to co-occupy thousands of enhancers associated with active genes and a small set of exceptionally large so called super-enhancers associated with key oncogenic drivers in many tumor cells (Loven, Hoke et al. 2013). Very recently, BRD4 was shown to stimulate elongation of both protein-coding transcripts and noncoding enhancer RNAs (eRNAs), in a manner dependent on bromodomain function (Kanno, Kanno et al. 2014).

BRD4 also interacts with transcription factors and may function as a coactivator. BRD4 bromodomains bind to acetylated RelA, thus stabilizing nuclear NF-κB and controlling the expression of downstream target genes (Zhang, Liu et al. 2012, Zou, Huang et al. 2013). BRD4 has been reported to enhance NF-κB activity in human kidney and lung carcinoma cells (Huang, Yang et al. 2009, Zhang,

Yang et al. 2009, Zhang, Prakash et al. 2012), but recent siRNA studies in melanoma cells indicate that BRD2 is the main BET protein involved in regulation of NF-κB. BET inhibitor treatment caused transcriptional downregulation of NF-κB target genes involved in inflammation and cell cycle regulation in line with the strong anti-inflammatory effects seen for BET inhibitors (Nicodeme, Jeffrey et al. 2010, Gallagher, Mijatov et al. 2014).

The acidic phosphorylation-dependent interaction domain (PDID) and basic residue-enriched interaction domain (BID) motifs (Fig. 1.8) independently recognize different regions of the tumor protein P53 (Wu, Lee et al. 2013). Phosphorylation of several PDID sites by casein kinase II guides the interaction with P53 and BID, and allows binding to acetylated histones for downstream gene activation (Wu, Lee et al. 2013). The same study showed that BRD4 also binds to other transcription factors such as the Myc/Max heterodimer and c-Jun, which impacts on the expression of downstream target genes especially in cancer (see below). BRD4 furthermore binds to ubiquitinated Stat3 (Ray, Zhao et al. 2014). The interaction regulates the downstream transcriptional program modulated by this factor which is implicated in cell proliferation and apoptosis. The BRD4 BD2 recognizes a diacetylated motif in the transcription factor Twist, ultimately leading to the activation of wingless-type MMTV integration site family, member 5A (WNT5A) expression which is involved in epithelial-mesenchymal transition, an essential process in basal-like breast cancer (Shi, Wang et al. 2014) (Fig. 1.12).

An interaction between the BET proteins BRD2, BRD3 and BRD4, and the N-terminal domain of the androgen receptor (AR) was recently reported (Asangani, Dommeti et al. 2014). This interaction is disrupted by a BET inhibitor and impairs AR recognition of regulatory regions of androgen target genes. AR mRNA levels were not altered upon JQ1 treatment in prostate cancer cells (Feng, Zhang et al. 2014). Interestingly, BRD3 and BRD4 also occupy regulatory regions of estrogen receptor (ER) target genes thereby controlling their expression (Asangani, Dommeti et al. 2014, Feng, Zhang et al. 2014, Nagarajan, Hossan et al. 2014) (Fig. 1.12).

BRD4 is also involved in cell cycle progression by controlling expression of Aurora B, an essential player in chromosomal segregation processes and a regulator of cyclin D1 and other G1-associated genes required for progression to the S phase (Mochizuki, Nishiyama et al. 2008, Yang, He et al. 2008, You, Li et al. 2009).

An implication of BRD4 in the oxidative stress response has newly been described (Hussong, Borno et al. 2014). The KEAP1/NRF2 pathway is deregulated following BET inhibitor treatment and binding of BRD4 to regulatory regions of the stress-related HMOX1 gene was reported (Fig. 1.12).

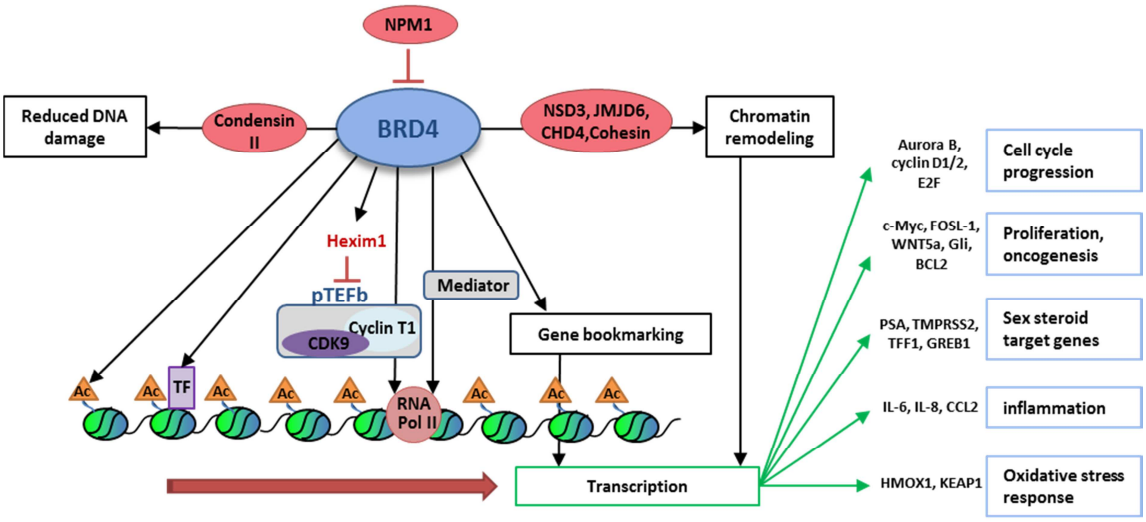

Figure 1.12 BRD4-interacting partners and implications for downstream gene regulation.
Black arrows point to proteins that interact with BRD4. Transcription factors (TF) include the Rel A subunit of NF-KB, AR, Twist, P53, c-Myc, c-Jun and Stat3. Representative regulated target genes for different cellular processes are shown on the right (Jung, Gelato et al. 2015).

BRD4 is one of the rare proteins, along with BRD2, that remains associated with chromosomes during mitosis, hence its denomination as a histone bookmark (Kanno, Kanno et al. 2004, Devaiah and Singer 2013). It marks the transcription initiation sites of numerous genes expressed during the G1 phase, thus favoring cell cycle progression. Although this binding could be expected to happen through bromodomain histone binding, published results strongly indicate that the conserved motif B, together with the integrity of the bromodomains, is required for attachment of BET proteins to mitotic chromosomes (Garcia-Gutierrez, Mundi et al. 2012).

1.2.1.4.4. BRD4 implication in response to DNA damage

Following treatment with ionizing radiation, BRD4 short isoform (794 amino acids) binds to acetylated histones, recruits the condensin II chromatin remodelling complex and reduces DNA damage response signaling (Fig. 1.11). Loss of this isoform results in relaxed chromatin structure, rapid cell-cycle checkpoint recovery and enhanced survival after irradiation, whereas functional gain of this isoform compacts chromatin, attenuates DNA damage response signalling and enhances radiation-induced lethality (Floyd, Pacold et al. 2013).

1.2.1.4.5. BRD4 implication in chromatin organization and remodeling

Cellular binding partners of the BRD4 ET region were identified using a proteomics approach. They include the histone methyltransferase NSD3 (or WHSC1L1 Wolf-Hirschhorn syndrome candidate 1-like 1) and the histone demethylase JMJD6, which adds another layer of complexity to the gene regulatory activity of BRD4 (Rahman, Sowa et al. 2011). Interestingly, JMJD6 also interacts with P-

TEFb and BRD4 as part of this complex plays an important role in controlling pause release (Liu, Ma et al. 2013).

The ET region additionally interacts with proteins involved in chromatin remodeling such as CHD4, which may also affect gene regulation (Rahman, Sowa et al. 2011). Also, through its interaction with architectural proteins such as mediator and cohesin, BRD4 plays an instrumental role in chromatin organization (Bonora, Plath et al. 2014).

In addition, crosstalk between histone acetylation and phosphorylation involving HDACs, protein phosphatase 1a (PP1α) and BRD4 has been shown. PP1α -mediated dephosphorylation of H3S10ph allows the deacetylation of nucleosomal H4K5/K8ac by HDAC1/2/3, thereby leading to the release of chromatin-bound BRD4 for subsequent recruitment of P-TEFb to enhance the expression of inducible genes (Hu, Lu et al. 2014).

Beside the bookmarking function, the association of BRD4 with mitotic chromosome is also important for the function of BRD4 in maintaining chromatin compaction (Zhao, Nakamura et al. 2011, Wang, Li et al. 2012).

1.2.1.4.6. BRD4 homodimerization

Motif B was identified in BET proteins between BD2 and the ET region, and is highly conserved among the subfamily (Fig. 1.8). It allows homo- and heterodimerization of BET proteins and is necessary for association with mitotic chromosomes (Garcia-Gutierrez, Mundi et al. 2012). However, pull-down analysis and immunofluorescence demonstrated that BRD4 proteins could interact with each other through the N terminal 1–470 aa domain containing BD1 and BD2 but not motif B. (Wang, Li et al. 2012).

1.2.2. BRD4 in cancer

Accumulating evidence has revealed the critical roles of BRD4 in cancer development and progression (Belkina and Denis 2012, Barbieri, Cannizzaro et al. 2013). The first clue linking BRD4 with cancer was the identification of the BRD4-NUT fusion oncogene which was recognized as an important mechanism in NUT midline carcinoma (NMC), an aggressive form of squamous carcinoma (French, Miyoshi et al. 2001, French, Miyoshi et al. 2003). More rarely, the NUT gene is found fused to the BRD3 gene (French 2013). Because NMCs arise from various anatomical sites, they cannot be categorized by their tissue of origin. Instead, NMC is defined genetically by the presence of chromosomal rearrangements involving the NUT gene (French 2012). Patient-derived NMC tumors are inhibited by the BET inhibitor JQ1 in *in vivo* xenograft models and the first clinical studies addressing this indication have already been initiated (Filippakopoulos, Qi et al. 2010, French 2013). The function of the NUT protein is not known. It is only constitutively expressed in early germ cells and within the brain (ciliary ganglion) and normally shuttles between the nucleus and cytoplasm.

However, it remains bound to chromatin when fused to BRD4 (French 2010). The resulting fusion protein recruits HAT proteins, thus leading to histone hyperacetylation, up-regulation of c-Myc and its target genes, and inhibition of cell differentiation (Reynoird, Schwartz et al. 2010, Grayson, Walsh et al. 2014). c-Myc protein belongs to the Myc family of transcription factors, which also includes N-Myc and L-Myc. High levels of c-Myc expression have been associated with almost all human cancers. This oncoprotein induces tumor initiation and progression by modulating the transcription of numerous genes. C-Myc dimerizes with MAX to form a c-Myc-MAX protein complex which directly binds to c-Myc-responsive element E-boxes at target gene promoters, thereby leading to transcription (Meyer and Penn 2008, Dang 2012).

Several studies indicate that BRD4 may contribute to cancer development through different mechanisms and BET-selective inhibitors such as JQ1 and I-BET151 (see below 1.2.1.4.7 BRD4 Inhibitors) (Filippakopoulos, Qi et al. 2010, Nicodeme, Jeffrey et al. 2010, Dawson, Prinjha et al. 2011) were extremely helpful for the demonstration of the essential role of BRD4 in growth control. Indeed, these inhibitors are effective against hematological cancers such as multiple myeloma (MM) through the suppression of c-Myc and downstream target genes (Delmore, Issa et al. 2011), acute myeloid leukemia (AML), and Burkitt's lymphoma (Dawson, Prinjha et al. 2011, Mertz, Conery et al. 2011, Zuber, Shi et al. 2011) by blocking the chromatin binding activity. In line with this, clinical studies with different BET inhibitors mainly addressing hematological tumors have recently been started.

BET inhibition has also recently shown efficacy in glioblastoma (Cheng, Gong et al. 2013, Pastori, Daniel et al. 2014) and medulloblastoma (Henssen, Thor et al. 2013) by downregulating c-Myc. In neuroblastoma, BET inhibitors also displace BRD4 from the N-Myc promoter region, downregulating N-Myc and its targets (Puissant, Frumm et al. 2013). BRD4 inhibition and cytotoxicity in neuroblastoma cell lines were also shown, irrespective of the N-Myc copy number or expression level, through direct suppression of N-Myc and of the anti-apoptotic protein BCL2.

The impact of BET inhibitors was also investigated in prostate cancer, where they prevented the growth of a patient-derived model with high c-Myc expression by direct downregulation of c-Myc and of BCL2 (Wyce, Degenhardt et al. 2013). Another study showed that JQ1 reduces the growth of the prostate cancer cells VCaP by inhibiting the direct association between BRD4 and AR, thus leading to diminished expression of androgen target genes (Asangani, Dommeti et al. 2014).

In human breast carcinomas, BRD4 induces a gene expression signature that efficiently predicts survival (Crawford, Alsarraj et al. 2008). JQ1 prevents binding of both BRD4 and BRD3 to the ER alpha promoter, reducing expression of downstream estrogen target genes (Feng, Zhang et al. 2014, Nagarajan, Hossan et al. 2014). *In vivo* anti-proliferative activity of BET inhibitors was also reported in a basal-like breast cancer model (Shi, Wang et al. 2014).

Lung adenocarcinoma cells growth is inhibited by the BRD4 inhibitor JQ1 through suppression of the oncogenic transcription factor FOSL-1 and its targets (Lockwood, Zejnullahu et al. 2012). Interestingly *in vivo* studies on a human lung adenocarcinoma cell line model showed efficacy not to be due to the regulation of c-Myc but to the prevention of the BRD4/NF-κB interaction (Zou, Huang et al. 2013). Nevertheless, in a small panel of non-small cell lung carcinoma models JQ1 response paralleled the abrogation of c-Myc expression (Shimamura, Chen et al. 2013).

JQ1 blocks the growth of several pancreas adenocarcinoma cell lines, by down-regulating c-Myc and FOSL1, as well as the architectural HMGA2 protein (Sahai, Kumar et al. 2014).

BRD4 is over-expressed in a number of primary and metastatic melanoma samples. Its implication in melanoma is further suggested by the effects of the BET inhibitors which show anti-proliferative activity *in vitro* in different cell lines by a reduction of c-Myc expression and an increase in p21 and p27 expression (Segura, Fontanals-Cirera et al. 2013) and i*n vivo* (Gallagher, Mijatov et al. 2014, Gallagher, Mijatov et al. 2014).

Although BRD4 is ubiquitously expressed, mice are reasonably tolerant to BET bromodomain inhibition so that efficacy in mouse tumor models could be achieved at tolerated doses (Filippakopoulos, Qi et al. 2010, Dawson, Prinjha et al. 2011, Delmore, Issa et al. 2011, Mertz, Conery et al. 2011, Zuber, Shi et al. 2011). As previously mentioned, BRD4 and the mediator complex are associated with most active enhancer and promoter regions in tumor cells, but both transcriptional activators are particularly enriched at super enhancers (Loven, Hoke et al. 2013). Treatment of MM tumor cells with the BET bromodomain inhibitor JQ1 led to preferential loss of BRD4 binding to super-enhancers and consequent transcription elongation defects that preferentially impacted genes with super-enhancers, including c-Myc (Loven, Hoke et al. 2013). This finding has been confirmed in other tumor types, including lymphoma and diffuse large B cell lymphoma (Chapuy, McKeown et al. 2013, Tolani, Gopalakrishnan et al. 2013) which offers an explanation for the specific repression of the transcription of tumor-promoting and lineage-specific genes by BET bromodomain inhibitors.

1.2.3. BET inhibitors

Increasing interest in BET proteins as targets for a variety of therapeutic applications including cancer has resulted in considerable activity from academia, biotechnology and pharmaceutical companies to identify BET inhibitors (Fig. 1.13 A.). JQ1, based on the structure of a compound series originally described by Mitsubishi, and I-BET762 were the first BET inhibitors published simultaneously in 2010 (Fig. 1.13 B.) (Filippakopoulos, Qi et al. 2010, Nicodeme, Jeffrey et al. 2010).

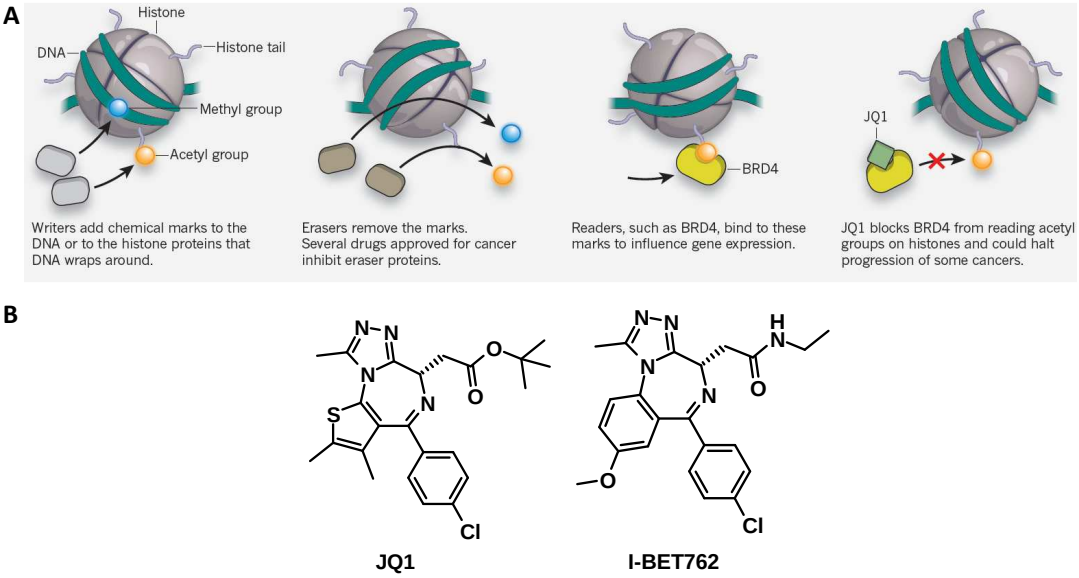

Figure 1.13 Mechanism of BET protein inhibition and chemical structure of first inhibitors.
A. Writers, erasers and readers orchestrate epigenetic modifications that regulate gene expression. The inhibitor JQ1 prevents the binding of the bromodomain reader protein BRD4 to the acetylated histone tails. Adapted from (Maxmen 2012).
B. The triazolo-thieno-diazepine JQ1 and the triazolo-benzo-diazepine I-BET762.

Since then BET inhibitors with different chemical scaffolds have been identified (Filippakopoulos and Knapp 2014, Gallenkamp, Gelato et al. 2014, Sanchez, Meslamani et al. 2014, Smith, Sanchez et al. 2014). These inhibitors interact directly with the acetyl-lysine-binding bromodomain pockets of all BET proteins, usually with little preference for BD1 or BD2. In several cases, crystal structures of the bromodomain-inhibitor complexes are established, revealing the contact interface involved and how the compounds mimic, at least partly, the natural acetyl-lysine ligand.

Four BET inhibitors are currently in early clinical trials for cancer indications, raising the hope that novel therapy options will soon be available for patients (Table 1.3). The oral compound I-BET762 (GlaxoSmithKline) was originally investigated in NMC and later in refractory hematological malignancies. OTX015 (OncoEthix) is tested orally in patients with hematological and selected solid malignancies, including recurrent glioblastoma multiform. CPI-0610 (Constellation Pharmaceuticals) is being evaluated orally in three phase I studies in patients with different hematological tumors including AML and MM. A study was initiated with the BET inhibitor TEN-010 (Tensha Therapeutics) which is tested subcutaneously in patients with solid tumors, including NMC.

Table 1.3 BET inhibitors in clinical development for cancer indications.
Adapted from (Jung, Gelato et al. 2015)

Compound	Company	Clinical phase	Indication	Identifier	Expected study completion
GSK 525762 (I-BET762)	GlaxoSmithKline	I/II I/II	NMC Hematological malignancies	NCT01587703 NCT01943851	12/2014 06/2015
OTX015	OncoEthix	I IB IIA	Hematological malignancies Selected advanced tumors Recurrent glioblastoma multiform	NCT01713582 NCT02259114 NCT02296476	07/2014 10/2016 10/2016
CPI-0610	Constellation Pharmaceuticals	I I I	Progressive lymphoma MM Acute leukemia, myelodysplastic syndrome, myelodysplastic/ myeloproliferative neoplasms	NCT01949883 NCT02157636 NCT02158858	05/2015 12/2015 12/2015
TEN-010	Tensha Therapeutics	I	Advanced solid malignancies	NCT01987362	10/2015

Surprisingly, it was observed that genes induced by the weak BET inhibitor RVX2135 (Resverlogix), were similar to those induced by the HDAC inhibitors vorinostat and panobinostat in Myc-induced murine lymphoma cells (Bhadury, Nilsson et al. 2014). This concept was described in NMC and called "the chemical equivalent of a smokescreen" (Maxmen 2012). It proposes that increasing histone acetylation upon HDAC inhibitor treatment would make NUT–BRD4 so busy reading acetylations elsewhere that it would overlook the oncogene regions. Vorinostat and panobinostat also induced cell-cycle arrest and cell death, and synergized with RVX2135 (Bhadury, Nilsson et al. 2014).

It has recently been discovered that several kinase inhibitors additionally exhibit a strong interaction with bromodomains and extensive screening showed that several compounds were also strong BET inhibitors (Ciceri, Muller et al. 2014). X-ray structures furthermore showed that these kinase inhibitors mimic the acetyl-lysine region and form similar hydrogen bonds inside the bromodomain pocket (Ember, Zhu et al. 2014). These unexpected findings suggest that part of the anti-tumor activity of kinase inhibitors may be due to an additional BET blocking activity.

BET inhibitors currently in development show promise as potent anticancer drugs against various solid and hematological malignancies. As BRD4 represents the best drug target for cancer therapy of the BET family, it will be crucial to thoroughly elucidate its mechanism of action in order to design more potent and specific BRD4 inhibitors.

2. Research outline

BRD4 is indispensable for cell proliferation, chromatin organization, and DNA damage repair. As outlined above, the interaction between BRD4 bromodomains and acetyl-lysine is essential for its cellular function. The goal of this study was to investigate systematically with several complementary methods the structural determinants of the interaction of BRD4 with its natural ligands and inhibitors.

To this end, the first aim was to obtain quantitative information on the interaction between the wild-type form of BRD4 bromodomains and acetylated peptides. The contribution to the binding of amino acid residues flanking the acetyl-lysines of the H4 N-terminal tail was analyzed in detail. Furthermore, the available co-crystal structures of BRD4 BD1 with acetylated H4 and with the BET inhibitor JQ1 were examined in light of the conservation of the residues involved across the bromodomain family. Amino acids whose mutation is likely to lead to measurable changes in binding affinity were selected and mutants were tested with biochemical and biophysical methods outside and inside the cell to obtain a classification of interacting residues based on their impact on the recognition of acetylated histone H4 or of JQ1.

The results should serve to advance the current understanding of the mechanisms underlying selective chromatin recognition by bromodomains and may help to guide the future design of more potent and specific BET inhibitors.

3. Materials and Methods

3.1. Materials

3.1.1. Equipment and materials

Table 3.1 Equipment and materials.
List of utilized equipment and materials with corresponding companies.

Name	Company
7900HT Fast Real-Time PCR System	Applied Biosystems
1000M polycarboxylate hydrogel sensor chips	Xantec
37°C incubator	Heraeus Instruments
6, 96-well culture plate clear	TPP
96-well culture plate white	Perkin Elmer
Biacore 2000	GE Healthcare
Biacore T200	GE Healthcare
Black microtiter plates	Greiner
Cell culture Flasks (25, 75, 162, 225 cm²)	Corning
Cells Incubator BBD 6220	Thermo Scientific
Centrifuge RC 5C Plus	Sorval
Countess cell counter	Invitrogen
E-Base	Invitrogen
E-Gel 1.2% agarose (GP)	Invitrogen
E-Gel 48 1% agarose (GP)	Invitrogen
E-Gel PowerBase v.4	Invitrogen
Electrophoresis Chamber	Bio-Rad
Heraeus Fresco 17 table centrifuge	Thermo Scientific
High-numerical-aperture (N. A. 1.3) 40x oil immersion objective	Zeiss GmbH
Inverted Zeiss Axio Observer, Z1 LSM710 microscope	Zeiss GmbH
LightSwitch Luciferase Assay Reagent	SwitchGear genomics
Microfluidizer	Microfluidics
Multifuge 3SR+	Thermo Scientific
Multitron II shacking 37°C incubator	Infors AG
Nanodrop	Thermo Scientific
NuPAGE 4-12% Bis-Tris Gel	Life technologies (Novex)
Parafilm M	Pechiney Plastic Packaging
PCR SoftStrips (0.2ml)	Eppendorf
PHERAstar FS microplate reader	BMG Labtech
Pipet filter tip (10µl, 2000µl, 1000µl)	Eppendorf
Pipetboy acu	Integra Biosciences
Pipettes	Eppendorf
Precision wipes	Kimtech Science
Reaction tubes (0.5ml, 1.5ml, 2ml)	Eppendorf
ReadyAgarose Wide Mini gels (8, 12, 20 wells)	Bio-Rad
Real-Time PCR System 7900HT Fast	Applied Biosystems
SA sensor chips	Biacore, GE Healthcare
Standard Power Pack P25	Biometra
Stripette (5, 10, 25, 50 ml)	Corning
SYNAPT G2-S mass spectrometer with an ESI ionization source	Waters
Tecan M1000	Tecan
Thermocycler Tetrad2	Bio-Rad
ThermoFluor system	Johnson & Johnson
Thermomixer Comfort	Eppendorf
UV light viewer	Biostep

Name	Company
Victor X3	Perkin Elmer
Vortex-Genie 2	Scientific Industries
Wide Mini-Sub Cell GT Systems	Bio-Rad

3.1.2. Chemicals, reagents and kits

Table 3.2 Chemicals and reagents.
List of utilized chemicals and reagents with corresponding companies.

Name	Company
Acetic acid	Sigma Aldrich
Ampicillin solution 100 mg/ml	Sigma
Anti-6His-XL665	CisBio
Anti-His D2	Cisbio
Blue Juice 10X	Invitrogen
BSA	Sigma
Calf Intestinal Alkaline Phosphatase (CIAP)	Invitrogen
CHAPS	Sigma
Coomassie Briliant Blue staining	Bio-Rad
DAPI (4',6-Diamidino-2-Phenylindole, Dihydrochloride)	Invitrogen
DMSO (Dimethyl Sulfoxide)	Sigma
DNA Ladder low and high Range, 1kb Plus	Invitrogen
Dual Glo Luciferase Assay System	Promega
EndoFree Plasmid Maxi Kit	Qiagen
Eu^{3+} cryptate-conjugated streptavidin	CisBio
Fugene HD Transfection Reagent	Promega
Glycerol	Sigma
HBS-P+	Biacore
HEPES pH 7.5	Applichem
Hispeed Plasmid Maxi Kit	Qiagen
His-trap columns	GE
Hot start Taq Master Mix kit	Qiagen
HTRF conjugate/lysis buffer	Cisbio
Imidazole	Sigma
Isopropyl-β-D-thiogalactopyranoside	Sigma-Aldrich
Kanamycin solution 50 mg/ml	Sigma
L-alanyl-L-glutamine	BioChrom AG
L-glutamine	Sigma-Aldrich
Lipofectamine 2000	Life Technologies
Methanol	Millipore
Mission LightSwitch Luciferase assay reagent	Switchgear genomics
NaCl	Sigma-Aldrich
Nanoluc detection system	Promega
Ni-NTA agarose	Macherey-Nagel
Ni-NTA Fast Start Kit	Qiagen
NuPAGE Sample Reducing Agent (10X)	Invitrogen
NuPAGE LDS Sample Buffer	Bio-Rad
NuPAGE MES SDS Running buffer 20X	Invitrogen
Paraformaldehyde	Sigma
Pluronic	Gibco, LifeTechnologies
Polyethylenimine	Polysciences
Potassium fluoride	Sigma
QIAprep Spin Miniprep Kit	Qiagen
Qiaquick gel extraction kit	Qiagen

Name	Company
QIAshredder	Qiagen
QIAquick PCR purification kit	Qiagen
QuickChange II XL Site-Directed Mutagenesis Kit	Agilent Technologies
Rapid DNA ligation Kit	Roche
Restriction enzyme AsuII=BstbI	New England Biolabs
Restriction enzyme BamHI	Roche
Restriction enzyme BglII	Roche
Restriction enzyme Bsu36I	Fischer
Restriction enzyme EcoRI	Roche
Restriction enzyme NheI	Roche
Restriction enzyme SalI	Roche
Restriction enzyme XbaI	Roche
Restriction enzyme XhoI	Roche
RNeasy Plus Mini Kit	Qiagen
Rotiphorese 10X TAE-Buffer	Carl Roth
Silicone oil DC200	Sigma Aldrich
Steadylite plus	Perkin Elmer
Streptavidin Eu chelate	W1024, Perkin Elmer
Superdex S75 26/60 column	GE
SuperScript III First-Strand Synthesis SuperMix for qRT-PCR	Invitrogen
Sypro Orange	Molecular Probe
TaqMan Fast Advanced Master Mix	Applied Biosystems
TCEP	CalBioChem
Tryptan Blue staining 0.4%	Invitrogen
Tween 20	Sigma
Ultra Pure Water	Biochrom
Vectashield Mounting medium for fluorescence	Vector Laboratories

3.1.3. Media

3.1.3.1. Bacteria media

The bacterial strains used in this work were cultured in LB (Luria Bertani) liquid medium: (tryptone, yeast extract, NaCl, NaOH) or solid medium (with agar) produced in the Quality Control Biology department of Bayer Healthcare.

3.1.3.2. Cell culture media

Table 3.3 Cell culture media.
The utilized eukaryote cell lines were cultured, washed, or stored using the following media.

Name	Company
DMEM	Biochrom
DMEM/Hams' F12 (1:1)	Biochrom
PBS Dulbecco (DPBS)	Biochrom
Fetal Bovine Serum (FBS)	Sigma
Sodium Pyruvate	GE Healthcare
Trypsin EDTA	GE Healthcare

3.1.4. Bacterial strains

Table 3.4 Bacterial strains.
Used *E. coli* strains with corresponding companies.

Name	Company
One Shot BL21(DE3)pLysS	Invitrogen
XL1-Blue competent cells	Stratagene
XL10-Gold ultracompetent cells	Stratagene

3.1.5. Human cell lines

The CAL-85-1 breast cancer cell line was obtained from the Deutsche Sammlung von Mikroorganismen und Zellkulturen GmbH (DSMZ), U-2 OS human bone osteosarcoma and HCT-116 human colon colorectal carcinoma cell lines were obtained from the American Type Culture Collection (ATCC). LAPC-4 human prostate cancer cells were kindly provided by Matthias Nees from the VTT Technical Research Centre of Finland.

3.1.6. Oligonucleotides

3.1.6.1. Mutation primers

Table 3.5 Mutation primers.
Mutants used in the TR-FRET, SPR, FP and Nano-BRET assays: Mutagenesis primers and their reverse sequence were synthesized by Eurofins MWG Operon.

Name	Sequence(5'-3')
W81A_for	CTATGGAAACACCAGTTTGCAGCTCCTTTCCAGCAGCCTGTGG
P82A_for	GGAAACACCAGTTTGCATGGGCTTTCCAGCAGCCTGTGGATG
L94A_for	GTGGATGCCGTCAAGCTGAACGCACCTGATTACTATAAGATCATT
Y97F_for	GTCAAGCTGAACCTCCCTGATTTCTATAAGATCATTAAAACGCCTATG
Y139F_for	CTATGTTTACAAATTGTTACATCTTCAACAAGCCTGGAGATGACATAG
N140A_for	GTTTACAAATTGTTACATCTACGCTAAGCCTGGAGATGACATAGTC
D144A_for	CATCTACAACAAGCCTGGAGCTGACATAGTCTTAATGGCAGAAG
D145A_for	CATCTACAACAAGCCTGGAGATGCTATAGTCTTAATGGCAGAAGCTC
I146A_for	CTACAACAAGCCTGGAGATGACGCAGTCTTAATGGCAGAAGCTCTGG
M149A_for	CCTGGAGATGACATAGTCTTAGCTGCAGAAGCTCTGGAAAAGCTC

3.1.6.2. Cloning primers

Table 3.6 Cloning primers.
The cloning primers are shown with the flanking restriction sites. The forward and reverse primer sequences are presented in 5' to 3' direction for cloning into the indicated vectors.

Name	Sequence(5'-3') with restriction site	target vector
H4_BamHI_for	GAATTGGGATCCTCTGGGCGAGGTAAAGG	pAD/pBD
H4_EcoRI_rev	GCGCGCGAATTCTCAACCGCCGAAACCATA	pAD/pBD
BRD4_BamHI_for	GAATTGGGATCCTCTGCGGAGAGCGGCCCTGGG	pAD/pBD
BRD4_XbaI_rev	GCGTCTAGATTAGGCAGGACCTGTTTCGGAGTC	pAD/pBD
BRD4_XhoI_for	CGGGCTCGAGCGGCGCGATCGCCATGTCTGCGGAGAGCGGC	pNL
BRD4_Bsu36I_rev	GCGTCTAGATTAGGCAGGACCTGTTTCGGAGTC	pNL
BRD4-1-545 _XbaI_rev	CGCTCTAGACTATTCCTTCTTGTCTTTCTCCTTTTTCTTTGG	pNL
BRD4-BD1_XbaI_rev	CGCTCTAGATCAGGAAACGCCAGGTTTTGCTGTCCC	pNL

Name	Sequence(5'-3') with restriction site	target vector
BRD4_for_EcoRI	GCG GAATTCATGTCTGCGGAGAGCGGC	pCMV6-XL4
BRD4s_rev_XbaI	GCGTCTAGATTAGGCAGGACCTGTTTCGGAGTC	pCMV6-XL4

3.1.6.3. Sequencing primers

Table 3.7 BRD4 sequencing primers.
The sequencing primers used for BRD4 sequencing after cloning or mutation are shown in the 5' to 3' direction.

Name	Sequence(5'-3')
BRD_seq1	AATAATAGCAGCAACAGC
BRD_seq2	GCTGGGAGGGGGCTTGCTC
BRD_seq3	GAGAGCTCCAGTGAGTCC
BRD_seq4	CTTCTTTTTTGACTTCGG
BRD_seq5	GAGCTGCCCCCTCACCTG
BRD_seq6	AGAGACCACTGCGTGCTG
BRD_seq7	CCCTCTGTGCAGCAGCAG
BRD_seq8	CTGCTGGGGTGGAGGC
BRD_seq9	CAGGAGCTGCGTGCTGCC
BRD_seq10	GGGTGAGTGGATCTTCTCC
BRD_seq11	TTCGAGCAGTTCCGCCGC
BRD_seq12	AGCGTGCTCGGCCTGAGCC
BRD_seq13	CTATTGTCAATATTTGAAG
BRD_seq14	CAATGTTTTGCCAGAAAATC
BRD_seq15	TGACTGGTTTTCTGTCCCC
BRD_seq16	GGCTGGGGTGTGGGGAAAG
BRD_seq17	CTCAGAGTGGTGCTCAAGAC
BRD_seq18	ATCATGATCTCGGTTTCTTC
BRD_seq19	GACCCAGACCCCTCAGCCG
BRD_seq20	CTGCTGCTCCTGGCGCCGAC
BRD_seq21	CAGAACGCACCGCCACCAGG
BRD_seq23	TGAGGAGCCGAGAGGACGAG

3.1.6.4. TaqMan® probes

Table 3.8 TaqMan® Gene Expression Assays used for quantitative PCR.

Gene symbol	name	reference
Hu Cyc	Cyclophilin A	4326316E
Myc	c-Myc	Hs00905030_m1
CCND1	Cyclin D1	Hs00765553_m1
FOSL1	FOS-like antigen 1	Hs04187685_m1
HEXIM1	Hexamethylene bis-acetamide inducible 1	Hs00538918_s1

3.1.7. Plasmid vectors

Table 3.9 Plasmid vector maps.
Plasmid vector origins and maps

Name	Source	plasmid map
pNIC28-Bsa4-BRD4#201	Structural Genomics Consortium (Oxford)	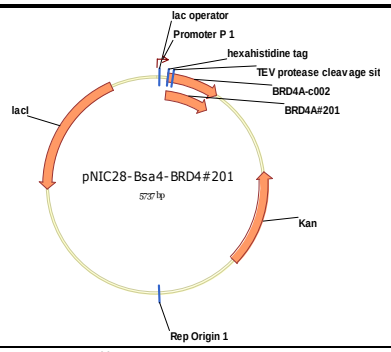
pcDNA6.2/N-EmGFP-BRD4	Structural Genomics Consortium (Oxford)	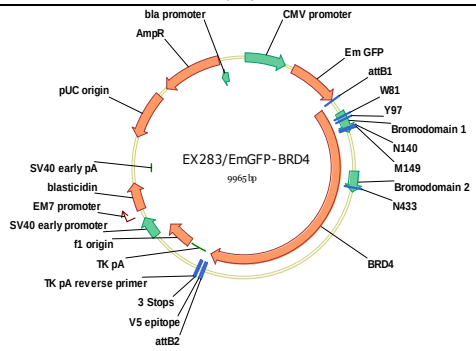
pAD	Mammalian Two-Hybrid Assay Kit (Agilent technologies)	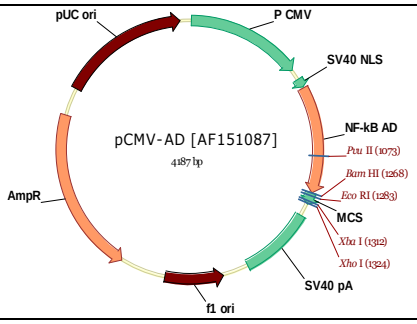
pBD	Mammalian Two-Hybrid Assay Kit (Agilent technologies)	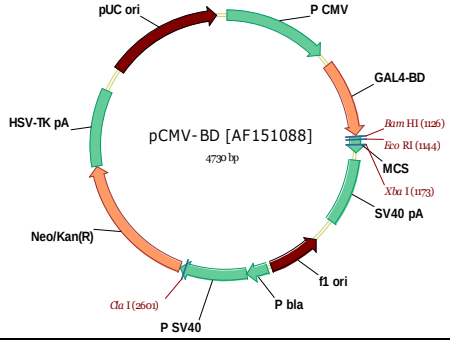

Name	Source	plasmid map
pFR-Luc	Mammalian Two-Hybrid Assay Kit (Agilent technologies)	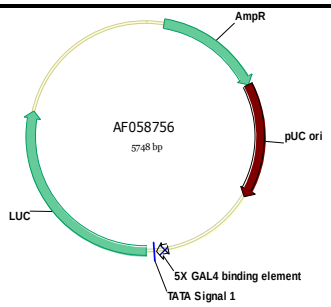
pNL-BRD4	Promega	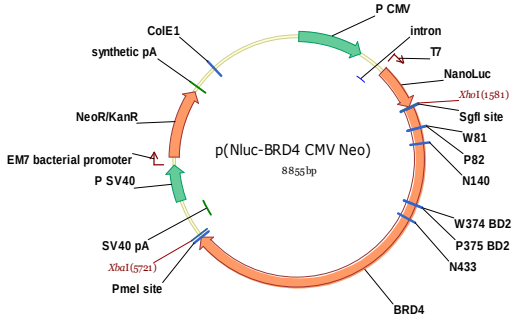
pH4-HaloTag	Promega	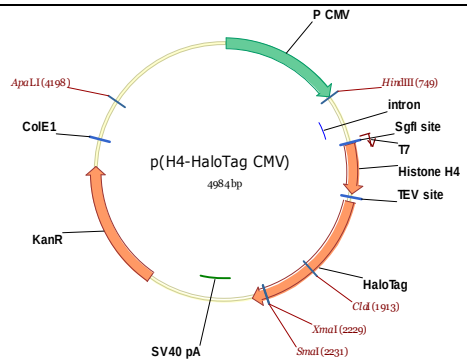
pCMV6-XL4-BRD4s	Origene 496978	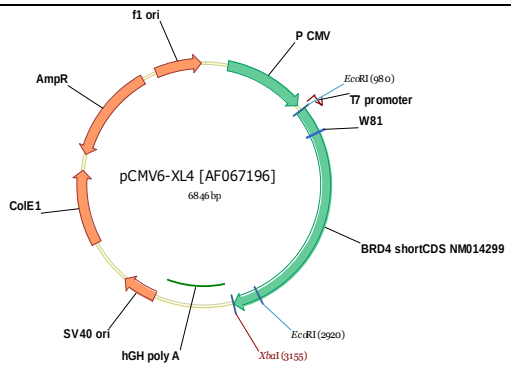
pLightSwitch	SwitchGear	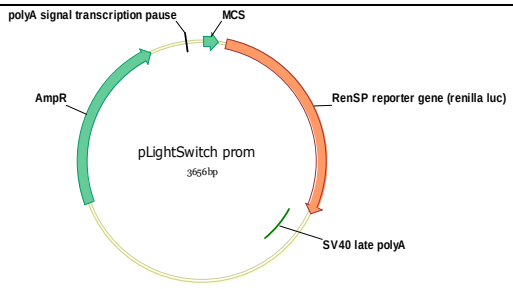

3.1.8. Peptides

Peptides corresponding to wild-type and mutant histone H4 (1-25) or to histone H3 (1-21) were synthesized and purified at Biosyntan and AnaSpec with or without a C-terminal biotin tag. Their purities (>90%) and identities were verified by liquid chromatography mass spectrometry (LC-MS).

Table 3.10 Peptide tails.
Sequences of modified peptide tails purchased from Biosyntan and Anaspec

Name	Sequence (^{1}a.a.^{n} + linker + label)	company
H4(ac)$_4$ K5K8K12K16	^{1}SGRGK(Ac)GGK(Ac)GLGK(Ac)GGAK(Ac)RHRKVLRDN^{25} GSGS - K(Biotin)	Biosyntan
H4 K5(ac)	^{1}SGRGK(Ac)GGKGLGKGGAKRHRKVLRDN^{25} GSGS - K(Biotin)	Biosyntan
H4 K8(ac)	^{1}SGRGKGG K(Ac)GLGKGGAKRHRKVLRDN^{25} GSGS - K(Biotin)	Biosyntan
H4 K12(ac)	^{1}SGRGKGGKGLGK(Ac)GGAKRHRKVLRDN^{25} GSGS - K(Biotin)	Biosyntan
H4 K16(ac)	^{1}SGRGKGGKGLGKGGAK(Ac)RHRKVLRDN^{25} GSGS - K(Biotin)	Biosyntan
H4 unacetylated	^{1}SGRGKGGKGLGKGGAKRHRKVLRDN^{25} GSGS - K(Biotin)	Biosyntan
H4 K5(ac)K8(ac)	^{1}SGRGK(Ac)GGK(Ac)GLGKGGAKRHRKVLRDN^{25} GSGS - K(Biotin)	Biosyntan
H4 K5(ac)K12(ac)	^{1}SGRGK(Ac) - GGKGLGK(Ac)GGAKRHRKVLRDN^{25} GSGS - K(Biotin)	Biosyntan
H4 K8(ac)K12(ac)	^{1}SGRGKGGK(Ac)GLGK(Ac)GGAKRHRKVLRDN^{25} GSGS - K(Biotin)	Biosyntan
H4 K12(ac)K16(ac)	^{1}SGRGKGGKGLGK(Ac)GGAK(Ac)RHRKVLRDN^{25} GSGS - K(Biotin)	Biosyntan
H4 K12(ac)K16(ac)K20(ac)	^{1}SGRGKGGKGLGK(Ac)GGAK(Ac)RHRK(Ac)VLRDN^{25} GSGS - K(Biotin)	Biosyntan
H4(ac)$_4$ unlabeled	^{1}SGRGK(Ac)GGK(Ac)GLGK(Ac)GGAK(Ac)RHRKVLRDN^{25} GSGS	Biosyntan
H3 K9(ac)K14(ac)	^{1}ARTKQTARK(Ac)STGGK(Ac)APRKQLA^{21} GGK(Biotin)	AnaSpec
H3 K9(ac)	^{1}ARTKQTARK(Ac)STGGKAPRKQLA^{21} GGK(Biotin)	AnaSpec
H3 K14(ac)	^{1}ARTKQTARKSTGGK(Ac) APRKQLA^{21} GGK(Biotin)	AnaSpec
H3 K27(ac)	^{21}ATKAAR-K(Ac)-SAPSTGGVKKPHRYRPG^{44}-GK(Biotin)	AnaSpec
RelA K310(ac)	^{301}EKRKRTYEFK(Ac)SIMKKSPFSG^{320} (Biotin)	AnaSpec
H4(ac)$_4$ S1A	^{1}AGRG K(Ac)GGK(Ac)GLGK(Ac)GGAK(Ac)RHRKVLRDN^{25}GSGS - K(Biotin)	Biosyntan
H4(ac)$_4$ G2A	^{1}SARGK(Ac)GGK(Ac)GLGK(Ac)GGAK(Ac)RHRKVLRDN^{25}GSGS - K(Biotin)	Biosyntan
H4(ac)$_4$ R3A	^{1}SGAGK(Ac)GGK(Ac)GLGK(Ac)GGAK(Ac)RHRKVLRDN^{25}GSGS - K(Biotin)	Biosyntan
H4(ac)$_4$ G4A	^{1}SGRAK(Ac)GGK(Ac)GLGK(Ac)GGAK(Ac)RHRKVLRDN^{25}GSGS - K(Biotin)	Biosyntan
H4(ac)$_4$ G6A	^{1}SGRGK(Ac)AGK(Ac)GLGK(Ac)GGAK(Ac)RHRKVLRDN^{25}GSGS - K(Biotin)	Biosyntan
H4(ac)$_4$ G7A	^{1}SGRGK(Ac)GAK(Ac)GLGK(Ac)GGAK(Ac)RHRKVLRDN^{25}GSGS - K(Biotin)	Biosyntan
H4(ac)$_4$ G9A	^{1}SGRGK(Ac)GGK(Ac)ALGK(Ac)GGAK(Ac)RHRKVLRDN^{25}GSGS - K(Biotin)	Biosyntan
H4(ac)$_4$ L10A	^{1}SGRGK(Ac)GGK(Ac)GAGK(Ac)GGAK(Ac)RHRKVLRDN^{25}GSGS - K(Biotin)	Biosyntan
H4(ac)$_4$ G11A	^{1}SGRGK(Ac)GGK(Ac)GLAK(Ac)GGAK(Ac)RHRKVLRDN^{25}GSGS - K(Biotin)	Biosyntan
H4(ac)$_4$ G13A	^{1}SGRGK(Ac)GGK(Ac)GLGK(Ac)AGAK(Ac)RHRKVLRDN^{25}GSGS - K(Biotin)	Biosyntan
H4(ac)$_4$ G14A	^{1}SGRGK(Ac)GGK(Ac)GLGK(Ac)GAAK(Ac)RHRKVLRDN^{25}GSGS - K(Biotin)	Biosyntan
H4(ac)$_4$ R17A	^{1}SGRGK(Ac)GGK(Ac)GLGK(Ac)GGAK(Ac)AHRKVLRDN^{25}GSGS - K(Biotin)	Biosyntan
H4(ac)$_4$ H18A	^{1}SGRGK(Ac) GGK(Ac)GLGK(Ac)GGAK(Ac)RARKVLRDN^{25}GSGS - K(Biotin)	Biosyntan
H4(ac)$_4$ R19A	^{1}SGRGK(Ac)GGK(Ac)GLGK(Ac)GGAK(Ac)RHAKVLRDN^{25}GSGS - K(Biotin)	Biosyntan
H4(ac)$_4$ K20A	^{1}SGRGK(Ac)GGK(Ac)GLGK(Ac)GGAK(Ac)RHRAVLRDN^{25}GSGS - K(Biotin)	Biosyntan
H4(ac)$_4$ V21A	^{1}SGRGK(Ac)GGK(Ac)GLGK(Ac)GGAK(Ac)RHRKALRDN^{25}GSGS - K(Biotin)	Biosyntan
H4(ac)$_4$ L21A	^{1}SGRGK(Ac)GGK(Ac)GLGK(Ac)GGAK(Ac)RHRKVARDN^{25}GSGS - K(Biotin)	Biosyntan
H4(ac)$_4$ R23A	^{1}SGRGK(Ac)GGK(Ac)GLGK(Ac)GGAK(Ac)RHRKVLADN^{25}GSGS - K(Biotin)	Biosyntan
H4(ac)$_4$ D24A	^{1}SGRGK(Ac)GGK(Ac)GLGK(Ac)GGAK(Ac)RHRKVLRAN^{25}GSGS - K(Biotin)	Biosyntan
H4(ac)$_4$ N25A	^{1}SGRGK(Ac)GGK(Ac)GLGK(Ac)GGAK(Ac)RHRKVLRDA^{25}GSGS - K(Biotin)	Biosyntan

3.1.9. Software

Table 3.11 Software used.

name	version	company
Schrödinger Release 2013-2: Maestro	version 9.5	Schrödinger, LLC, New York, NY, 2013
PyMol Molecular Graphics System	Version 1.3	Schrodinger, LLC;
Vector NTI	NTI 10	Life technologies
Thermofluor++	version 1.3.7	3-Dimensional Pharmaceuticals

name	version	company
GraphPad Prism	version 6.0	GraphPad
BIA evaluation software	2000 and T200	Biacore, GE Healthcare
Zen microscope control software	ZEN 2010	Zeiss GmbH
Microsoft Office	2010	Microsoft
Adobe Illustrator	CS5	Adobe

3.2. Methods

3.2.1. Site-directed mutagenesis

Point mutations were introduced into the pNIC28-Bsa4-BRD4#201 constructs using appropriate forward and reverse primers (Table 3.5) and the QuickChange II XL Site-Directed Mutagenesis Kit, following the manufacturer´s instructions. The generated products were digested with DpnI for 1 h at 37 °C, and transformed into XL10-Gold ultracompetent bacteria. Plasmid DNA was purified from individual colonies using the QIAprep Spin Miniprep Kit. Presence of the desired mutations was confirmed by DNA sequencing (SMB Services in Molecular Biology GmbH).

3.2.2. Protein expression and purification

3.2.2.1. Mutants expression

His_6-tagged protein domains BRD4 BD1 or BD2 wild-type were expressed and purified by the Protein Technologies department from the pNIC28-Bsa4-BRD4#201 construct. BRD4 mutants were expressed similarly, as described before (Filippakopoulos, Qi et al. 2010). Briefly, the expression plasmids were transformed into One Shot BL21(DE3)pLysS bacteria and grown overnight. Then the culture was diluted 1:1000 in fresh medium and cell growth was allowed at 37 °C to an optical density of about 0.5 (OD600) before the temperature was decreased to 18 °C. Protein expression was thereafter induced overnight at 18 °C in presence of 0.5 mM isopropyl-β-D-thiogalactopyranoside (IPTG).

3.2.2.2. Affinity chromatography purification

The mutated variants were purified by affinity chromatography using the Ni-NTA columns, following the instructions for purification under native conditions. For each mutant, both elution fractions contained in elution buffer were monitored by Sodium Dodecylsulfate Polyacrylamide Gel Electrophoresis (SDS-PAGE) and then pooled.

3.2.2.3. SDS-PAGE

The protein extraction fractions were collected and analyzed by SDS-PAGE: 13 µL of eluate were mixed with 2 µL reducing agent and 5 µL sample buffer. 15 µL of this sample solution were separated on a 4-12 % BisTris Gel in MES SDS Running buffer for 1 h at 200 V. SDS-PAGE gel was removed from

plastic and rinsed in deionized water and incubated for 1 h with Coomassie stain. The gel was then rinsed twice with deionized water and destained with destaining solution containing 80 % methanol and 20 % acetic acid for 2 hours with knotted wipes. The gel was then rinsed with water and scanned.

3.2.2.4. Size-exclusion chromatography purification

A second purification step using size exclusion chromatography with a Superdex S75 16/60 column was performed. The column was first washed with water and equilibrated with 1 column volume (120 ml) running buffer (10 mM HEPES pH 7.5; 150 mM NaCl; 0.5 mM TCEP). Affinity chromatography eluates were then manually injected in the column. Proteins were first eluted in running buffer in 0.5 mL fractions (W81A, P82A, L94A) and then in 1 ml fractions on a deep well 96-well plate, 1 ml being sufficient for appropriate separation. The proteins were detected by monitoring their UV absorbance (280 nm) during elution. Purity of the fractions corresponding to their absorbance peak was confirmed by SDS-PAGE.

3.2.2.5. LC-MS

LC-MS analysis of purified proteins confirming the presence of mutations was performed by the Protein Technologies department.

3.2.3. Cloning

For the generation of Mammalian two Hybrid constructs in pAD and pBD vectors, BRD4 short isoform cDNA (NM_014299), was amplified by Polymerase Chain Reaction (PCR) in a Thermocycler using Hot start Taq Master Mix kit following the manufacturer´s instructions. pcDNA6.2/N-EmGFP-BRD4 wt and mutants were used as template DNA with BRD4_BamHI_for and BRD4_XbaI_rev forward and reverse primers (Table 3.6), which respectively contained the BamHI and XbaI restriction sites. H4 cDNA was similarly amplified from H4 True clone (BC020884) with H4_BamHI_for and H4_EcoRI_rev primers (Table 3.6).

To generate pNL-BRD4 mutants and truncated variants, BRD4 sequences were amplified from pcDNA6.2/N-EmGFP-BRD4 wt and mutants using BRD4_XhoI_for coupled with BRD4_Bsu36I_rev, BRD4-1-545 _XbaI_rev or BRD4-BD1_XbaI_rev (Table 3.6).

pCMV6-XL4-BRD4s (BRD4 short isoform NM_014299) constructs were generated using pcDNA6.2/N-EmGFP-BRD4 wt and mutant with BRD4_for_EcoRI and BRD4s_rev_XbaI primers (Table 3.6).

Agarose gel electrophoresis on an E-gel using an electric current to separate the negatively charged DNA fragments according to their size was used to verify DNA amplification. When correct amplification of a DNA fragment was visualized, the DNA fragments were purified directly from the

PCR reaction mixture using the PCR purification Kit based on silica-gel-membranes which bind to DNA in high-salt buffer and elute it with low-salt buffer.

The resulting purified PCR products and the target vectors were further digested with enzymes recognizing the specific restriction sites (Table 3.2) at 37°C in the appropriate buffer, as recommended by the manufacturer.

To purify inserts and vectors after restriction enzyme cleavage ReadyAgarose gels were used for 1h30 at 90V in TAE buffer and the gel fragment containing the vector or insert were excised. The excised agarose gel fragments were weighed and purified using a Gel Extraction Kit following the manufacturer's instructions and based on the same principle as the PCR purification kit.
The digested vectors were then dephosphorylated by incubation with the Calf Intestinal Alkaline Phosphatase (CIAP) for 5 min at 37 °C to prevent re-ligation and CIAP was inactivated at 65°C for 15 min. The insert and the opened dephosphorylated plasmids were ligated using the Rapid DNA Ligation Kit. The product was then used to transform XL1-Blue supercompetent cells following the manufacturer's protocol.
Bacterial colonies were allowed to grow at 37 °C overnight on LB-Agar plates supplemented with the appropriate antibiotic corresponding to the resistance gene contained in the plasmid (100 µg/ml ampicillin or 50µg/ml kanamycin). The colonies were tested for the presence of plasmids with the expected insert by PCR using insert-specific primers (Table 3.7) and visualized on an agarose E-Gel. Positive clones were then amplified in 4 ml culture medium containing the appropriate antibiotic, the plasmid purified with the Plasmid Mini Kit and the insert sequenced (SMB Services in Molecular Biology GmbH).
Positive clones were further cultured in 200 ml LB medium containing the appropriate antibiotic and plasmids were purified with Plasmid Maxi Kit.

3.2.4. Binding experiments outside a cellular context

3.2.4.1. Crystal structures

The crystal structures of BRD4 in complex with the acetylated H4 K5(ac)K8(ac) peptide and JQ1 (PDB codes 3UVW and 3MXF, respectively) were downloaded from the RCSB protein databank (www.rcsb.org) and analyzed with the Maestro and PyMOL softwares.

3.2.4.2. Thermal Shift Assay (TSA)

In the TSA, 0.4 µg of BRD4 BD1 protein were mixed with 5x Sypro Orange and adjusted to a final volume of 5 µl with 100 mM HEPES buffer pH 7.5 and 150 mM NaCl. For binding experiments, 1%

DMSO or JQ1 in serial dilution (0.14 µM to 100 µM, 3-fold) were added to the mixture. In order to protect samples from evaporation, they were overlaid with 1 µl silicone oil DC200. Melting curves were recorded using a ThermoFluor system after heating the samples from 25 °C up to 95 °C while measuring the fluorescence intensity of the dye with the excitation and emission filters set to 465 nm and 590 nm, respectively. For data analysis, melting curves (fluorescence intensity changes at increasing temperatures) were fitted using a first derivative method (Brandts and Lin 1990) in order to determine the melting point Tm and the unfolding enthalpy ΔH_u using the evaluation software provided by the manufacturer of the instrument. A series of thermal melting curves were collected in presence of varying inhibitor concentrations. The heat capacity of protein unfolding (ΔCp_u) was assumed to be independent of the temperature and estimated from the size of the protein, using the following equation (Myers, Pace et al. 1995): ΔCp_u=-119+0.20(-907+93(#residues)). The standard enthalpy of binding (ΔH^o_b) was calculated as follows (Layton and Hellinga 2010): $\Delta H^o_b = \Delta H^o_{u(DMSO)} - \Delta H^o_{u(JQ1\ 100\mu M)}$. The difference of positive free energy of unfolding ($\Delta\Delta G_u$) was calculated for each inhibitor concentration using $\Delta\Delta G_{u(JQ1,T)} = \Delta H_{u(JQ1)}(1-Tm_{(DMSO)}/Tm_{(JQ1)}) + \Delta Cp_u[Tm_{(JQ1)}-Tm_{(DMSO)}+Tm_{(DMSO)} \ln(Tm_{(DMSO)}/Tm_{(JQ1)})]$ (Layton and Hellinga 2010). The extrapolated standard free energy change $\Delta\Delta G^o_u$ value in function of the JQ1 concentration was fitted using the GraphPad Prism software and the following equation to obtain estimate K_D^o values (Layton and Hellinga 2010): Y=-RTm$_{(DMSO)}$ln{1+[X-Pt-2*K_D^o+sqrt((X+Pt+2 K_D^o)^2)-(4*Pt*X))]/(2 K_D^o), R being the gas constant and Pt the BRD4 concentration.

Standard free energy of binding (ΔG^o) and entropy (ΔS^o) were calculated with the equations: $\Delta G^o = -RT*\ln(1/K_D^o)$ and $-T\Delta S^o = \Delta G^o - \Delta H^o_b$. In order to facilitate comparisons $d\Delta G^o$ was also calculated: $d\Delta G^o = \Delta G^o$ (mt) - ΔG^o (wt).

3.2.4.3. Time-Resolved Fluorescence Resonance Energy Transfer (TR-FRET)

The TR-FRET binding assay used to measure the interaction of BRD4 with acetylated peptides was a modified version of a previously described protocol (Nicodeme, Jeffrey et al. 2010). The experiments were performed in 384-well black small volume microtiter plates in a buffer composed of 50 mM Hepes, pH 7.5, 50 mM NaCl, 400 mM KF , 0.5 mM CHAPS and 0.05% BSA in a final volume of 5-10 µl (n = 4). BRD4 (100 nM) protein domains were mixed with 200 nM of the biotin-labeled histone peptides and incubated for 30 min at room temperature. The protein-peptide complexes at equilibrium were then detected with 5 nM of Eu^{3+} cryptate-conjugated streptavidin and 10 nM of anti-6His-XL665. To analyze the binding of mutated histone peptides at different ionic strengths, Streptavidin Eu chelate was used instead of cryptate as fluorescence donor, and KF was replaced by NaCl at concentrations of 20, 100 and 500 mM. After 3 h of further incubation at 4 °C, the plates

were measured in a PheraStar reader using the homogeneous time-resolved fluorescence (HTRF) module (excitation: 337 nm with 10 flashes, emission: 620 and 665 nm). The 665 nm / 620 nm ratios were converted to Delta F (Delta F (%) = (Ratio sample-Ratio background)*100/(Ratio background)) to normalize experiments performed at different days and with different readers.

For competition assays 50 nM BRD4 BD1 and 500 nM BD2 protein were pre-incubated with serial dilutions of the unlabeled H4 (1-25) K5(ac)K8(ac)K12(ac)K16(ac) tetra-acetylated peptide (15 nM to 250 µM, 2-fold) or with JQ1 (0.61 nM to 10 µM, 2-fold) for 30 min at room temperature. The plates were then processed as described above. IC_{50} values were calculated by plotting the log [Competitor / Inhibitor] vs. mean normalized response data from at least two independent experiments measured in triplicate and fitting it to a 4-parameter equation with variable Hill slope: Y = Bottom + (Top-Bottom)/(1+10^((LogIC_{50}-X)*Hill slope), using the GraphPad Prism software. The IC_{50} values obtained under these experimental conditions can be expressed as K_D (=Ki) based on the Cheng-Prusoff equation (Cheng and Prusoff 1973): Ki= IC_{50}/(1+[L]/K_D). Free energy of binding ΔG and dΔG were calculated as described above.

3.2.4.4. Surface Plasmon Resonance (SPR)

SPR interaction analyses were conducted on Biacore 2000 and T200 instruments using standard buffers and protocols (Biacore™ Assay Handbook, www.gelifesciences.com/biacore). For peptide binding assays, BRD4 BD1 and BD2 (50 µg/ml in 25 mM HEPES pH 7) were immobilized on 1000M polycarboxylate hydrogel sensor chips at densities varying between 2000 and 3000 RU using standard amine coupling methods based on EDC/NHS chemistry at densities varying between 2000 and 3000 RU. The analyte was an unlabeled tetra-acetylated H4 peptide flowed over the surface by injecting serial, 2-fold dilutions (0.16 to 20 µM) in running buffer (HBS-P+) over all surfaces at a flow rate of 30 µl/min. The association phase was followed during 60 s and the complexes were allowed to dissociate in buffer during 600 s before regenerating the surface with 1 M NaCl. The kinetic and steady-state data obtained were fitted to the Langmuir 1:1 and a single-site equilibrium binding equation using the BIA evaluation software.

A reverse set-up was also used to evaluate the binding of the BRD4 BD1 wt and mutants to histone tails. Briefly, SA sensor chips were coated by injecting a 10 µM solution of the biotinylated tetra-acetylated H4 peptide used for TR-FRET assays at a flow rate of 10 µl/min until capture levels of 1100-1200 RU were achieved. To validate the surface, the wild-type protein was titrated on the chip at concentrations varying from 0.02 to 20 µM and the affinity parameters for the interaction were calculated as described above. After confirming that the K_D was in agreement with known and reverse set-up values, all mutant and wild-type proteins were injected at a single concentration of 10 µM until equilibrium was established. Double referenced binding responses at equilibrium were used

to calculate the surface activity or binding percentage: % Binding = (RUeq/Rmax)*100, where Rmax describes the binding capacity of the surface: Rmax=((MW (analyte))/(MW (ligand)))*RL, and RL is the immobilization level of the ligand (H4 peptide in this case).

3.2.4.5. Fluorescence Polarization (FP)

The affinity of the BRD4 variants for JQ1 (tert-butyl[(6S)-4-(4-chlorophenyl)-2,3,9-trimethyl-6H-thieno[3,2-f][1,2,4]triazolo[4,3-a][1,4]diazepin-6-yl]acetate)) was estimated with an FP binding assay using the tetramethylrhodamine (TAMRA)-labeled JQ1 derivative 5-{[5-({[(6S)-4-(4-chlorophenyl)-2,3,9-trimethyl-6H-thieno[3,2-f][1,2,4]triazolo[4,3-a][1,4]diazepin-6-yl]acetyl}amino)pentyl]carbamoyl}-2-[6-(dimethylamino)-3-(dimethyliminio)-3H-xanthen-9-yl]benzoate.

The fluorescent probe was validated before, its ability to displace the H4 peptide in the TR-FRET assay described above was assessed beforehand and the K_D was found to be comparable to that of JQ1 (data not shown). For K_D determinations, 10 nM of the JQ1-TAMRA probe were incubated in 384-well small volume black microtiter plates with serial (1:2) dilutions of each BRD4 variant (0.61 nM to 10 µM) in a buffer containing 10 mM HEPES pH 7.5 (Applichem), 150 mM NaCl (Sigma), 0.005% Tween 20 (Sigma) and 0.5 mM TCEP (CalBioChem). After 30 min incubation at room temperature, the plates were measured in a Tecan M1000 plate reader using its FP module and excitation / emission wavelengths of 530 nm and 570 nm, respectively. For K_D determinations the background-corrected polarization values were plotted against the concentrations of BRD4 and the data were fitted to a one site binding equation: $Y=Bmax*X/(K_D + X)$, where Y is the specific and Bmax the maximal binding, using the GraphPad Prism software. Free energy of binding ΔG was calculated as described above.

3.2.5. Experiments in a cellular context

3.2.5.1. Thawing, culturing and seeding of cell lines

The thawing of cryo-preserved cells required their quick collection in 10 ml of pre-warmed appropriate culturing medium which was followed by a centrifugation step for 5 min at 300 g and room temperature to remove all residual DMSO. Afterwards the cells were resuspended in 12 ml of the recommended medium and transferred to a T75 flask. The cells were incubated for 24h in an incubator set to 37°C, 95% O2, 5% CO2 and 5% humidity, and the medium was replaced with fresh one after 24h. The cells were passaged when reaching 80-90% confluency and cultivated using 25 cm^2, 75 cm^2 and 162 cm^2 cell culture flasks. For passaging, the cells were washed using 10 ml DPBS and then treated with 0.5-2 ml trypsin. The cells were incubated for 2-5 min at 37 °C. Cell detachment was ensured via microscopy and the cells were diluted in fresh culture medium and transferred into new cell culture flasks using a dilution factor of 1:5 to 1:15, depending on doubling

times. For all experiments, viable cells were counted using the Countess and Tryptan Blue staining and plated at the desired cell densities.

3.2.5.2. Transfection

Plasmid transfections were carried out with FuGENE HD. Cells were seeded in 96-, or 6-well plates and the transfection was performed the day after using 3 µl reagent per 1 µg DNA. GFP was used in order to verify the transfection efficiency.

3.2.5.3. Fluorescence microscopy

U-2 OS cells were grown in 4-well chambers and transfected with 1 µg expression constructs encoding N-EmGFP-BRD4 (wild-type or mutants). Media was removed and cells washed twice with PBS. The cells were fixated with 4 % paraformaldehyde for 10 min at room temperature. Cells were washed 3 times with PBS and stained with DAPI (300 nM in PBS) for 5 min at room temperature. Then the chambers were washed with water and air-dried. Silicone sealing and plastic chambers were then removed. A coverslip was put on the slide with one drop of Vectiashield.

The imaging system consisted of a Zeiss LSM 710 with a 63x oil immersion objective. GFP fluorescence and DAPI imaging were carried out with an argon-ion laser of 365 and 488 nm, and filters to detect emission light of 445 and 525 nm respectively.

3.2.5.4. Mammalian two-hybrid assay

The assay utilizes hybrid genes to detect protein-protein interactions in mammalian cells via the activation of reporter-gene expression. The mammalian two-hybrid reporter plasmid, pFR-Luc (see Figure 3.1), contains a synthetic promoter with five tandem repeats of the yeast GAL4 binding sites that control expression of the luciferase gene. Luciferase reporter-gene expression occurs as a result of reconstitution of a functional transcription factor caused by the association of two-hybrid proteins.

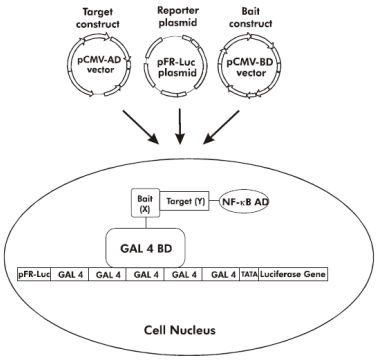

Figure 3.1 Schematic representation of the Mammalian Two-Hybrid Assay Kit.
Interaction between protein X (GAL4 BD-X fusion protein) and protein Y (NF-κB AD-Y fusion protein) brings the activation domain (AD) into close proximity with the DNA-binding domain (BD), resulting in activation of reporter gene expression through GAL4 binding sites.

The kit contains four control plasmids:

- The pBD-NF-κB control plasmid expressing the GAL4 DNA binding domain and the transcription activation domain of NF-κB as a hybrid protein.
- The pBD-p53 control plasmid expressing the GAL4 binding domain and amino acids 72–390 of murine p53 as a hybrid protein.
- The pAD-SV40T control plasmid expressing a hybrid protein which contains the NF-κB transcription activation domain fused to amino acids 84–708 of the SV40 large T-antigen.
- The pAD-TRAF control plasmid expresses the NF-κB transcriptional activation domain and amino acids 297–503 of TRAF.

H4 and BRD4 inserts were fused with NF-κB AD and GAL4 BD in pAD and pBD as described in section 3.2.3.

U-2 OS cells (8 x 10^3cells/well) were plated on a 96-well plate, allowed to attach and recover for 24 hours and then co-transfected with pFR-Luc and pAD and pBD (Table 3.9) containing the appropriate inserts, or control plasmids. One day after transfection 100 µL/well of steadylite Plus Luciferase substrate were added and plates incubated for 15 min at room temperature under light protection. Luminescence was then measured using the 420 Multilabel Counter VICTOR3 with a 1 sec reading time.

3.2.5.5. Nano-BRET assay

BRET (Bioluminescence Resonance Energy Transfer) is based on the efficient Resonance Energy Transfer between a bioluminescent donor moiety and a fluorescent acceptor moiety. BRET differs from FRET in that it uses luminescence generated during substrate conversion by luciferase as the energy donor. Here we used the NanoLuc™ (Nluc), a 19.1 kDa, ATP-independent luciferase that utilizes a coelenterazine analog (furimazine) to produce high intensity, glow-type luminescence. The HaloTag® Fusion Protein is 34.1 kDa protein from halophilic bacterial hydrolase to which the ligand covalently attaches. Using Nluc fused with BRD4 as the donor and HaloTag® fused with H4 and binding the acceptor ligand, we were able to monitor protein-protein interactions.

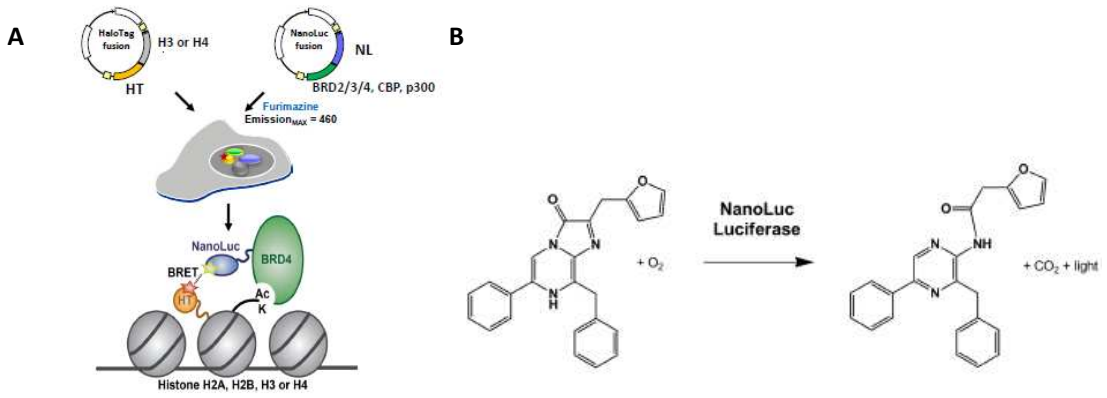

Figure 3.2 Schematic representation of the NanoBRET assay.
A. Assay principle B. NanoLuc™ (NL) utilizes a coelenterazine analog (furimazine) to produce high intensity, glow-type luminescence.

HCT-116 or U-2 OS cells (8 x 10^5cells/well) were plated on a 6-well plate, allowed to attach and recover for 4-6 hours at 37°C, 5% CO2 and then co-transfected with 2 µg Histone H4-HaloTag (Table 3.9) and 0.02 µg NanoLuc-BRD4 plasmids (Table 3.9) with 8 µl FuGENE HD in OPTI-MEM medium. Twenty hours post-transfection the cells were collected, cell density was adjusted to 2 x 10^5 cells/ml in OPTI-MEM medium with DMSO (control sample) or with 100 nM NanoBRET 618 fluorescent ligand (experimental sample), and then re-plated in a 96-well assay white plate. For inhibitor activity measurement JQ1 in DMSO was added at final concentrations between 0-10 µM and the plates were incubated for 4hrs at 37°C in the presence of 5% CO_2. Nano-Glo luciferase substrate was added to both control and experimental samples at a final concentration of 10 µM. Readings were performed within 10 minutes using the 420 Multilabel Counter VICTOR3 equipped with 510/60 nm and 660/100 nm bandpass filters with a 1 sec reading setting. A corrected BRET signal was calculated as the ratio of the emission at 610 nm/450 nm for experimental samples (i.e. those treated with NanoBRET fluorescent ligand) subtracted by the emission at 610 nm/450 nm for control samples. Corrected BRET ratios are expressed as milliBRET units (mBU), where 1 mBU corresponds to the corrected BRET ratio multiplied by 1000.

3.2.5.6. RNA extraction and reverse transcription

Cells were transfected or treated as indicated for each experiment, cell lysates homogenized using QIAshredder and total RNA extracted using the RNeasy Plus Mini Kit. The RNA concentration was measured using the Nanodrop device. To transcribe RNA into DNA, first-strand cDNA synthesis was performed starting with 0.5 to 4 µg of total RNA with the random primers using SuperScriptTM III reverse transcriptase.

3.2.5.7. Quantitative PCR

Quantitative real-time PCR (qPCR) allows to amplify and simultaneously quantify a targeted DNA molecule normalized to a constitutive housekeeping gene (here cyclophilin A). Sequence-specific DNA probes (TaqMan® Gene Expression Assays) consisting of oligonucleotides labelled with a fluorophore were used. qPCR quantification was performed on a Fast Real-Time PCR System using the standard cycling program (95 °C for 20 s, 40 cycles of 95 °C for 3 s followed by 60 °C for 30 s). The specific TaqMan gene expression assays used were purchased from Applied Biosystems (Table 3.8). As template 6 ng of cDNA per reaction was added.

For the interpretation of the qPCR results the "ΔΔCt method" was used: the cycle threshold (Ct) value of the gene of interest obtained for each sample was normalized to the Ct value of human cyclophilin A (ΔCt) and then to the control sample (ΔΔCt). Results are expressed as fractions ($2^{-\Delta\Delta Ct}$) in comparison to the control.

3.2.5.8. Luciferase transactivation assay

pLightSwitch vectors (Table 3.9) containing promoter regions (c-Myc, CCND1, FOS) cloned in front of the renilla luciferase (RenSP), or no promoter (empty luc) were used. Renilla Luciferase is an oxidative enzyme with bioluminescence activity. The expression results in a measurable light production after colenterazine administration which corresponds to the activity of the analyzed promoter. U-2 OS cells were seeded into 96-well plates at a concentration of 8,000 cells/per well. The next day, expression plasmids for wild-type BRD4 short isoform or mutant form (pCMV6-XL4-BRD4s 10, 50 or 100 ng/well) were co-transfected together with 100 ng/well plightswitch reporter vector harboring the promoters of interest or empty control. Measurement of luciferase emission light was carried out after 24 h in a Victor multilabel reader, following the addition of 100 µl light switch Reagent. For all points the average value of six wells treated in parallel was taken.

4. Results

4.1. BRD4 BD1 and BD2 binding to various acetylated peptides

Genome-wide analysis showed BRD4 binding to correlate with acetylation marks at positions H3K9, H3K27, H4K5 and H4K8 (Zhang, Prakash et al. 2012, Loven, Hoke et al. 2013). *In vitro* assays showed binding of full-length BRD4 or of individual BD1 and BD2 to different histone tails with various methods (Table 1.2) (Filippakopoulos and Knapp 2012). The first aim of the work was to obtain quantitative information on the interaction between the wild-type (wt) form of BRD4 bromodomains and acetylated peptides.

4.1.1. TR-FRET analysis of BRD4 BD1 and BD2 binding to acetylated peptides

The binding of purified BRD4 BD1 and BD2 to 14 peptides covering the H3 or H4 tails and containing one or several acetylated lysines was determined. In addition, the binding to one peptide derived from the acetylated region of RelA recently shown to interact with BRD4 was tested (Huang, Yang et al. 2009) (Fig. 4.1 A). The strongest binding signals were recorded for the interactions of BRD4 BD1 and BD2 with peptides bearing multiple acetylation sites, except for the H3K9(ac)K14(ac) and the H4K5(ac)K12(ac) peptides. On the other hand, only low binding to the mono-acetylated H3 and H4 peptides was observed (Fig. 4.1 A). No significant binding to RelA was observed. In several, but not all cases, better signals were detected for BD1 than for BD2.

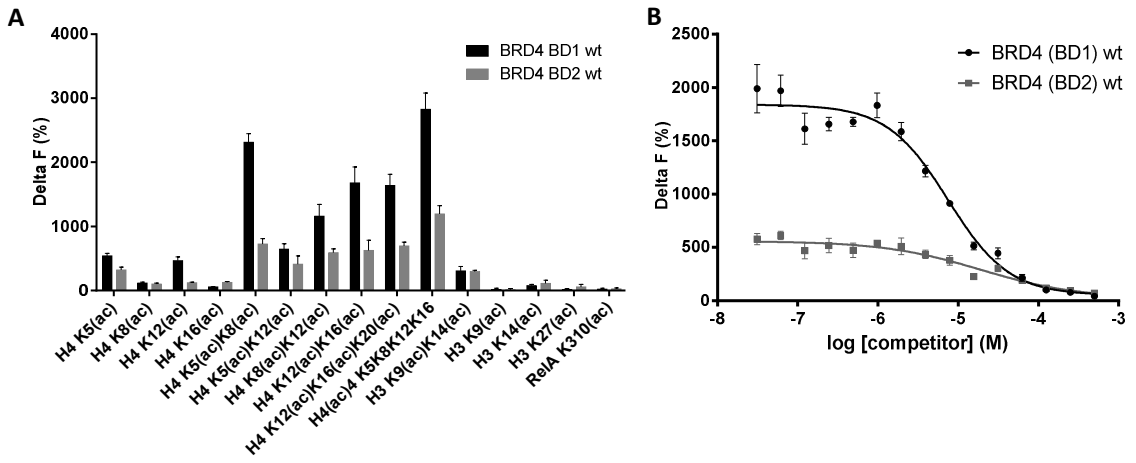

Figure 4.1 TR-FRET analyses of BRD4 BD1 and BD2 binding to acetylated peptides.
A. TR-FRET quantification of BRD4 BD1 and BD2 (100 nM) binding to acetylated peptides derived from H3, H4 or RelA (200 nM each).
B. Determination of BRD4 BD1 and BD2 affinities to H4 K5(ac)K8(ac)K12(ac)K16(ac) using a TR-FRET homogeneous competition assay. 200 nM biotinylated H4 peptide and 50 nM BRD4 BD1 or 500 nM BRD4 BD2 were titrated with unlabeled H4 peptide at the concentrations indicated. Delta F values were plotted against the concentrations of unlabeled peptide (competitor). The fitting of data to the 4-parameter equation served to calculate the dissociation constants (K_D) indicated in the text.

Based on the strong signal measured, the tetra-acetylated H4 peptide was selected for a more detailed study. It was used as a displacement probe in a competitive binding assay with the aim to compare in detail the affinities of the wild-type and mutant BRD4 bromodomains for this peptide. The exquisite sensitivity of the TR-FRET technology allowed the concentrations of BRD4 BD1 and BD2, and of the peptide to be kept far below the affinity constants previously reported for the interaction (Vollmuth, Blankenfeldt et al. 2009, Chung and Witherington 2011, Filippakopoulos, Picaud et al. 2012). Under these conditions, the non-biotinylated tetra-acetylated H4 peptide should quantitatively displace the fluorescent probe in a dose-dependent fashion and with an IC_{50} equivalent to the dissociation constant for the interaction (Cheng and Prusoff 1973). Using this experimental set-up dissociation constants of 4.8 µM and 30.6 µM were determined for BD1 and BD2, respectively (Fig. 4.1 B).

4.1.2. SPR analysis of BRD4 BD1 and BD2 binding to tetra-acetylated H4

In order to gain more insight into the binding mode and further validate the results described above, BRD4 BD1 and BD2 interactions with the H4 tetra-acetylated peptide were additionally analyzed using the SPR method. The binding sensorgrams obtained for both BRD4 bromodomains indicated fast equilibration kinetics for the interaction (Fig. 3.2) and the rates were often beyond the limits of what can be accurately measured by the reading instrument.

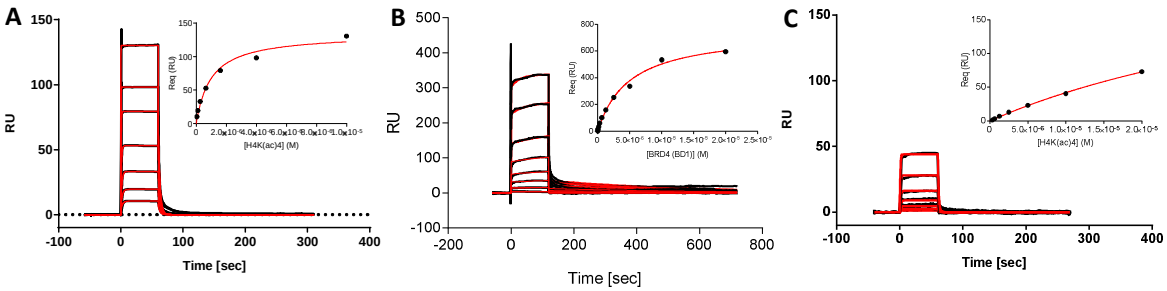

Figure 4.2 SPR analysis of BRD4 BD1 and BD2 binding to tetracetylated H4.
A. SPR sensorgram of the interaction between BRD4 BD1 (immobilized on a 1000M polycarboxylate chip) and histone H4 K5(ac)K8(ac)K12(ac)K16(ac).
B. SPR sensorgrams of the interactions between biotinylated H4K5(ac)K8(ac)K12(ac)K16(ac) captured on a SA chip with increasing concentrations of BRD4 BD1
C. SPR sensorgrams of the interaction between BRD4 BD2 (immobilized on a 1000M polycarboxylate chip) and histone H4 K5(ac)K8(ac)K12(ac)K16(ac)
The insets in A, B and C show SPR equilibrium resonance values plots, from which K_D values indicated in the text were calculated. Red lines represent the fit of the data to the Langmuir 1:1 and single-site equilibrium binding equations. All data represent the mean values of multiple replicates.

For BRD4 BD1, binding analyses through immobilizing the bromodomain or the acetylated histone on the chip surface (Fig. 4.2 A. and B. respectively) and plotting the steady-state responses at different analyte concentrations (insets Fig. 4.2) yielded full saturation curves from which $K_{D(eq)}$ values of 4.9

and 2.4 µM respectively were estimated. Immobilizing BRD4 BD2 and plotting the steady-state responses at different H4 K5(ac)K8(ac)K12(ac)K16(ac) concentrations yielded partial binding saturation curves from which $K_{D(eq)}$ values of 32.5 µM was estimated (Fig 4.2 C.). These values were in excellent agreement with the affinity constants measured in the TR-FRET competition assay.

4.1.3. Influence of amino acids neighboring acetyl-lysines on H4 recognition by BRD4

4.1.3.1. TR-FRET analysis of BRD4 BD1 binding to mutated H4

The TR-FRET assay described above was used to analyze in detail the binding of BRD4 BD1 to tetra-acetylated H4 mutated at different positions and in presence of different salt concentrations (Fig. 4.3). Altogether, the interaction of all H4 peptides with BRD4 BD1 was found to be strongly reduced at 500 mM NaCl concentration, compared to 20 and 100 mM. In order to determine whether the amino acids of the H4 peptide located around the acetyl lysine marks and which do not directly interact with the bromodomain pocket nevertheless had an impact on the interaction, these residues were individually mutated to alanine and the corresponding peptides evaluated for BRD4 BD1 binding.

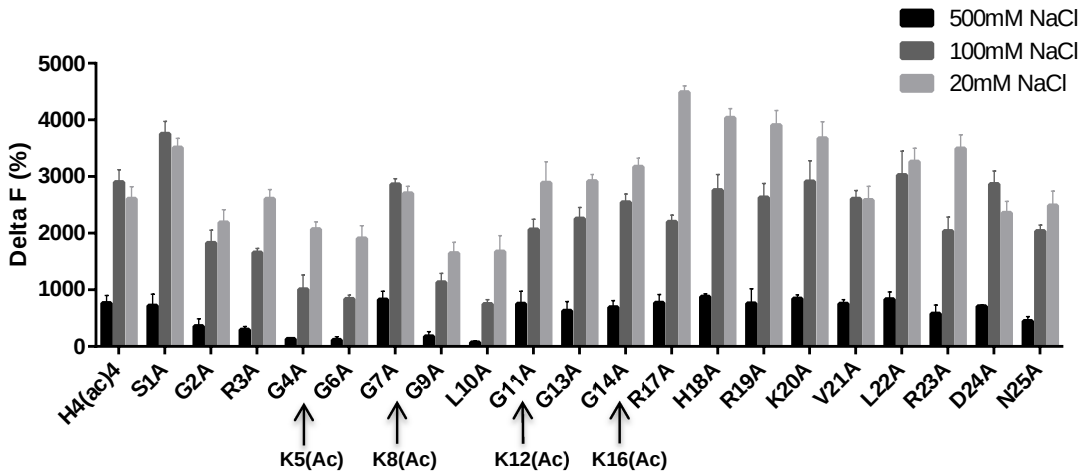

Figure 4.3 Alanine scanning of the tetra-acetylated H4 tail with BRD4 BD1.
The bar chart shows the average blank-subtracted TR-FRET delta F (%) values corresponding to the interaction of BRD4 BD1 (100 nM) at increasing concentrations of NaCl with tetra-acetylated histone H4 peptides (200 nM each) modified as indicated. The data represent the mean values of multiple replicates.

Changing the residues that flank acetylated K5 and K8 to alanine led to significantly weaker BRD4 BD1 binding, especially at high ionic strengths, with the notable exception of the G7 position (Fig. 4.3). In contrast, mutations at positions R17, H18, R19 or K20, L22 and R23 or at position S1 slightly strengthened the binding of BRD4 BD2 to the acetylated H4 peptide especially at low salt concentrations.

4.1.3.2. TR-FRET analysis of BRD4 BD2 binding to mutated H4

The same assay was used to analyze in detail the binding of BRD4 BD2 to the alanine mutated tetra-acetylated H4 (Fig. 4.4). The interaction of all H4 peptides with BRD4 BD2 was found to be reduced at 100 mM NaCl concentration compared to 20 mM and completely abolished at 500 mM.

Changing the residues that flank acetylated K5 to alanine led to weaker BRD4 BD2 binding at 100 mM NaCl, and mutations at positions G14, R17, H18, K20 or L22, or at position S1 strengthened the binding of BRD4 BD2 to the acetylated H4 peptide at 20 mM salt concentration.

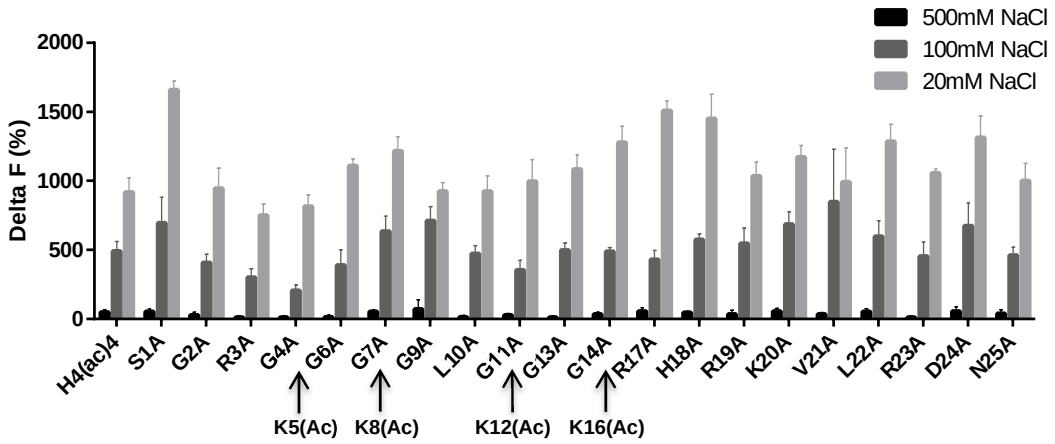

Figure 4.4 Alanine scanning of the tetra-acetylated H4 tail with BRD4 BD2.
The bar chart shows the average blank-subtracted TR-FRET delta F (%) values corresponding to the interaction of BRD4 BD2 (100 nM) at increasing concentrations of NaCl with tetra-acetylated histone H4 peptides (200 nM each) modified as indicated. The data represent the mean values of multiple replicates.

4.2. BRD4 bromodomain structure analysis and mutation

To better understand the binding mode of BRD4 BD1 and the precise contribution of each relevant amino acid, co-crystal structures were analyzed to decide which residues to select for a detailed mutational analysis.

4.2.1. BRD4 BD1 point mutants selection

The individual interactions of BRD4 BD1 with H4 K5(ac)K8(ac) (Fig. 4.5 A.) and with JQ1 (Fig. 4.5 B.) in the available co-crystal structures were examined in light of the conservation of the residues involved across the bromodomain family (Fig. 4.5 C.). This allowed selecting ten amino acids whose mutation is likely to lead to measurable changes in binding affinity (Fig. 4.6).

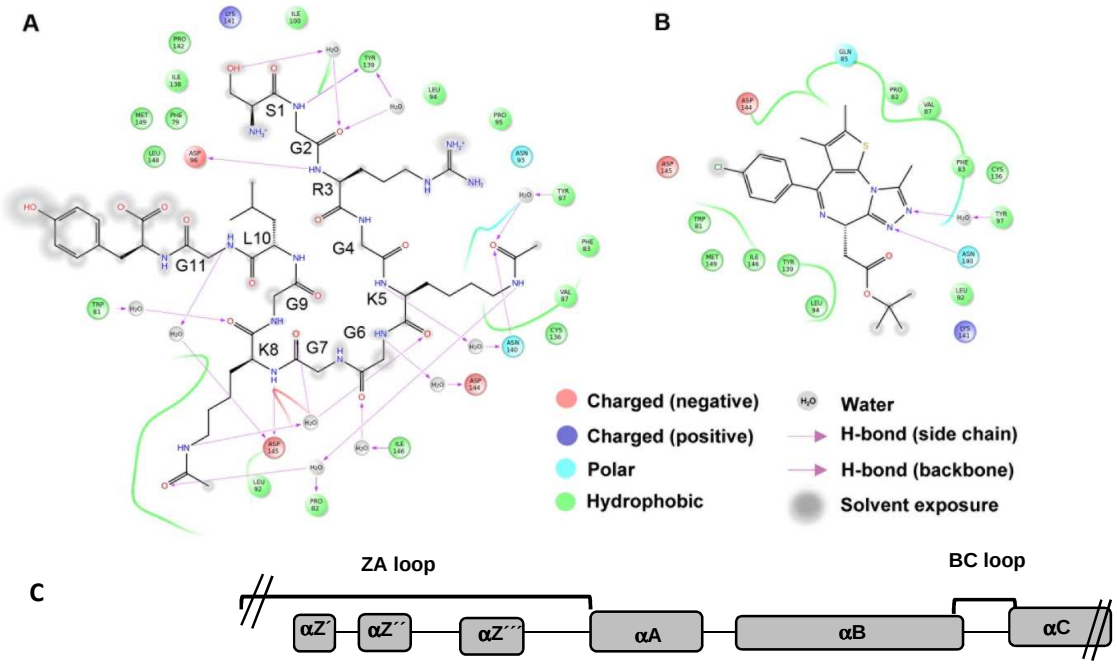


```
Inter_BD
hBRD4_BD1          81-150     WPFQQPVDAVKLNLPDYYKIIKTPMDMGTIKKRLENNYYWNAQECIQDFNTMFTNCYIYNKPGDDIVLMA
hBRD4_BD2         374-443     WPFYKPVDVEALGLHDYCDIIKHPMDMSTIKSKLEAREYRDAQEFGADVRLMFSNCYKYNPPDHEVVAMA
Interspecies
hBRD4_BD1          81-150     WPFQQPVDAVKLNLPDYYKIIKTPMDMGTIKKRLENNYYWNAQECIQDFNTMFTNCYIYNKPGDDIVLMA
mBRD4_BD1          92-161     WPFQQPVDAVKLNLPDYYKIIKTPMDMGTIKKRLENNYYWNAQECIQDFNTMFTNCYIYNKPGDDIVLMA
rBRD4_BD1          81-150     WPFQQPVDAVKLNLPDYYKIIKTPMDMGTIKKRLENNYYWNAQECIQDFNTMFTNCYIYNKPGDDIVLMA
dBRD4_BD1          81-150     WPFQQPVDAVKLNLPDYYKIIKTPMDMGTIKKRLENNYYWNAQECIQDFNTMFTNCYIYNKPGDDIVLMA
Inter_BET
hBRD4_BD1          81-150     WPFQQPVDAVKLNLPDYYKIIKTPMDMGTIKKRLENNYYWNAQECIQDFNTMFTNCYIYNKPGDDIVLMA
hBRD2_BD1          97-166     WPFRQPVDAVKLGLPDYHKIIKQPMDMGTIKRRLENNYYWAASECMQDFNTMFTNCYIYNKPTDDIVLMA
hBRD3_BD1          57-126     WPFYQPVDAIKLNLPDYHKIIKNPMDMGTIKRRLENNYYWSASECMQDFNTMFTNCYIYNKPTDDIVLMA
hBRDT_BD1          47-116     WPFQRPVDAVKLKLPDYYTIIKNPMDLNTIKKRLENKYYAKASECIEDFNTMFSNCYLYNKPGDDIVLMA
Inter_BRD
I     hPCAF        746-813     WPFMEPVK--RTEAPDYYEVIRSPMDLKTMSERLKNRYYVSKKLFMADLQRVFTNCKEYNAPESEYYKCA
II    hBRD4_BD1    81-150      WPFQQPVDAVKLNLPDYYKIIKTPMDMGTIKKRLENNYYWNAQECIQDFNTMFTNCYIYNKPGDDIVLMA
III   hCBP         110-179     LPFRQPVDPQLLGIPDYFDIVKNPMDLSTIKRKLDTGQYQEPWQYVDDVWLMFNNAWLYNRKTSRVYKFC
IV    hBRD7        155-222     AFFSFPVTDFIA--PGYSMIIKHPMDFSTMKEKIKNNDYQSIEELKDNFKLMCTNAMIYNKPETIYYKAA
V     BAZ2B     1887-1954      WPFLLPVN-LKL-VPGYKKVIKKPMDFSTIREKLSSGQYPNLETFALDVRLVFDNCETFNEDDSDIGRAG
VII   hTFIID_1  1403-1470      YPFHTPVNAKVVK--DYYKIITRPMDLQTLRENVRKRLYPSREEFREHLELIVKNSATYNGPESQYTKTA
VIII  hSMARCA4  1526-1582      ------------LPEYYELIRKPVDFKKIKERIRNHKYRSLNDLEKDVMLLCQNAQTFNLEGSLIYEDS
```

Figure 4.5 Conservation of key interacting residues within the bromodomain family.
A. Two-dimensional representation of BRD4 BD1 contacts with K5(ac)K8(ac) H4 region as seen in the three-dimensional structure of the complex (PDB-code 3UVW).
B. Two-dimensional representation of BRD4 BD1 interactions with JQ1 as seen in the three-dimensional structure of the complex (PDB-code 3MFX).
For A and B, properties of the interacting residues and nature of the interactions are indicated in the legend.
C. Alignment of selected bromodomain protein sequences. Bold characters indicate the residues that were mutated in the BRD4 BD1 sequence. Equivalent positions in other bromodomains are also in bold and highlighted in red when they are not conserved. Residues analyzed in previous works and mentioned in the introduction are underlined. Roman figures denote the different bromodomain subfamilies. No member of family VI is shown due to the low sequence conservation in the compared region. Secondary structure elements (α-helices) of human BRD4 are displayed above the sequence alignment. h, human; m, mouse; r, rat; d, drosophila.

Four out of the ten residues chosen are located in the ZA loop, namely the hydrophobic W81 and P82 which belong to the WPF shelf, and L94 and Y97, which face the binding pocket. Furthermore two residues in the αB helix were chosen, N140, which forms the key hydrogen bond interaction, but whose mutation in BRD3 intriguingly does not significantly affect binding to GATA1, and Y139. Finally

the positively charged D144 was selected in the BC loop, and D145 and I146 in the αC helix, which enclose the hydrophobic shelf, and M149, which may affect the ZA channel and the hydrophobic shelf, though not being directly part of the pocket.

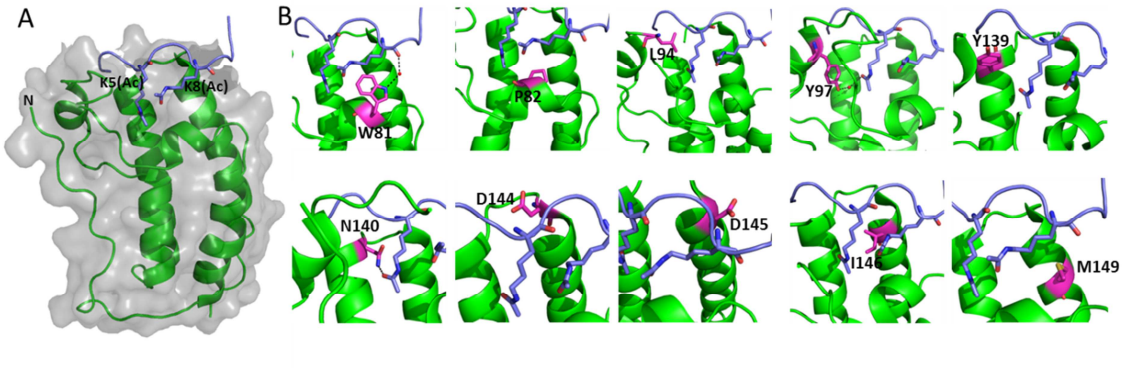

Figure 4.6 Position of selected mutations in the crystal structure of BRD4 BD1 in complex with the H4 K5(ac)K8(ac).
A. and B. Position of selected mutations in the crystal structure of BRD4 BD1 in complex with theH4 K5(ac)K8(ac). The BD1 region and the H4 tail are shown in green and slate blue, respectively.
A. Protein surface representation (grey) was added to visualize BRD4 BD1.
B. Residues chosen for mutation are shown in pink as sticks, hydrogen bonds as dotted line and water molecules as red spheres.

These ten amino acids are entirely conserved across BD1 in the BET family and play distinct roles in the interaction with histone H4 and JQ1 (Fig. 4.5. A and B). They are also found in BD2, with the exception of D144, D145, and I146 which are substituted for histidine, glutamic acid and valine, respectively (Fig. 4.5). These residues were individually mutated to alanine, except Y97 and Y139 which were mutated to phenylalanine, in order to keep the same overall conformation while eliminating the hydroxyl group that may undergo phosphorylation or be involved in hydrogen bonding.

4.2.2. BRD4 site-directed mutagenesis, and expression and purification of mutants

Mutants were produced similarly to wt BRD4 BD1 and BD2 in an *E. coli* strain bacteria stimulated with IPTG. Bacteria were lysed and His-tagged protein extracted by immobilized metal ion affinity chromatography purification using the Ni-NTA columns. After this first purification step, presence of mutants was confirmed by SDS-polyacrylamide gel electrophoresis (SDS-PAGE) at an expected mass (17.5 kDa).

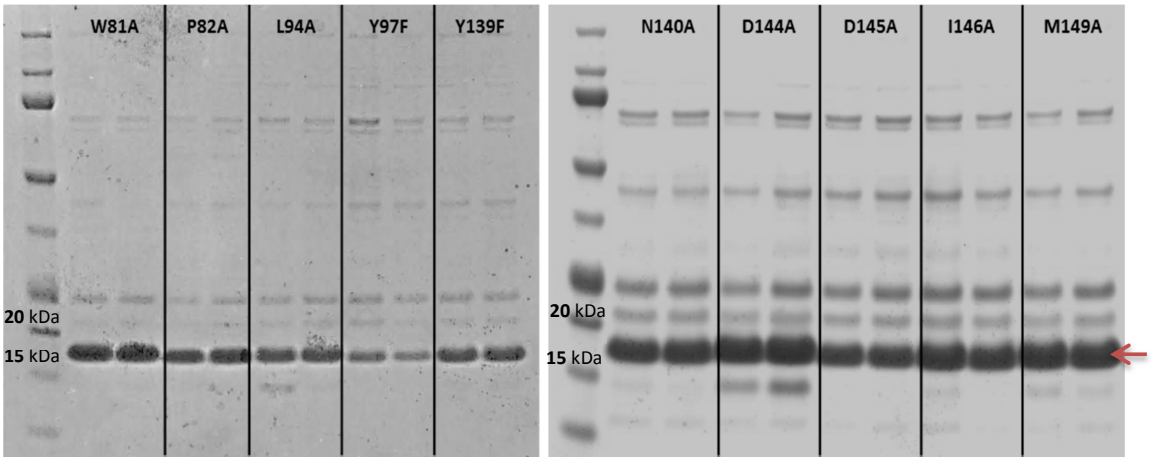

Figure 4.7 SDS-PAGE after immobilized metal ion affinity chromatography purification.
For each mutated protein, both elution fractions were collected and analyzed by SDS-PAGE. The red arrow indicates BRD4 BD1 variants at 17.5 kDa.

The expression yields of the mutants was unequal, BRD4 Y97F being the one with the lowest expression. The gel electrophoresis also indicated the presence of other proteins with different molecular weights that needed to be eliminated (Fig. 4.7).

A second purification step using size exclusion chromatography was then performed. The fractions were collected and monitored by SDS-PAGE, and the correctly purified fractions were pooled together (Fig. 4.8).

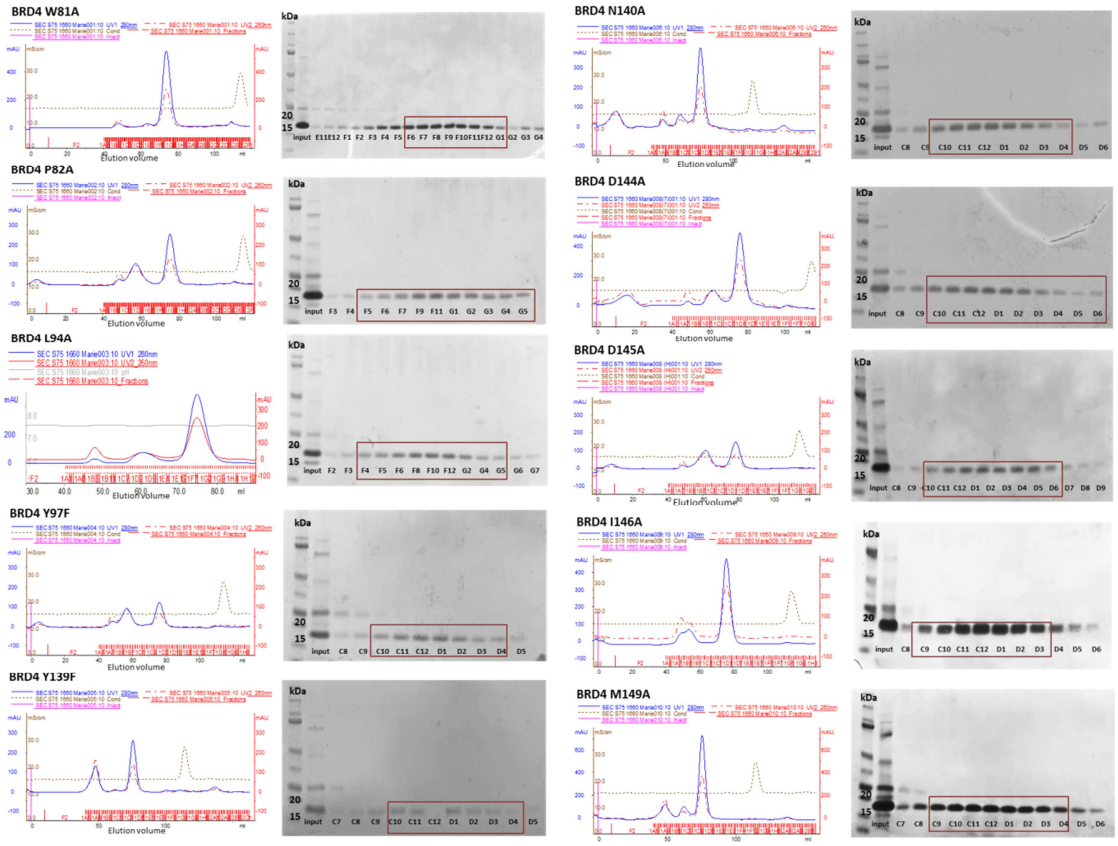

Figure 4.8 Size-exclusion chromatography elution profile of purified His-tagged BRD4 BD1 mutants. Purification from a Superdex 75 column at a flow rate of 1 ml/min. The first wells contain the ladder proteins and the second wells the samples before SEC purification (input). The proteins were eluted in 1mL fractions (except for W81A, P82A, L94A 0.5ml fractions). The fraction names correspond to the position on the 96-well plate. Red box indicates pooled fractions.

4.2.3. BRD4 BD1 mutants quality control

The exact mass of each BRD4 BD1 variant and the presence of the mutation were confirmed by LC-MS analysis in the Protein Technologies department.

Differential scanning fluorimetry/TSA melting curves of mutated and wild-type BRD4 BD1 domains were comparable, indicating correct folding (Fig. 4.9). However two mutants, namely Y97F and I146A showed less stability with lower melting temperatures than the wild-type BRD4 (BD1) which was only correlated to a lower expression yield for Y97F.

A

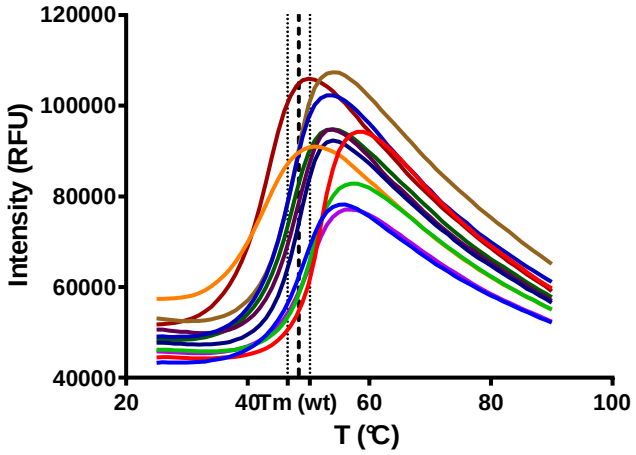

B

BRD4 BD1 variant	Melting temperature (°C)
BRD4 wt	48.4 ± 0.6
W81A	51.8 ± 0.4
P82A	50.1 ± 0.4
L94A	49.9 ± 0.5
Y97F	42.1 ± 0.8
Y139F	46.7 ± 0.3
N140A	47.3 ± 0.3
D144A	48.1 ± 0.4
D145A	47.7 ± 0.3
I146A	43.0 ± 0.3
M149A	46.9 ± 0.4

Figure 4.9 Folding analyses of BRD4 mutants.
A. Thermal Shift assay melting curves of BRD4 (BD1) wt (blue) and mutants. Melting temperature (Tm) of wt form with standard deviation is shown.
B. Tm of BRD4 BD1 variants extracted from the melting curves with standard deviations.

4.3. Affinity determinants for BRD4 chromatin recognition

4.3.1. BRD4 BD1 mutants binding to histone outside a cellular context

4.3.1.1. TR-FRET analysis of BRD4 BD1 mutants binding to H4 peptides

Binding of BRD4 BD1 mutants to H4 peptides was analyzed by TR-FRET as previously done for wild-type BD1 and BD2. Altogether, a reduction of the TR-FRET signals was observed for all mutants compared to the wild-type (Fig. 4.10 A). Like for the wild-type BD1, the strongest binding was generally observed for the tetra-acetylated H4 peptide and the di-acetylated H4 peptide harboring acetylated K5 and K8. Conversely, very weak or no binding was seen for all mono-acetylated H4 peptides. Among the mutant proteins, P82A, Y139F, D144A and I146A displayed the highest binding signals for the tetra-acetylated and most di-acetylated peptides. W81A, L94A, D145A and M149A had significantly reduced binding activity whereas Y97F and N140A showed the weakest interaction.

A

	BRD4 wt	W81A	P82A	L94A	Y97F	Y139F	N140A	D144A	D145A	I146A	M149A
unacetylated	3 ±9	3 ±9	-8 ±6	1 ±7	-6 ±5	-7 ±7	-6 ±1	-6 ±10	-7 ±10	-2 ±12	4 ±5
H4 K5(ac)	87 ±63	24 ±18	22 ±25	4 ±12	-4 ±5	38 ±20	0 ±61	4 ±24	1 ±8	-2 ±8	-1 ±9
H4 K8(ac)	16 ±8	12 ±9	11 ±7	6 ±12	9 ±7	9 ±14	7 ±7	15 ±16	15 ±7	7 ±9	7 ±8
H4 K12(ac)	86 ±11	34 ±14	27 ±10	0 ±14	0 ±12	6 ±1	6 ±5	1 ±8	6 ±5	-4 ±5	4 ±8
H4 K16(ac)	-7 ±14	-5 ±7	-6 ±4	-8 ±6	-7 ±16	-6 ±12	-3 ±8	-12 ±8	-2 ±9	-15 ±13	-14 ±7
H4 K5(ac)K8(ac)	2463 ±104	311 ±86	1166 ±129	453 ±78	146 ±33	1490 ±218	159 ±29	737 ±43	210 ±17	1048 ±133	270 ±69
H4 K5(ac)K12(ac)	309 ±21	203 ±45	177 ±97	38 ±21	6 ±9	106 ±86	7 ±12	105 ±56	73 ±18	15 ±9	40 ±9
H4 K8(ac)K12(ac)	431 ±11	251 ±41	228 ±34	36 ±16	13 ±5	140 ±36	2 ±5	148 ±39	111 ±29	30 ±6	125 ±65
H4 K12(ac)K16(ac)	548 ±12	67 ±10	169 ±18	44 ±13	-8 ±7	36 ±21	-11 ±8	578 ±68	73 ±34	24 ±92	42 ±25
H4 K12(ac)K16(ac)K20(ac)	861 ±65	192 ±39	331 ±87	337 ±30	21 ±7	190 ±26	24 ±7	761 ±39	255 ±32	162 ±18	151 ±21
H4 K5(ac)K8(ac)K12(ac)K16(ac)	2763 ±237	725 ±56	1440 ±91	851 ±192	246 ±44	1543 ±115	271 ±61	1547 ±145	767 ±59	1230 ±127	554 ±68

<11
11-50
51-500
501-1000
1001-2000
>2000

B

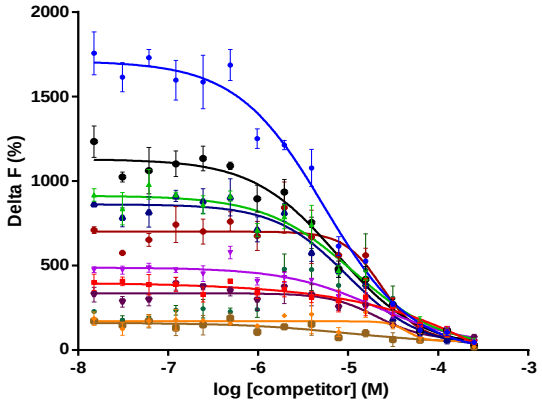

C

BRD4 BD1 variant	K_D (µM)	ΔG (kJ mol^{-1})
BRD4 wt	4.8 ± 0.4	-30.4
W81A	52.2 ± 5.0	-24.4
P82A	11.2 ± 0.7	-28.3
L94A	39.8 ± 15	-25.1
Y97F	n.i.	
Y139F	8.5 ± 1.4	-28.9
N140A	n.i.	
D144A	6.9 ± 2.9	-29.5
D145A	23.8 ± 3.3	-26.4
I146A	17.1 ± 9.8	-27.2
M149A	~72.7 ± 10	~-23,6

Figure 4.10 Binding analysis of BRD4 BD1 mutants to acetylated peptides by TR-FRET.
A. TR-FRET delta F (%) quantification (±SD) of BRD4 BD1 (wild-type and mutants, 50 nM each) binding to different acetylated H4 histone tails (200 nM each).
B. Determination of BRD4 BD1 affinity to H4 K5(ac)K8(ac)K12(ac)K16(ac) with a TR-FRET homogeneous competition assay. 200 nM biotinylated H4 peptide and 50 nM protein were titrated with unlabeled H4 peptide at the concentrations indicated. Delta F values were plotted against the concentrations of unlabeled peptide (competitor). The fitting of the normalized data (not shown) to the 4-parameter equation described in the method section (colored lines) served to calculate the K_D values indicated in the table C. All data represent the mean values of multiple replicates each.
C. Mean values of the affinity parameters derived from TR-FRET (±SD) are listed. Values not shown could not be interpreted (n.i.).

In order to confirm that the reduced TR-FRET signals at single concentrations of protein and peptide were an indicator of affinity decrease, the previously established TR-FRET competition assay for a precise quantification of the K_D values was used. As expected, the P82A, Y139A, D144A and I146A mutations had only a limited impact on the affinities in comparison to the wild-type protein. The affinities of D145A and L94A were more markedly reduced (5- and 8-fold, respectively) whereas for the W81A and M149A mutants the affinities were less than 10-fold that of the wild-type form (Fig. 4.10 B. and C.). The affinities of Y97F and N140A could not be quantified reliably due to the small dynamic window of the competition assay for these mutants.

4.3.1.2. SPR analysis of BRD4 BD1 mutants binding to tetra-acetylated H4

The above-described results were further confirmed by SPR analysis with immobilized H4 K5(ac)K8(ac)K12(ac)K16(ac) peptide, the surface having previously been validated with the wild-type BRD4 BD1 (Fig 4.2. B). The RU and % surface activity (= % binding) values obtained from the injection of a single concentration (near K_D) of wild-type or mutated bromodomain were therefore considered to be a *bona fide* estimate of the affinity of the protein for the immobilized peptide.

A

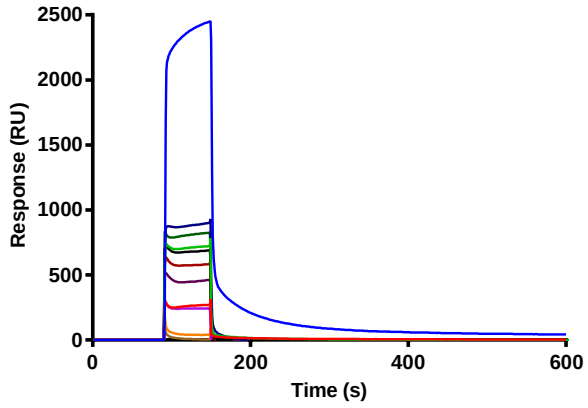

B

BRD4 BD1 variant	Binding (%)
BRD4 wt	100
W81A	10.8
P82A	29
L94A	9.7
Y97F	1.6
Y139F	27.8
N140A	0.2
D144A	36.5
D145A	18.7
I146A	23.8
M149A	34

Figure 4.11 Binding analysis of BRD4 BD1 mutants to acetylated peptides by SPR.
A. SPR sensorgrams of the interaction of BRD4 BD1 (wild-type and mutants, 10 µM each) with a biotinylated H4 K5(ac)K8(ac)K12(ac)K16(ac) peptide captured on a Biacore SA chip.
B. Surface activity (= % binding) compared to wt derived from SPR sensorgrams are listed.

In these experiments, all mutants showed a reduced interaction compared to the wild-type form. The effects were most pronounced for W81A, L94A, Y97F and N140A for which the remaining binding was roughly 10 % or less (Fig. 4.11).

4.3.2. BRD4 BD1 mutants chromatin binding analysis in a cellular context

4.3.2.1. BRD4 wild-type and mutants cellular localization and mobility

To state the cellular localization of BRD4 full-length protein wild-type and mutated form EmGFP-tagged plasmids fused with BRD4 were transfected in osteosarcoma U-2 OS cells and observed by fluorescence microscopy. BRD4 asparagine mutant was used, the asparagine being mutated to alanine in both BRD4 bromodomains (N140A in BD1 and N433A in BD2).

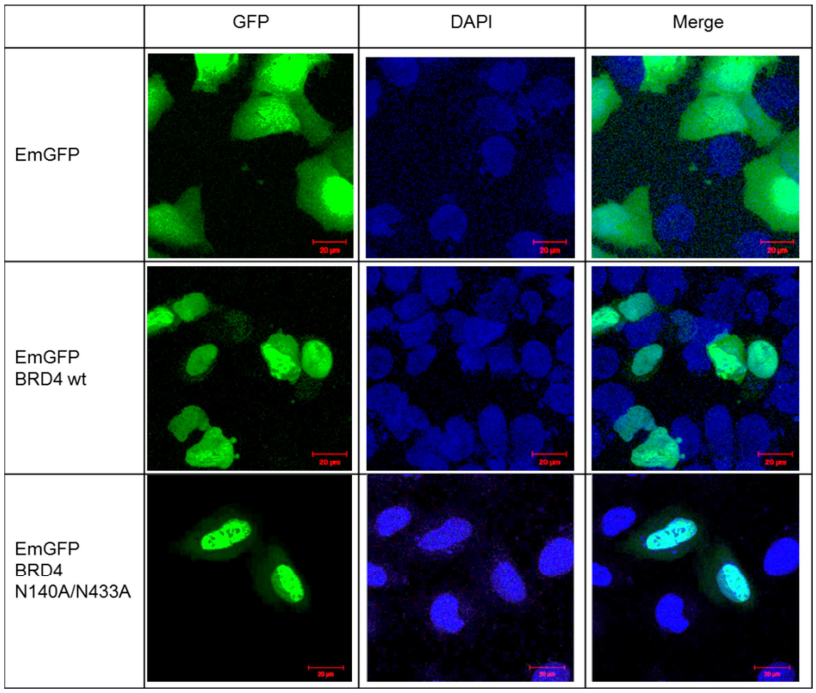

Figure 4.12 Cellular localization of BRD4 wt and asparagine mutant.
U-2 OS cells transfected with EmGFP fused with indicated inserts, followed by fixation and DAPI staining. All pictures were taken at 63x magnification using confocal microscopy. DAPI is shown in blue, EmGFP in green.

EmGFP control plasmid showed fluorescence in the nucleus and cytoplasm of transfected U-2 OS cells. EmGFP-tagged BRD4 wild-type and the N140A/N433A form both showed only nuclear expression of the fused protein.

Fluorescence recovery After Photobleaching (FRAP) experiments were performed by M. Philpott in Oxford to assess the intracellular mobility of the most impaired BRD4 mutants in their recognition of acetylated histone H4 peptides in biochemical assays, namely those with mutated W81, Y97, N140 and M149 (Jung, Philpott et al. 2014). All BRD4 BD1 and BD2 mutants showed a quicker recovery of fluorescence intensity than the wild-type protein in the cell nuclei, indicative of displaced and freely diffusing proteins. For all mutants, the enhanced half-fluorescence recovery was comparable to that seen for BRD4 wild-type in JQ1-treated cells.

4.3.2.2. Two-hybrid analysis of BRD4 interactions

Mammalian two-hybrid assay allows detection of protein-protein interactions in a cellular context. When interacting, fused proteins create a functional transcription activator by bringing the activation domain into close proximity with the DNA-binding domain. This can be detected by expression of the luciferase reporter gene.

Luciferase reporter plasmid (pFR-luc) was transfected in U-2 OS cells with 2, 20 or 80 ng pBD-NF-κB positive control plasmid expressing the GAL4 DNA-binding domain and the transcription activation

domain of NF-κB as a hybrid protein. The maximal induction of the luciferase reporter gene was already reached with 2 ng pBD-NF-κB plasmid (Fig. 4.13 A).

The pBD-p53 control plasmid expresses the GAL4 binding domain and amino acids of murine p53 as a hybrid protein. The pAD-SV40T control plasmid expresses a hybrid protein which contains the NF-κB transcription activation domain fused to amino acids of the SV40 large T-antigen. The pBD-p53 and pAD-SV40T plasmids, whose expressed proteins interact *in vivo*, were used as positive control to verify that induction of the luciferase reporter gene could occur (Fig. 4.13 B.).

The pAD-TRAF control plasmid expresses the NF-κB transcriptional activation domain and amino acids of TRAF. The pBD-p53 and pAD-TRAF control plasmids, expressing proteins which do not interact *in vivo*, were used as negative control to verify that the luciferase gene was not induced in the absence of an interaction (Fig 4.13 B.).

At all three concentrations (2, 20 or 80 ng pAD and pBD plasmid) the difference between positive and negative controls relative light units showed a good assay window especially with 20ng plasmids (Fig. 4.12. A and B).

BRD4 and H4 were respectively fused with both the DNA-binding domain of the yeast protein GAL4 in a pBD vector and with the transcriptional activation domain of the mouse protein NF-κB in a pAD vector. In this assay, BRD4 and H4 showed only background interaction with an emission light below the negative control in both fused configurations. Nevertheless it could be observed that BRD4 fused with the yeast protein GAL4 mouse (pBD-BRD4) and H4 with NF-κB (pAD-H4) resulted in a higher signal (Fig. 4.12. C).

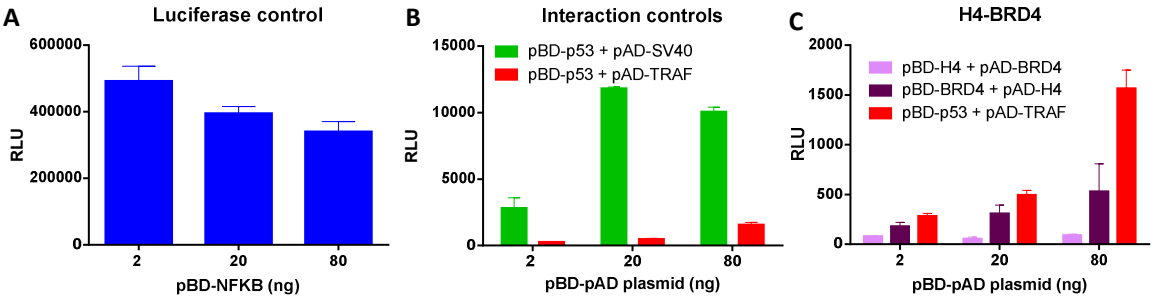

Figure 4.13 Mammalian two-Hybrid assay: H4-BRD4 interaction.
50ng reporter gene was transfected with 2, 20 or 80 ng pCMV-AD (abbreviated pAD) and pCMV-BD (abbreviated pBD) plasmid in U-2 OS cells. The amount of light, as measured by the luminometer, is expressed in Relative Light Units (RLU).
A. Luciferase emission control after pBD-NF-κB and pFR-luc cotransfection
B. Positive (pBD-p53 + pAD-SV40) interacting and negative non-interacting control (pBD-p53 + pAD-TRAF) co-transfected with luciferase reporter plasmid.
C. BRD4-H4 interaction (pBD-H4 + pAD-BRD4 and pBD-BRD4 + pAD-H4) compared to negative control.

Further, 20 ng pAD and pBD plasmids, which previously showed the better assay window using control vectors (Fig 4.12. B.) were co-transfected with 50 or 100 ng pFR-Luc reporter plasmid. In addition, both BRD4 fused p-AD and p-BD plasmids were also co-transfected.

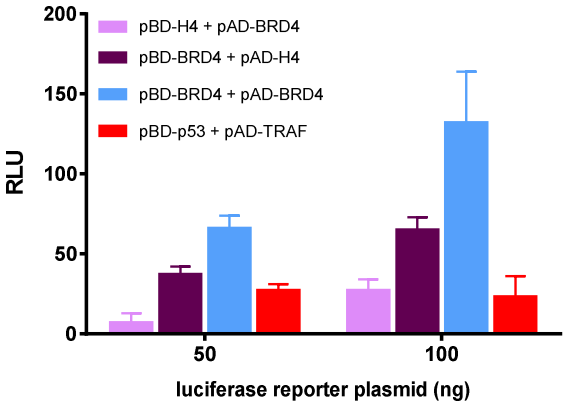

Figure 4.14 Mammalian two-hybrid assay: BRD4 homodimerization.
U-2 OS cells were transfected with 20 ng p-AD and 20 ng p-BD with inserts indicated in the legend, and with 50 or 100 ng luciferase reporter plasmid (pFR-Luc). The amount of light, as measured by the luminometer, is expressed in Relative Light Units (RLU).

Doubling the transfected luciferase reporter plasmid doubled the luciferase emission induced by interacting proteins except for the negative control plasmids expressing non interacting proteins which induced a constant low luciferase emission. Like in the previous two-hybrid experiment, the transfection of pBD-BRD4 and pAD-H4 showed a higher signal than pAD-BRD4 and pBD-H4. This interaction induced a weak luciferase emission with 50 ng luciferase reporter plasmid, but higher than the negative control with 100 ng pFR-luc plasmid.

Furthermore, an interaction between AD-BRD4 and BD-BRD4 could be observed at both reporter plasmid concentrations confirming the possibility of a BRD4 homodimerization.

4.3.2.3. Nano-BRET analysis of BRD4 variants binding to H4

BRET (Bioluminescence Resonance Energy Transfer) is based on the efficient Resonance Energy Transfer between a bioluminescent donor moiety and a fluorescent acceptor moiety. Here we used the NanoLuc (Nluc), a 19.1 kDa luciferase to produce high intensity luminescence and the HaloTag Fusion Protein, a 34.1kDa protein for covalent attachment of the acceptor substrate. When the donor (Nluc) and acceptor (substrate binding to HaloTag) are in close proximity, the energy resulting from catalytic degradation of the coelenterazine derivative substrate is transferred to the substrate, which will then emit fluorescence at its characteristic wavelength (Fig 3.2). Both emissions are measured at different wavelengths and a corrected BRET ratio is calculated as indicated in section 3.2.5.5 indicating the level of protein-protein interaction.

Nano-BRET using Nluc and HaloTag fused respectively with BRD4 and H4 allowed the direct monitoring of protein-protein interaction in the cell. This method was used to compare the binding

of different BRD4 constructs to the H4 peptide in a cellular context. The corrected BRET ratio was constant in different cell lines and independent of the Nanoluc-BRD4 protein expression level which can be monitored by donor emission measurement. To test the influence on binding to H4 of different regions, truncated BRD4 variants were also produced. Two BRD4 point mutants were also tested namely N140A and W81A (Fig 4.15 A).

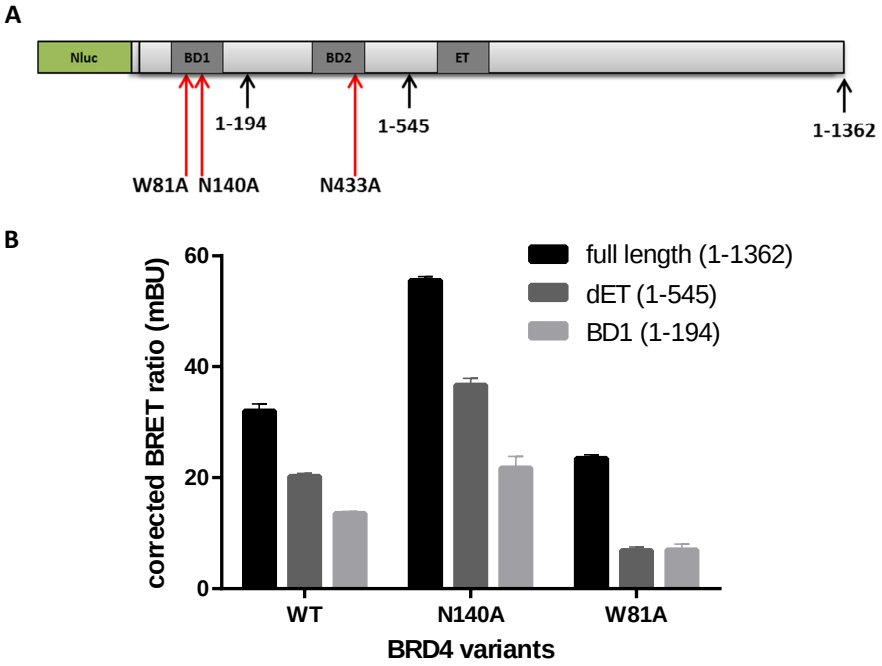

Figure 4.15 Nano-BRET in cell binding analysis of BRD4 variants to H4.
A. Schematic representation of BRD4 (grey) fused with Nluc (green). Mutation sites are indicated by red arrows and cutting sites for truncated variants by black arrows indicating the length of the constructs.
B. Corrected BRET ratio calculated from emission light measured in HCT-116 cells transfected with 2 µg pNL-BRD4 and 0.02 µg pH4-HaloTag. BRD4 truncated variants are indicated in the legend and mutations for each variant on the horizontal axis.

Shortening the length of BRD4 wild-type reduced the BRET ratio signal indicating that the interaction between BRD4 and histone H4 was reduced and suggesting that not only the bromodomains are involved in the interaction with the chromatin.

Surprisingly, the N140A mutant which previously showed dramatic loss of binding to H4, had an improved binding compared to the wild-type BRD4. Similar results were observed with the double mutant N140A (BD1) and N433A (BD2) not shown here. The same trend was observed, for the N140A BRD4 shorter variants compared to wild-type truncated forms. Only the W81A mutation showed reduced binding of BRD4 to histone H4 for all BRD4 variants compared to non-mutated BRD4 forms.

4.4. Affinity determinants for BRD4 recognition by the small molecule inhibitor JQ1

Although JQ1 efficiently mimics the acetyl-lysine group and occupies the same space in the BRD4 BD1 pocket, it does not make exactly the same interactions with the protein as the acetylated H4 does (Fig. 4.5 A and B). An important point to investigate was whether the reduction of BRD4 BD1 mutant interaction with histone peptides translated into a quantitative loss of inhibitor binding.

4.4.1. Mutants binding to JQ1 analysis outside a cellular context

4.4.1.1. Fluorescence polarization analysis of BRD4 mutants binding to a JQ1 derivative

JQ1 was labeled with fluorescent TAMRA and titrated with increasing concentrations of BRD4 wild-type and mutants. Fluorescent TAMRA excited with a plane-polarized light rotates and emits light into a different plane. Therefore, when the TAMRA molecule binds to a large molecule such as BRD4 through its JQ1 moiety, the emitted light is less depolarized. Fluorescence polarization of the probe was used as indicator for complex formation (Fig. 4.16).

A

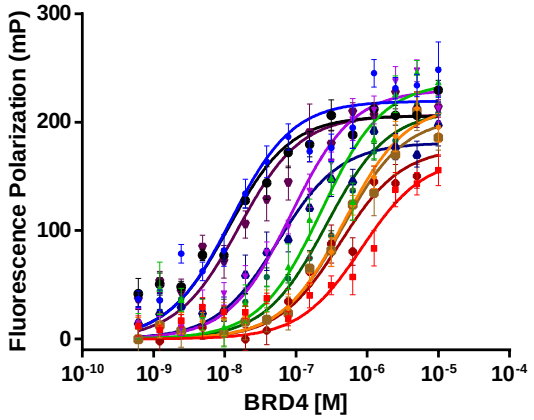

B

BRD4 BD1 variant	K_D (nM)	ΔG (kJ mol^{-1})
BRD4 wt	14.5 ± 3.3	-45
W81A	834.7 ± 281.5	-35
P82A	229.3 ± 59.7	-38
L94A	85.3 ± 14.8	-40
Y97F	474.8 ± 73.8	-36
Y139F	11.4 ± 2.2	-45
N140A	447.8 ± 70.6	-36
D144A	56.6 ± 11.3	-41
D145A	15.8 ± 3.7	-45
I146A	414.8 ± 100.7	-36
M149A	267,8 ± 77.1	-38

Figure 4.16 FP analysis of BRD4 BD1 wild-type and mutant binding to TAMRA-labeled JQ1.
A. The TAMRA labeled JQ1 tracer (10 nM) was titrated with increasing concentrations of protein as indicated and blank-subtracted fluorescence polarization values were plotted vs. [Protein]. The lines show the fit of the data to a single-site equilibrium binding equation.
B. The K_D values obtained from these fits are indicated in the table.

The results indicate that JQ1 binding to the Y139F and D145A mutants was not significantly different compared to wild-type BRD4 BD1. The strongest effects were observed for P82A, Y97F, N140A, I146A and M149A, and especially for the W81A mutant.

4.4.1.2. Thermal stabilization analysis of BRD4 mutants by JQ1

To test whether the results obtained using a JQ1-derivative recapitulated the interactions of the parent compound with BRD4, the effects of JQ1 on unfolding thermodynamics of the BRD4 BD1 mutants were analyzed using TSA. To this end melting curves of the wild-type and of each mutant at increasing ligand concentrations were recorded. As previously reported (Filippakopoulos, Qi et al. 2010), JQ1 binding resulted in thermal stabilization of BRD4 BD1 and raising ligand concentrations increased the protein thermal stability (Fig. 4.17. A).

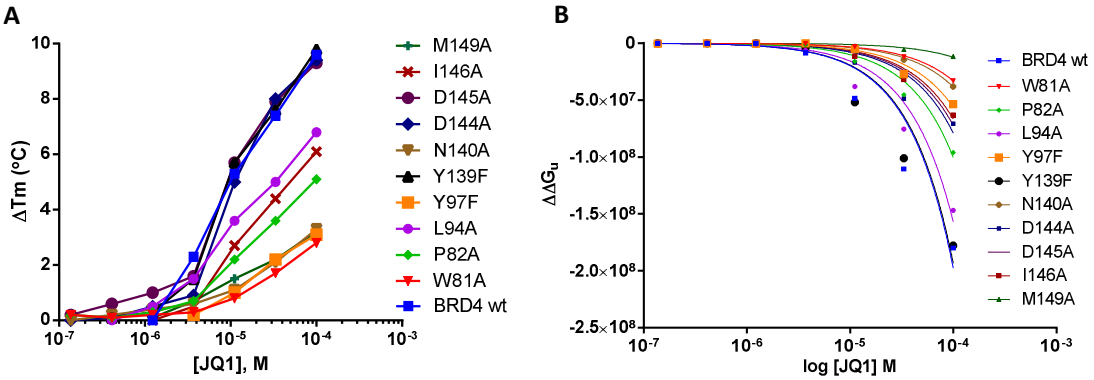

C

BRD4 BD1 variant	ΔTm* (°C)	K_D^o (nM)	ΔG (kJ mol^{-1})	ΔH^o_b (kJ mol−1)	$-T\Delta S^o$ (kJ mol−1)
BRD4 wt	9.6 ± 0.6	1	-51-3	-13.8	-37.5
W81A	2.8 ± 0.4	13,7	-44.9	-9.2	-35.7
P82A	5.1 ± 0.2	3,64	-48.2	-17.4	-30.8
L94A	6.9 ± 0.4	2,14	-49.5	-17.7	-31.8
Y97F	3.1 ± 0.6	10,5	-45.6	-15.5	-30.1
Y139F	9.8 ± 0.3	1,0	-51.5	-18.7	-32.8
N140A	3.3 ± 0.4	8.6	-46	-11.9	-34.1
D144A	9.5 ± 0.6	1	-51.3	-9.9	-41.4
D145A	9.2 ± 0.6	1.1	-51.2	-6.5	-44.7
I146A	6.1 ± 0.3	2.4	-49.2	-8.8	-40.4
M149A	3.2 ±0.3	9.7	-45.7	-0.5	-45.3

Figure 4.17 TSA analysis of BRD4 BD1 wild-type and mutant affinity and stabilization thermodynamics of binding to JQ1.

A. Thermal stabilization (ΔTm) of BRD4 BD1 by JQ1 with raising ligand concentrations.

B. The compound-induced changes in free energy of unfolding ($\Delta\Delta G^o_u$) were plotted vs. [JQ1] and the data were fitted to the equation described in the materials and methods section (colored lines). These fits served to calculate the K_D^o values shown in table

C. Mean values of the thermal stabilization measured with 100 µM JQ1 and affinity and thermodynamics parameters derived from TSA measurements (±SD).

Analysis of the melting points of the mutants in the presence of 100 µM JQ1 revealed that the W81A, Y97F, N140A and M149A forms were the least stabilized by JQ1, whereas the mutants P82A, L94A and I146A showed a moderate stabilization profile (Fig. 4.17.A and C). Conversely, JQ1 stabilized the

Y139F, D144A and D145A mutants as strongly as wild-type BD1. The ΔTm values at 100 µM JQ1 were in good agreement with the affinities of the mutants for JQ1 in the FP assay (Fig 4.15).

Encouraged by these results the ΔTm and ΔH_u parameters obtained from the experiments were used to estimate the binding enthalpy ΔH^o_b and evaluate the impact of JQ1 on the protein stability change $\Delta\Delta G^o_u$ (Fig. 4.17.B). Using the appropriate equations and making assumptions discussed elsewhere (Myers, Pace et al. 1995, Matulis, Kranz et al. 2005, Layton and Hellinga 2010)) K_D^o values for the interaction of JQ1 with the different mutants were also derived. The results of these studies are summarized in the table (Fig 4.17.C) The calculated standard binding enthalpy ΔH^o_b of BRD4 BD1 wild-type to JQ1 of -13,8 kJ mol^{-1} was in the same range as the -8,42 kcal mol^{-1} ΔH_{obs} previously measured by ITC (Filippakopoulos, Qi et al. 2010). Loss of stabilization by JQ1 translated into loss of relative free energy of binding ΔG^o, which however remained negative along with the binding enthalpy ΔH^o_b and entropy changes $T\Delta S^o$ (Fig 4.17.C). As anticipated from the ΔTm values, the thermodynamic data obtained from the TSA experiments supported the affinity ranking of the mutants obtained using the FP assay.

4.4.1.3. TR-FRET analysis of BRD4 BD1 mutants binding to acetylated peptides

The impact of BD1 mutations on JQ1 binding are expected to influence the inhibitory activity of the compound. Therefore the interaction of JQ1 with each purified mutant was determined in the TR-FRET competition assay, using biotinylated H4 tetra-acetylated peptide as tracer (Fig. 4.18). The K_D of JQ1 for those mutants with sufficient affinity to the H4 tetra-acetylated to allow an appropriate assay window was calculated. W81A, Y97F, N140A and M149A were therefore excluded from this analysis.

A

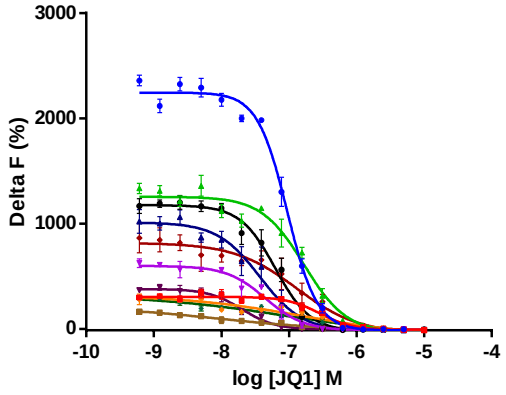

B

BRD4 BD1 variant	K_D (nM)	ΔG (kJ mol^{-1})
BRD4 wt	105.7 ± 13.9	-39.4
W81A	n.i.	
P82A	174.1 ± 13.9	-38.2
L94A	42.8 ± 2.3	-41.6
Y97F	n.i.	
Y139F	61.3 ± 16.5	-40.8
N140A	n.i.	
D144A	44.0 ± 11.4	-41.6
D145A	16.8 ± 4.6	-43.9
I146A	112.0 ± 23.5	-39.3
M149A	n.i.	

Figure 4.18 TR-FRET competition assay.
A. 200 nM biotinylated H4 peptide and 50 nM wild-type or mutant proteins were titrated with JQ1 at the concentrations indicated in the graph. Plots of the Delta F data vs. [JQ1] were fitted to the 4-parameter equation described in the Experimental Procedures section (colored lines) in order to calculate the K_D values indicated in the table.
B. Mean values of the affinity and thermodynamics parameters derived from TR-FRET measurements (±SD) are listed. Values not shown could not be interpreted (n.i.).

JQ1 was a better inhibitor of the interaction of BRD4 with the H4 peptide when L94, Y139, D144 and D145 were mutated to alanine especially for D145A where a 6-fold increase of inhibitory activity was observed. JQ1 showed similar inhibition for I146A or a slightly decreased one for P82A, in comparison to the wild-type protein.

4.4.2. BRD4 mutants binding analysis to JQ1 in a cellular context

4.4.2.1. Nano-BRET analysis of JQ1 inhibition of BRD4 mutants binding to H4

In order to assess the relevance of our findings with JQ1 in a cellular context, the Nano-BRET assay was also used to analyze 2 BRD4 point mutants, namely N140A and W81A.

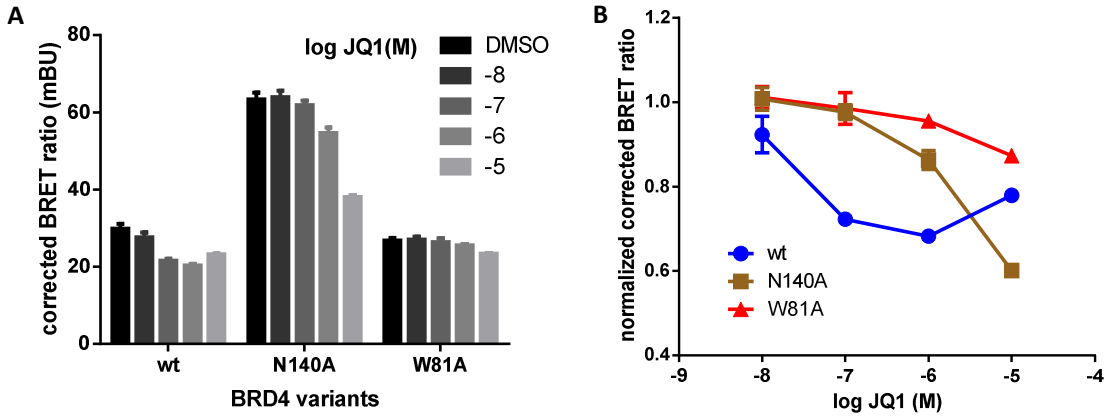

Figure 4.19 Determination of cellular inhibition of BRD4-H4 interaction with the NanoBRET assay.
A. Corrected BRET ratio of BRD4 wt and mutants interacting with H4 with increasing concentrations of JQ1.
B. Normalization of corrected BRET ratio to DMSO treatment.

As previously shown (4.3.2.3), mutants show different basal binding to H4, so that normalized ratio was also used to compare JQ1 inhibition (Fig. 4.19). Both mutated forms were less sensitive to JQ1 inhibition, confirming the loss of JQ1 affinity shown in extracellular TSA experiments.

4.4.2.2. In cell stabilization of BRD4 mutants by JQ1

A novel assay system which detects changes in BRD4 BD1 protein levels in cell lysates by TR-FRET was developed (Schulze, Moosmayer et al. 2014), built on the fact that ligand-induced stabilization of proteins has recently been shown to take place in living cells (Martinez Molina, Jafari et al. 2013). Small molecule inhibitors of BRD4 bromodomains can increase the half-life of the targeted protein in cells, and incubation of cells expressing BRD4 BD1 with JQ1 led to a dose-dependent and saturable increase of the TR-FRET signals, indicative of increased protein levels. The EC_{50} value measured for stabilization of wild-type BRD4 was 0.1 µM, in concordance with the IC_{50} determined in the biochemical TR-FRET competition experiment. In line with the biochemical data, mutated BRD4 variants that were least recognized by JQ1, namely W81, P82, Y97, N140 and M149 showed am increased EC_{50} in the cellular stabilization assay (from 7-fold to over 100-fold), indicative of a reduced recognition by JQ1 inside cells. The effects were most pronounced for the N140 and especially the M149A mutants (Jung, Philpott et al. 2014).

4.5. Mechanistic analysis of BRD4 role in transcription

4.5.1. Effect of JQ1 treatment on endogenous gene expression in prostate cancer cells

The expression of numerous genes in prostate cancer cells is under the control of steroid hormones. As a ligand-dependent transcription factor, the androgen receptor (AR) interacts with androgen

response elements (ARE) in various androgen target genes to activate and more rarely repress transcription. Typical target genes upregulated by the AR code for different proteases, including the prostate specific antigen (PSA, also known as kallikrein-related peptidase 3, KLK3), and the kallikrein-related peptidase 2 (KLK2) (DePrimo, Diehn et al. 2002). To analyze the effect of JQ1 on these regulated genes, and also on AR and on c-Myc, AR-positive LAPC-4 prostate cancer cells were cultured and mRNA levels were determined by quantitative PCR after JQ1 treatment with or without the synthetic androgen analogue R1881 (Fig. 4.20).

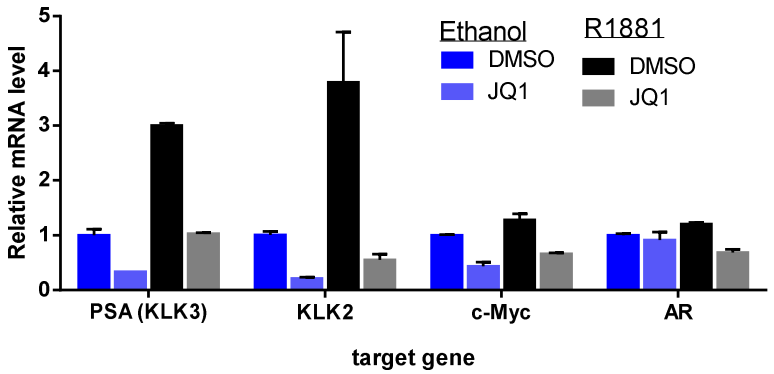

Figure 4.20 qPCR expression of genes in AR-positive prostate cancer cell line treated with androgen analog and JQ1.
LAPC-4 cells were treated for 7 hours with 1 nM R1881 or vehicle (Ethanol 0.1 %) and 100 nM JQ1 or vehicle (DMSO 0.01 %), total RNA was prepared and the PSA, KLK2, c-Myc and AR transcript levels were determined by quantitative PCR. Results calculated from multiple replicates were normalized for each gene to vehicle control (Ethanol + DMSO).

As expected, the androgen analog increased PSA and KLK2 expression but had only limited effect on c-Myc and AR expression. JQ1 reduced the basal expression of PSA, KLK2 and c-Myc. Androgen-induced expression of PSA and KLK2 was reduced to basal levels upon JQ1 treatment. AR and c-Myc expression was decreased by JQ1 after androgen analog treatment.

4.5.2. Effect of JQ1 treatment on endogenous gene expression in BRD4 low expressing cells

CAL-85-1 breast cancer cells show low BRD4 expression, as determined in a broad in-house cell panels. c-Myc, Cyclin D1 (CCND1), FOSL-1 and HEXIM1 have previously been shown to be regulated by BRD4 in different cancer cell lines (see introduction). CAL-85-1 cells were first tested to measure the effect of BET inhibition on the expression of these BRD4 target genes (Fig. 4.21).

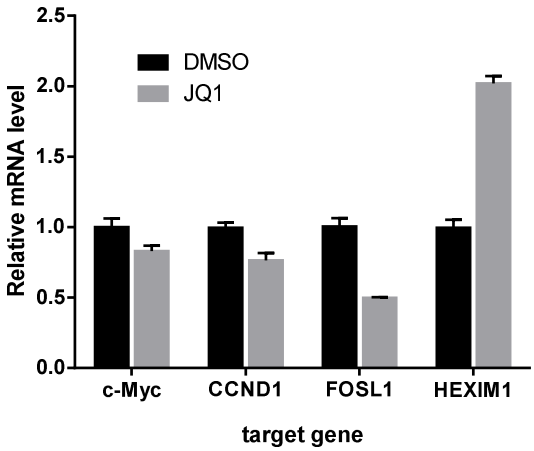

Figure 4.21 qPCR expression of c-Myc, Cyclin D1, FOSL1 and Hexim1 in CAL-85-1 breast cancer cell line treated with JQ1.
CAL-85-1 cells were treated for 18 hours with 200 nM JQ1 or vehicle (DMSO), total RNA was prepared and the c-Myc, CCND1, FOSL1 and HEXIM1 transcript levels were determined by quantitative PCR. Results were calculated from three replicates normalized to vehicle control.

BET inhibition by JQ1 slightly reduced the expression of c-Myc and cyclin D1, decreased the expression of FOSL-1 but increased the expression of HEXIM1.

4.5.3. Effect of BRD4 overexpression on endogenous gene expression in BRD4 low expressing cells

To analyze the effect of BRD4 overexpression, the same BRD4 low expressing cells were used. BRD4 wild-type and asparagine mutant, which showed loss of binding to the H4 peptide, were transfected and the mRNA of target genes was quantified (Fig. 4.22). Transfection efficiency was verified using GFP plasmids and fluorescence microscopy.

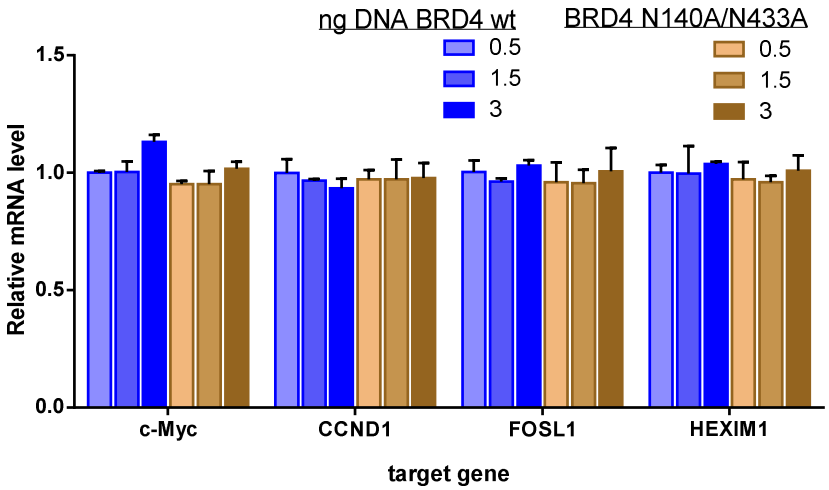

Figure 4.22 qPCR expression of c-Myc, Cyclin D1, FOSL1 and HEXIM1 in CAL-85-1 breast cancer cell line overexpressing BRD4.
CAL-85-1 cells were transfected for 24 hours with BRD4wt or double mutant N140A/N433A, total RNA was prepared and the c-Myc, CCND1, FOSL1 and HEXIM1 transcript levels were determined by quantitative PCR. Results calculated from three replicates normalized to 0.5ng BRD4 wt.

BRD4 wild-type and mutant overexpression for 24 hours did not affect the transcription of the endogenous genes previously shown to be influenced by JQ1 treatment. The same results were also observed after 72 hours overexpression.

4.5.4. Promoter transactivation by BRD4 overexpression

To compare the effect of BRD4 wild-type and mutant on promoter activity, c-Myc, Cyclin D1, and FOS promoters cloned in front of a luciferase reporter gene were co-transfected with BRD4 wild-type and an asparagine double mutant (N140A/N433A). The luciferase vector containing no promoter (empty luc) was used as a control (Fig 4.23).

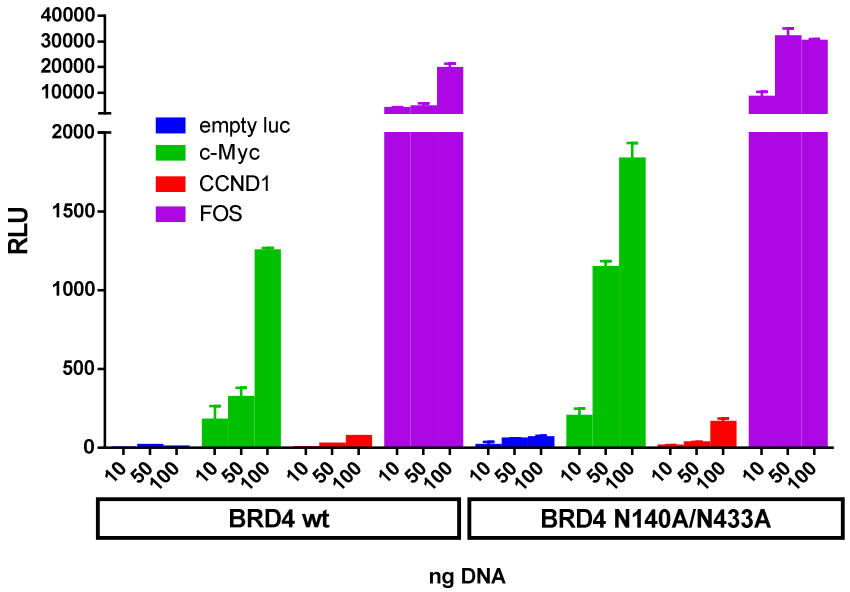

Figure 4.23 Cyclin D1, c-Myc and FOS promoter activity after BRD4 overexpression in U-2 OS.
U-2 OS cells were co-transfected for 24 hours with 100ng pLightSwitch plasmids containing the c-Myc, CCND1, FOS promoter or no promoter (empty luc) together with 10, 50 or 100ng BRD4 wt or double mutant N140A/N433A. The amount of light, was measured by the luminometer for six replicates, and expressed in Relative Light Units (RLU).

Luciferase emission light intensity shows that growing BRD4 concentrations increased the activity of the transfected constructs, especially for the c-Myc promoter. Surprisingly, mutation of BRD4 at the essential N140 and N433 residues did not impair this induction but increased the activity of the promoter, in an even stronger fashion than with wild-type BRD4.

5. Discussion

BET proteins play a pivotal role in cancer, mainly as part of regulatory complexes involved in the control of transcription elongation. BRD4 is the best-studied member of the family and its diverse biological activities rely on its role in the functional transition between chromatin targeting and transcriptional regulation (Chiang 2009, Devaiah and Singer 2013). The recent identification of selective and potent BET inhibitors allowed a profound understanding of the function of this protein group. Importantly, these compounds showed efficacy in several cancer models, which ultimately led to the initiation of clinical studies, mainly in patients with hematological tumors.

A detailed understanding of the BRD4 bromodomain residues engaged in acetylated lysine and inhibitor binding will be essential for the identification of compounds with an improved pharmacological profile.

5.1. BRD4 binding to acetylated peptides

5.1.1. BRD4 BD1 and BD2 binding profiles

Using different biophysical and biochemical methods the binding profiles of BRD4 BD1 and BD2 to different acetylated H4 and H3 peptides was first compared. The results of the binding measurements allowed to identify the tetra-acetylated peptide H4 K5(ac)K8(ac)K12(ac)K16(ac) and the di-acetylated peptide H4 K5(ac)K8(ac) as the best binding partners of BRD4 BD1 and BD2. Furthermore, the fast kinetics of the interactions between BRD4 BD1 or BD2 and the tetra-acetylated H4 were shown for the first time. BRD4 BD1 had a more than 6-fold higher affinity for the tetra-acetylated H4 peptide than BD2, with affinity constant values comparable to those previously reported using ITC (Filippakopoulos, Picaud et al. 2012). Altogether, these results strongly suggest that the first bromodomain is the main player in BRD4 recognition of acetylated histones.

Binding of BRD4 to tetra-acetylated H4 was strongly impaired at high salt concentration, raising the question whether transient local changes of ionic strength in the nucleus may influence the binding of BRD4 to chromatin.

A weaker interaction was observed for a H3-derived di-acetylated peptide, in line with previous data generated with peptide arrays. These studies analyzed the recognition of numerous acetylated histone-derived peptides by different BET and non-BET bromodomains using SPOT arrays. They revealed important differences in the recognition pattern, including individual binding profiles for the BET BD1 and BD2 regions (Filippakopoulos, Picaud et al. 2012).

The limited binding seen for mono-acetylated peptides suggests that synergistic effects between different acetylation marks are needed for recognition. Indeed, this is a general feature found for most bromodomains, as previously shown by peptide array and ITC data (Filippakopoulos, Picaud et

al. 2012). Also, structural studies performed with BRDT have revealed that two acetylation marks are recognized by a single bromodomain, thus mediating cooperative effects (Moriniere, Rousseaux et al. 2009).

The distance between acetylation marks was also noted to be important. A six amino acid space between H4 acetylated lysines reduced the binding of BRD4 BD1 compared to a two or three residue spacing. Indeed the two closely spaced acetylation marks of the H4K5(ac)K8(ac) have been shown to both fit into BRD4 BD1 by cocrystallization (Filippakopoulos, Picaud et al. 2012).

5.1.2. Influence of amino acids neighboring acetyl-lysines on H4 recognition by BRD4

Furthermore the nature of the amino acids located between modified lysines was found to have an impact on the interaction of the tetra-acetylated H4 peptide with BRD4 BD1 and BD2. Multiple glycine residues are present in the H4 tail between K5 and K16, suggesting flexibility of this region to be important for recognition by reader proteins. First experiments performed with a di-acetylated peptide had already shown that G6, but not G7, needed to be conserved to maintain strong binding by BRD4 BD1 (Filippakopoulos, Picaud et al. 2012). The role of G6 in the tetra-acetylated H4 peptide was here confirmed and additionally G4 and G9 were also shown to have an impact on accessibility and recognition by BRD4 BD1. The importance of glycine residues near histone marks has recently been reported in childhood tumors where a mutation in the histone variant H3.3 leading to a glycine to arginine or valine exchange modified the neighboring H3K36me3 profile (Bjerke, Mackay et al. 2013). Interestingly, the loss of binding was found to be dependent on the salt concentration. Given the position outside of the BRD4 binding pocket and the solvent exposure of the residues, this strongly suggests that the solvent interferes with the H4 conformation needed for optimal binding to BRD4.

L10 makes hydrophobic interactions outside of the BD1 binding pocket, which may explain the impact of the mutation to a less hydrophobic amino acid on binding.

S1 mutation to alanine increased the binding of BRD4 BD1 and BD2. This polar residue is involved in hydrogen interaction with a water molecule but mutation to alanine allows hydrophobic interactions with BRD4 neighboring residues.

Surprisingly, mutating the polar and charged R17, H18, R19 or K20 to alanine slightly increased the binding of BRD4 BD1 to the acetylated H4 peptide at low ionic strength conditions. These residues do not engage in the binding pocket, suggesting an indirect underlying cause such as higher solubility of the mutated histone peptide in low salt concentrations compared to the non-mutated peptide form.

5.2. Comparing affinity determinants for BRD4 chromatin and JQ1 recognition

The crystal structures of BRD4 BD1 bound to the acetylated H4 peptide or to different inhibitors show the compounds to mimic acetyl-lysine but also to engage in somewhat different interactions. Based on these observations ten amino acids belonging to the binding pocket were selected for site-directed mutagenesis and thorough analysis of the corresponding mutated BRD4 BD1 region outside a cellular context. Key amino acids for histone and JQ1 binding were additionally analyzed in a cellular context.

5.2.1. Affinity determinants for BRD4 chromatin and JQ1 recognition outside a cellular context

The affinity of the 10 selected mutants for H4 and JQ1 measured outside the cell was compared to the wild-type. Using TR-FRET and TSA experiments, the results allowed to establish an affinity map of BRD4 and altogether identify three different groups of mutations which similarly or differentially impacted histone and JQ1 binding to BRD4 outside a cellular context.

5.2.1.1. Affinity map of BRD4 interactions with H4 and JQ1 outside a cellular context

The affinity of the ten mutants for H4 and JQ1 was compared to the wild-type form using the free energy of binding calculated from the competitive TR-FRET and TSA experiments. Altogether, the results allowed to draw a three-dimensional affinity map of the BRD4 pocket engaged in interactions with histone H4 (Fig. 5.1. A) or with JQ1 (Fig. 5.1. B). The loss of absolute free energy of binding of each mutant compared to wild-type BD4 BD1 was color-coded, depending on the difference measured in an extracellular context.

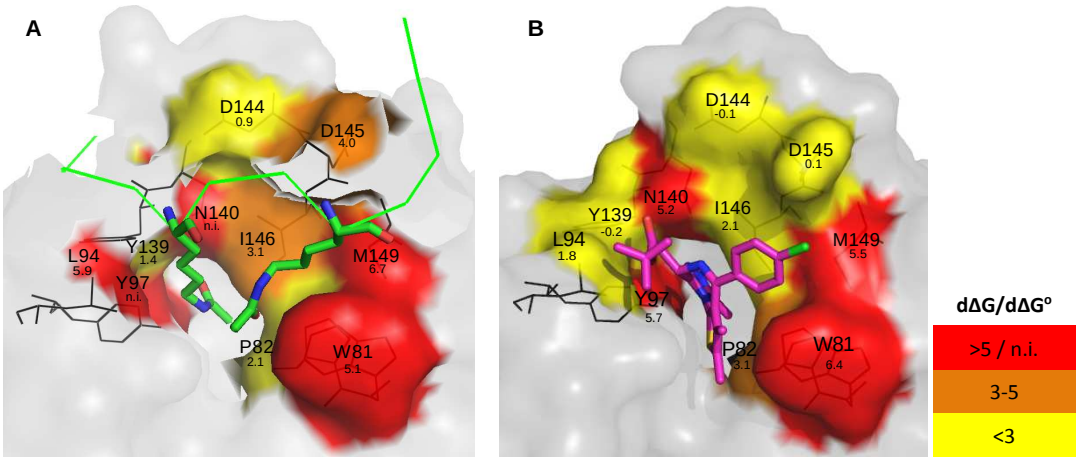

Figure 5.1 Three-dimensional affinity map of BRD4 interactions with H4 tail and JQ1.
Residues investigated in this study are highlighted in the crystal structures of BRD4 complexed with H4K5(ac)K8(ac) (A) and JQ1 (B). The colors represent the loss of absolute free energy of binding (dΔG) associated with the individual mutations. dΔG values were calculated by subtracting free energy of binding of the wild-type from the mutants. Non-mutated BRD4 regions are shown in grey, the H4K5(ac)K8(ac) peptide is shown in green and JQ1 in magenta. The dΔG values were calculated from the TR-FRET experiment (panel A) and the dΔG° values from the TSA experiment (panel B).

From these results, three different groups of mutations could be identified.

5.2.1.2. Residues with marginal contribution to histone and JQ1 recognition

This first group includes D144 and Y139. For both these mutated residues, the JQ1 and histone-binding affinities were only slightly altered in comparison to the wild-type protein, indicating a marginal role in binding of either partner.

Interestingly, the BD1 residue D144 is replaced by histidine in BD2, which can affect both the overall structure and the local charge, and possibly account for the different functions of these bromodomains.

5.2.1.3. Residues with different contribution for histone and JQ1 recognition

A second group with a mixed profile was identified. It includes residues P82, I146, L94 and D145.

The P82A mutation had little effect on H4 peptide binding but led to affinity loss towards JQ1. These results show that the interactions of P82 with H4 that include two indirect hydrogen bonds with the acetylation marks are rather weak, while the interactions with JQ1 are strong due to hydrophobic forces engaged with the thiophene group of the compound.

The I146A mutation showed a strong loss of affinity for H4 while binding to JQ1 was only partially affected. Interestingly, the nature of this gatekeeper residue varies outside of the BET family suggesting this position to be essential for the diversity of bromodomain functions. In BRDT,

introducing a large, bulky residue at this position entirely suppresses reorganization of hyper-acetylated chromatin (Moriniere, Rousseaux et al. 2009).

The L94A mutation led to a strong loss of affinity to the histone H4 tail, whereas binding to JQ1 was only weakly affected. This exact mutation was very recently used to generate a "hole" in the BRD4 bromodomain pocket for a new "bump-and-hole" approach aiming at engineering a BRD4 mutant that can be selectively blocked by compounds that target this modified bromodomain only. These dedicated compounds bear a sterically bulky "bump" that can only be accommodated by the modified pocket engineered in the protein. The authors show with Bio-layer Interferometry (BLI) that the binding of biotinylated acetylated histone H4 peptides to wild-type and mutated BRD4 was similar, and claim that the constructs retained the same ability to bind tetra-acetylated H4 even though the K_D measured in their ITC experiments was ninefold higher than in presence of the wild-type BRD4 BD1 (Baud, Lin-Shiao et al. 2014). For this particular method, the results shown here suggest that P82 could be a better position than L94 due to the more limited impact on histone binding. On the other hand, mutating a proline residue may also have an unexpected impact on the overall conformation of the pocket, due to the special properties of this residue.

Concerning D145, the affinity loss calculated for the mutant indicates that this residue forms medium-strength hydrogen bonds directed towards the H4 backbone but does not interact with the nearby chlorophenyl group of JQ1.

Competitive experiments involving JQ1 and tetra-acetylated H4 were performed with this mixed profile group. They showed that JQ1 was a better inhibitor of the interaction of BRD4 with the H4 peptide when L94 and D145 were mutated to alanine, whereas it showed similar inhibition for I146A or a slightly decreased one for P82A, in comparison to the wild-type protein.

These data reveal that residues with a mixed profile between loss of binding to histone and to JQ1 exist suggesting that resistance mutations compatible with bromodomain binding are possible.

5.2.1.4. Key residues for histone and JQ1 recognition

Here mutants where important losses of histone and JQ1 binding were noted. The prime example is N140, for which a strong reduction of binding properties was expected, based on previous studies, due to the formation of an essential hydrogen bond with the carbonyl group of the acetyl mark and with the 3-methyl-1,2,4-triazole ring of JQ1 (Muller, Filippakopoulos et al. 2011, Hewings, Rooney et al. 2012). Indeed, the N140 position has already been shown to be essential for the reading function of many, but not all bromodomains (Filippakopoulos, Picaud et al. 2012). For instance, the corresponding mutation in BRD3 BD1 has no impact on binding to GATA1 (Gamsjaeger, Webb et al. 2011), suggesting that the interaction between a bromodomain and its acetylated partner may in some instances follow different rules.

The Y97 mutant also had severely impaired binding properties. Cocrystal structures indicate that Y97 interacts indirectly, by hydrogen bonding through a water molecule, with the acetylated lysine (Vollmuth, Blankenfeldt et al. 2009) and also with JQ1 (Filippakopoulos, Qi et al. 2010). The effects observed in these experiments are in line with comparable mutations in BRD2 and BRD3, showing Y97 to be critical for binding to mono-acetylated H4 (Umehara, Nakamura et al. 2010) and to GATA1 (Gamsjaeger, Webb et al. 2011), respectively.

Interestingly, molecular dynamic simulations (Steiner, Magno et al. 2013) showed both N140 and Y97, as well as Y139, to be located in a flexible region (see also Fig. 3.6) allowing rotation between an inward and an outward position, which may affect recognition of the acetyl-lysine binding site.

Two other residues were essential for peptide and inhibitor binding, namely the hydrophobic amino acids W81 and M149. Both positions are known to be essential in BRD3 BD1 for its interaction with the GATA1 peptide (Gamsjaeger, Webb et al. 2011). Interestingly, an alanine residue is found at the W81 position in the BRD7 bromodomain, which has only low binding affinity for acetylated peptides (Sun, Liu et al. 2007). W81, together with P82 and F83 form the hydrophobic WPF shelf (Prinjha, Witherington et al. 2012, Vidler, Brown et al. 2012). In this study, the hydrophobic interaction between JQ1 and W81 was as important as the hydrogen bonds formed with Y97 and N140.

The effects were less pronounced for the M149 mutation, but still very marked. Importantly W81 and M149, together with I146, form the hallmark signature of the BET bromodomain group and are predictive of high druggability (Vidler, Brown et al. 2012). In the BET family, the position corresponding to M149 is conserved whereas in the BAZ family it is replaced by the small amino acids alanine or cysteine, which allow the tryptophan to move close to residue 149, thereby removing the ZA channel and hydrophobic shelf (Vidler, Brown et al. 2012). Altogether these data show that W81, Y97, N140 and M149 are key amino acids for histone and JQ1 binding which inhibitors need to address for efficient inhibition of BRD4. The mutants of this group were further investigated to analyze if these results translated in a cellular context.

5.2.2. Translation in a cellular context

5.2.2.1. Chromatin binding

Biochemical and biophysical binding analysis have shown that W81, Y97, N140 and M149 are key amino acids for histone and JQ1 binding which is why members of this group were additionally analyzed in a cellular context.

Using FRAP an impaired chromatin recognition for all of the corresponding mutants was observed (Jung, Philpott et al. 2014).

In the mammalian two-hybrid assay it was not possible to show an interaction between BRD4 wild-type and H4. Multiple reasons can explain this. First, the weak interaction between BRD4 and H4 (K_D

>1 µM) may not be detectable in this assay, as noted previously (Estojak, Brent et al. 1995). Second, the acetylation status of the H4 protein expressed by the transfected plasmid is uncertain. Third, H4 needs a proper context for interaction with BRD4 and promoter activation on the reporter plasmid. The yeast two-hybrid method is based on the same principle. In *S. cerevisiae*, two genes encode each of the four core histones. This low copy number stands in contrast to mice and humans with more than 50 copies of histone genes. *S. cerevisiae* was also used as a model system for studying histones acetylation (Rando and Winston 2012). However, up to now, no two-hybrid data were published using histones. On the other hand, a yeast two-hybrid assay showed that BET proteins dimerize through the conserved motif B (Garcia-Gutierrez, Mundi et al. 2012). We could here confirm the interaction between two BRD4 proteins in a mammalian system.

In contrast to the mammalian two-hybrid assay the Nano-BRET technology allows to monitor in-cell protein-protein interaction without transcription activation of a reporter gene. The first publication on this new technology came out very recently and described the measurement of the displacement of NanoLuc-tagged BRPF1 (bromodomain and PHD finger containing protein family) bromodomain construct from Halo-tagged histone H3.3. with different inhibitors (Demont, Bamborough et al. 2014). Using this technology the interaction between BRD4 wild-type and histone H4 could be observed. The signal was proportional to the length of the protein suggesting additional interactions due to BD2 and other domains to take place. Indeed, it was previously shown when extracting transfected BRD4 short and long isoforms from whole cell lysates that the BRD4 long isoform was a stronger binder of diacetylated H4K5(ac)K8(ac) peptides whereas the short isoform had a greater range of acetylated histone binding pattern including H3K18(ac) and H3K14(ac)K18(ac) diacetylated peptides (Alsarraj, Faraji et al. 2013). For BRD2 the interaction with chromatin was also shown not to be solely due to bromodomain interaction with histone acetylation but that the C-terminal part was also crucial for association with chromatin (Hnilicova, Hozeifi et al. 2013).

Although both FRET and BRET rely on the energy transfer between two proteins in close proximity, surprisingly the loss of binding shown with BRD4 BD1 in the TR-FRET assay using the asparagine mutant was not observed with the Nano-BRET assay, either with the full-length protein or the protein shortened before the ET domain or with the BD1 domain only. The fact that the mutated BD1 bromodomain shows higher binding than the corresponding wild-type excludes a role of additional interactions due to other regions of BRD4. The mutation to alanine could possibly confer conformational changes or differences in post-translational modifications which enhance the binding to H4. In FRAP experiments the N140A and N140F mutants showed a quicker recovery of fluorescence intensity indicative of displaced and freely diffusing proteins and are thus in line with the TR-FRET binding experiments (Jung, Philpott et al. 2014).

On the other hand the W81A mutation confirmed the key role of this position in a cellular context as measured with the Nano-BRET assay and also with FRAP experiments (Jung, Philpott et al. 2014).
These results suggest a context-dependent binding mode of the BRD4 bromodomain to the H4 histone at least regarding the hydrogen bonding formed by the N140.

5.2.2.2. JQ1 binding

JQ1 competitively inhibits BRD4 wild-type binding to H4 in a cellular context but compared to TR-FRET experiments it could not completely abolish the Nano-BRET signal even when using only BD1 as binding partner. This was also observed with other bromodomain proteins like BRPF1 using the same method (Demont, Bamborough et al. 2014). In FRAP experiments JQ1 showed competitive displacement of BRD4 from chromatin (Filippakopoulos, Qi et al. 2010). Treatment of MM cells with JQ1 dramatically but not completely reduced the levels of BRD4 genome-wide binding. There was a ~60% reduction at enhancers and ~90% reduction at promoters while the loss was nearly complete only at super-enhancers (Loven, Hoke et al. 2013), indicating that residual BRD4 binding to chromatin remains at some locations following inhibitor treatment.
JQ1 inhibition of W81A and N140A BRD4 mutants binding to H4 was strongly impaired in the cellular assay, in accordance with the extracellular binding experiments and cellular stabilization assays performed where those same BRD4 BD1 mutants had a strongly reduced binding to JQ1 (Jung, Philpott et al. 2014, Schulze, Moosmayer et al. 2014).
The mixed translation of extracellular results to a cellular context raises the question whether the differentially impaired binding of BRD4 mutants to histone and JQ1 can be translated into an altered impact of BRD4 inhibitors on cellular function.

5.2.2.3. Translation in a cellular mechanistic context

To monitor the effects of mutants BRD4 overexpression in transfected cells and minimize possible artefacts linked to the silencing of endogenous BRD4 and concomitant overexpression, low BRD4 expressing cells were used. These cells showed reduced expression of c-Myc, CCND1 and FOSL1, and increased HEXIM1 transcription upon JQ1 treatment. However, overexpressing BRD4 in these cells did not affect the expression levels of these four genes, regardless whether the wild-type or the asparagine mutant form was transfected. Similar results were also observed in the HCT-116 cell line expressing comparable endogenous BRD4 levels compared to other cell lines.
Most experiments studying the effects of BRD4 level variations on target gene expression described in the literature were performed with the knock-down technology but rarely with overexpression. The only results reported so far are the decreased HMOX1 levels and concomitant CoPP induction (Hussong, Borno et al. 2014). In addition BRD4 stimulated Aurora B promoter activity and increased Aurora B protein levels upon overexpression in C33A retinoblastoma cells (You, Li et al. 2009).

Here a transactivation assay was also tested, showing growing activity of the c-Myc, Cyclin D1 and FOS promoters upon BRD4 overexpression. Surprisingly BRD4 N140A/N433A had an even stronger effect on the activity of each promoter. This correlates with the Nano-BRET results showing higher binding of this mutant to the histone. If mutating this residue to alanine genuinely increased BRD4 binding to H4 in the cell and increased transcription activation while losing JQ1 sensitivity, this would suggest that a resistance mutation combined with BRD4 gain of function would be possible.

It was demonstrated before that mammalian cells are capable of rapidly assembling non-integrated circular DNA into typical "minichromosomes" containing nucleosomes with a 190 bp repetitive spacing, depleted in histone H1 and containing highly acetylated forms of histone H4 (Reeves, Gorman et al. 1985). This suggests that the effects of BRD4 overexpression on gene regulation of an artificial, plasmid-located promoter can be monitored in such an artificial system. The question remains though whether the effects seen with the Nano-BRET and transactivation assays take place on the plasmid nucleosomes or on the endogenous chromatin. Since the wrapping of the nucleosomes is slightly bigger and the modifications of the histones are possibly not identical, there may still be important differences in the results generated in these experiments.

The diverse biological roles of BRD4 have been proposed to rely on its functional transition between chromatin targeting and transcriptional regulation (Chiang 2009, Devaiah and Singer 2013) and the link between chromatin-bound BRD4 and transcriptional regulation is unclear. BRD4 persistently associates with chromosomes during mitosis for transmitting epigenetic memory across cell divisions. During interphase, BRD4 plays a key role in regulating the transcription of signal-inducible genes by recruiting P-TEFb to promoters. In stress-induced situations BRD4 needs to be released from histone interaction mostly through signal-triggered deacetylation of nucleosomal histone H4 by HDAC1/2/3 at acetylated-lysine 5/8 (H4K5ac/K8ac) in order to interact with P-TEFb and play its role in transcription activation (Ai, Hu et al. 2011, Hu, Lu et al. 2014). In line with this, another hypothesis would be that mutating the essential asparagine residue reduces the interaction with H4 as shown in the extracellular results but potentiates BRD4 transcriptional activity. BRD4 could stay in close proximity to the histone N-terminus and with this conformation generate a higher BRET signal. According to the providers, the donor and acceptor must be close (<10nm) to generate a signal in BRET. In view of the size of a nucleosome which is about 11 nm this hypothesis seems plausible.

5.3. Effect of JQ1 treatment on endogenous gene expression in prostate cancer cells

BRD4 physically interacts with the N-terminal domain (NTD) of AR in a large multi-protein complex composed of AR, BRD4 and RNA Pol II and this high-affinity interaction (K_D = 70 nM measured in a biophysical experiment) can be disrupted by JQ1 (Asangani, Dommeti et al. 2014). As a consequence,

the expression of androgen-induced expression of PSA, KLK2 and c-Myc is strongly reduced, which can be to due either to AR NTD/BRD4 binding inhibition or disruption of the transcription complex with P-TEBb and RNA Pol II. Hormone therapy with AR antagonists or lyase inhibitors for advanced prostate cancer obliterates androgen signalling but these therapies usually fail after about 18 months and the disease progresses to metastatic castration-resistant prostate cancer (CRPC) (Myung, Banuelos et al. 2013). Asanghani *et al.* highlighted different efficiencies of a BRD4 inhibitor and of anti-androgens such as bicalutamide and enzalutamide on recruitment of AR and BRD4 to target genomic loci and on *in vitro* and *in vivo* efficacies. Inhibiting AR target gene expression through blockade of the AR NTD gives hope for a new option in CRPC treatment, less likely to be affected by acquired resistance associated with AR antagonists, usable either as a monotherapy or in combination with current anti-androgen therapies.

5.4. Conclusion

This work contributes to a better understanding of the interactions of the important cancer target BRD4 with histone and JQ1 inhibitor and should help to both better understand the biology of this protein and help in the better design of future inhibitors.

First, the best acetylated binding partners for BRD4 bromodomains could be identified. The impact of histone residues neighboring the acetylation sites was also demonstrated. Then, biophysical and biochemical extracellular experiments on mutated forms allowed the drawing of a bromodomain affinity map and identified the BRD4 key residues W81, Y97, N140 and M149 for histone and JQ1 binding but also interestingly residues with a mixed profile between loss of binding to histone and to JQ1 such as P82, L94, D145 and I146.

The translation of these results into a cellular context was challenging. No effect could be seen on the transcription activation of endogenous genes shown to be regulated by JQ1. Furthermore the binding and mechanistic results obtained in cells were surprising. The key role of N140, which is the sole BRD4 BD1 residue forming a direct hydrogen bond with the acetyl moiety was questioned.

A cellular assay is usually more physiologically relevant and less artificial than biochemical and biophysical assays because intact cells and native cellular environment are used, but whether this also applies to artificial plasmid DNA inside the cell remains open.

The contribution of individual amino acids in histone and inhibitor recognition by BRD4 was elucidated but the context-dependent BRD4 interactions which implicate multiple interacting partners creates a complex environment which still requires better understanding. Furthermore the link between BRD4 bromodomains interaction with histone acetyl-lysine and BRD4 functions in cell proliferation, chromatin organization, and additional functions such as DNA damage repair needs to be further elucidated.

5.5. Outlook

Malignancies are characterized by extensive global reprogramming of epigenetic patterns, including gains or losses in DNA methylation and changes in histone marks. Furthermore, high-resolution genome-sequencing efforts have discovered a wealth of mutations in genes encoding epigenetic regulators that have roles as “writers”, “readers” or “erasers” of DNA methylation and/or chromatin states (Plass, Pfister et al. 2013) which may be the scope of next-generation inhibitors. Genetic defects were identified in DNMTs (Yan, Xu et al. 2011), in HMTs (Kleer, Cao et al. 2003, Sneeringer, Scott et al. 2010, Asangani, Ateeq et al. 2013) and in histone demethylases (Jones, Jager et al. 2012, Plass, Pfister et al. 2013). For example gain-of-function mutations that increase the catalytic activity of EZH2 and NSD2 histone methyltransferases are found in distinct subsets of B-cell neoplasms, which promote cell transformation by elevating the global level of H3K27 tri-methylation or H3K36 di-methylation, respectively (Shen and Vakoc 2015).

Histone acetylation is also affected in cancer and specific HDAC1 mutations are associated with high HDAC5 expression and with a sensitization of cells to the HDAC inhibitor panobinostat (Masica and Karchin 2013) suggesting that HDAC mutations could be used as predictive biomarkers.

Finally, chromosomal translocations involving chromatin regulator genes as exemplified with BRD4-NUT, can lead to the formation of fusion oncoproteins that directly modify chromatin.

Aside from the BRD4 translocation in NMC, no BRD4 mutation in cancer patients has been described in the literature up to now. Rare BRD4 mutations in single patients are listed by the International Cancer Genome Consortium (ICGC) and were mainly found in esophageal, ovarian and thyroid cancer.

This work showed that disturbing individual interactions between BRD4 and its acetylated protein partners can have a significant impact on substrate binding. In addition, the impact of mutating histone residues was also demonstrated.

Mutations in histone H3 have been identified in certain pediatric cancers which cause reprogramming of H3K27 and H3K36 methylation by interfering with histone methyltransferase activity (Shen and Vakoc 2015). The histone pattern can be mutated at the epigenetic modification sites (Yuen and Knoepfler 2013) but also at nearby histone marks like the H3.3G34 (Bjerke, Mackay et al. 2013).

An extended knowledge on the contribution of individual BRD4 amino acids to histone and JQ1 binding can be relevant in the context of clinical use of BET inhibitors. For instance, following the approval of tyrosine kinase inhibitors, a number of resistance mechanisms originating from single point mutations of the targeted kinase have been identified in patients (Sierra, Cepero et al. 2010). Frequently, these mutations decrease the affinity of the drug for the kinase domain, while the catalytic activity is maintained. Mutations affecting amino acids surrounding the binding site of the

drug and reducing the availability of the target region towards the inhibitor without interfering with ATP binding have furthermore been described (Zhang, Yang et al. 2009). Also, some mutations increase the affinity of the kinase for ATP, thus reducing the efficacy of the ATP-competitive inhibitors (Yun, Mengwasser et al. 2008).

As exemplified in the case of tyrosine kinase inhibitors, point mutations in protein regions targeted by drugs are a frequent escape mechanism observed in treated cancer patients. At this early stage, no instances of acquired resistance to BET inhibition have been reported but new technologies such as genome-wide DNA sequencing and comparative gene expression profiling should help to understand the molecular mechanisms involved, once resistant tumors arise. An early understanding of which bromodomain residues are likely to be involved in escape mechanisms from current BET small-molecule inhibitors may already guide the development of next-generation compounds. Future analysis of clinical samples will show whether such mutations occur in patients treated with BET inhibitors.

A deeper understanding of the role of individual amino acids in histone and inhibitor recognition as provided here can also improve the development of new methods like the very recently described “bump and hole experiments” giving the hope to identify the individual roles of single BET proteins in human physiology and disease (Baud, Lin-Shiao et al. 2014).

Somatic gain-of-function mutations that drive cancer pathogenesis are well established opportunities for therapeutic intervention, as mentioned above. A broader clinical impact for epigenetic therapies in oncology requires an increased understanding of the interplay between genetic and epigenetic alterations, and will guide the design of novel therapeutic strategies. The fact that only four years have elapsed between the initial description of BET inhibitors and the first positive results in clinical studies shows how intensive and combined efforts from both academia and pharmaceutical industry can quickly lead to a successful translation that benefits patients and there is great hope that new treatment paradigms for cancer based on such principles will emerge in the years to come.

Zusammenfassung

Bromodomain Protein 4 (BRD4) ist ein Mitglied der Bromodomain und extra-terminalen Domain (BET) Proteinfamilie. Es bindet an azetylierte Histone über seine beide Bromodomäne BD1 und BD2 und bildet einen Komplex mit dem positiven Transkriptionselongationsfaktor b, der die Phosphorylierung von RNA-Polymerase II steuert, und letztlich zu einer Stimulation der Transkriptionselongation führt. Die wesentliche Rolle von BRD4 bei der Zellproliferation und Krebswachstum wurde in mehreren Studien berichtet.

Hier wurde die Bindung von BRD4 BD1 und BD2 zu verschiedenen Partnern analysiert. Die Ergebnisse zeigen, dass die stärksten Wechselwirkungen mit Di- und Tetra-acetylierte Peptide aus dem Histon 4 (H4) erfolgten. Weiterhin konnte gezeigt werden, dass mehrere H4 Aminosäuren in der Nähe der azetylierten Lysinen auch maßgeblich die Bindung beeinflussen. Zehn verschiedene BRD4 BD1 Mutanten wurden erzeugt und ihre Affinitäten zu dem azetyliertem Histonende und dem BET-Inhibitor JQ1 wurden mit mehreren biochemischen und biophysikalischen Methoden untersucht. Insgesamt zeigen die Ergebnisse, dass W81, Y97, N140 und M149 eine ähnliche wichtige Rolle spielen bei der Erkennung von azetylierten Histonen und von JQ1. P82, L94, D145 und I146 haben eine differenziertere Rolle, was darauf hinweist, dass verschiedene Arten von Wechselwirkungen stattfinden und dass Resistenzmutationen mit BRD4-Funktion kompatibel sind. Die Auswirkungen der Schlüsselmutationen wurden anschließend in einer zellulären Umgebung analysiert.

Unsere Studie erweitert das Wissen über den Beitrag einzelner BRD4 Aminosäuren zur Histon- und JQ1-Bindung und kann bei der zukünftigen Gestaltung neuen BET-Antagonisten mit verbesserten pharmakologischen Eigenschaften nützlich sein.

Summary

Bromodomain protein 4 (BRD4) is a member of the bromodomain and extra-terminal domain (BET) protein family. It binds to acetylated histone tails via its tandem bromodomains BD1 and BD2, and forms a complex with the positive transcription elongation factor b which controls phosphorylation of RNA polymerase II, ultimately leading to stimulation of transcription elongation. An essential role of BRD4 in cell proliferation and cancer growth has been reported in several recent studies.

Here the binding of BRD4 BD1 and BD2 to different partners was analyzed and showed that the strongest interactions took place with di- and tetra-acetylated peptides derived from the histone 4 (H4) N-terminal tail. Several H4 residues neighboring the acetylated lysines were also found to significantly influence binding. Ten different BRD4 BD1 mutants were generated and their affinities to acetylated histone tails and to the BET inhibitor JQ1 were analyzed using several complementary biochemical and biophysical methods. Altogether, the results show that W81, Y97, N140 and M149 play similarly important roles in the recognition of acetylated histones and JQ1. P82, L94, D145 and I146 have a more differentiated role, suggesting that different kinds of interactions take place and that resistance mutations compatible with BRD4 function are possible.

The impact of the key mutations was further analyzed in a cellular environment. Our study extends the knowledge on the contribution of individual BRD4 amino acids to histone and JQ1 binding, and may help in the design of new BET antagonists with improved pharmacological properties.

References

Ai, N., X. Hu, F. Ding, B. Yu, H. Wang, X. Lu, K. Zhang, Y. Li, A. Han, W. Lin, R. Liu and R. Chen (2011). "Signal-induced Brd4 release from chromatin is essential for its role transition from chromatin targeting to transcriptional regulation." Nucleic Acids Res **39**(22): 9592-9604.

Allfrey, V. G., R. Faulkner and A. E. Mirsky (1964). "Acetylation and methylation of histones and their possible role in the regulation of RNA synthesis." Proc Natl Acad Sci U S A **51**: 786-794.

Alsarraj, J., F. Faraji, T. R. Geiger, K. R. Mattaini, M. Williams, J. Wu, N. H. Ha, T. Merlino, R. C. Walker, A. D. Bosley, Z. Xiao, T. Andresson, D. Esposito, N. Smithers, D. Lugo, R. Prinjha, A. Day, N. P. Crawford, K. Ozato, K. Gardner and K. W. Hunter (2013). "BRD4 short isoform interacts with RRP1B, SIPA1 and components of the LINC complex at the inner face of the nuclear membrane." PLoS One **8**(11): e80746.

Asangani, I. A., B. Ateeq, Q. Cao, L. Dodson, M. Pandhi, L. P. Kunju, R. Mehra, R. J. Lonigro, J. Siddiqui, N. Palanisamy, Y. M. Wu, X. Cao, J. H. Kim, M. Zhao, Z. S. Qin, M. K. Iyer, C. A. Maher, C. Kumar-Sinha, S. Varambally and A. M. Chinnaiyan (2013). "Characterization of the EZH2-MMSET histone methyltransferase regulatory axis in cancer." Mol Cell **49**(1): 80-93.

Asangani, I. A., V. L. Dommeti, X. Wang, R. Malik, M. Cieslik, R. Yang, J. Escara-Wilke, K. Wilder-Romans, S. Dhanireddy, C. Engelke, M. K. Iyer, X. Jing, Y. M. Wu, X. Cao, Z. S. Qin, S. Wang, F. Y. Feng and A. M. Chinnaiyan (2014). "Therapeutic targeting of BET bromodomain proteins in castration-resistant prostate cancer." Nature **510**(7504): 278-282.

Barbieri, I., E. Cannizzaro and M. A. Dawson (2013). "Bromodomains as therapeutic targets in cancer." Brief Funct Genomics **12**(3): 219-230.

Bartholomeeusen, K., Y. Xiang, K. Fujinaga and B. M. Peterlin (2012). "Bromodomain and extra-terminal (BET) bromodomain inhibition activate transcription via transient release of positive transcription elongation factor b (P-TEFb) from 7SK small nuclear ribonucleoprotein." J Biol Chem **287**(43): 36609-36616.

Baud, M. G., E. Lin-Shiao, T. Cardote, C. Tallant, A. Pschibul, K. H. Chan, M. Zengerle, J. R. Garcia, T. T. Kwan, F. M. Ferguson and A. Ciulli (2014). "Chemical biology. A bump-and-hole approach to engineer controlled selectivity of BET bromodomain chemical probes." Science **346**(6209): 638-641.

Baylin, S. B. and P. A. Jones (2011). "A decade of exploring the cancer epigenome - biological and translational implications." Nat Rev Cancer **11**(10): 726-734.

Beck, S., I. Hanson, A. Kelly, D. J. Pappin and J. Trowsdale (1992). "A homologue of the Drosophila female sterile homeotic (fsh) gene in the class II region of the human MHC." DNA Seq **2**(4): 203-210.

Belkina, A. C. and G. V. Denis (2012). "BET domain co-regulators in obesity, inflammation and cancer." Nat Rev Cancer **12**(7): 465-477.

Belkina, A. C., B. S. Nikolajczyk and G. V. Denis (2013). "BET protein function is required for inflammation: Brd2 genetic disruption and BET inhibitor JQ1 impair mouse macrophage inflammatory responses." J Immunol **190**(7): 3670-3678.

Berger, S. L., T. Kouzarides, R. Shiekhattar and A. Shilatifard (2009). "An operational definition of epigenetics." Genes Dev **23**(7): 781-783.

Berkovits, B. D., L. Wang, P. Guarnieri and D. J. Wolgemuth (2012). "The testis-specific double bromodomain-containing protein BRDT forms a complex with multiple spliceosome components and is required for mRNA splicing and 3'-UTR truncation in round spermatids." Nucleic Acids Res **40**(15): 7162-7175.

Berkovits, B. D. and D. J. Wolgemuth (2013). "The role of the double bromodomain-containing BET genes during mammalian spermatogenesis." Curr Top Dev Biol **102**: 293-326.

Bhadury, J., L. M. Nilsson, S. Veppil Muralidharan, L. C. Green, Z. Li, E. M. Gesner, H. C. Hansen, U. B. Keller, K. G. McLure and J. A. Nilsson (2014). "BET and HDAC inhibitors induce similar genes and biological effects and synergize to kill in Myc-induced murine lymphoma." Proc Natl Acad Sci U S A **111**(26): E2721-2730.

Bird, A. (2002). "DNA methylation patterns and epigenetic memory." Genes Dev **16**(1): 6-21.

Bird, A. P. (1986). "CpG-rich islands and the function of DNA methylation." Nature **321**(6067): 209-213.

Bisgrove, D. A., T. Mahmoudi, P. Henklein and E. Verdin (2007). "Conserved P-TEFb-interacting domain of BRD4 inhibits HIV transcription." Proc Natl Acad Sci U S A **104**(34): 13690-13695.

Bjerke, L., A. Mackay, M. Nandhabalan, A. Burford, A. Jury, S. Popov, D. A. Bax, D. Carvalho, K. R. Taylor, M. Vinci, I. Bajrami, I. M. McGonnell, C. J. Lord, R. M. Reis, D. Hargrave, A. Ashworth, P. Workman and C. Jones (2013). "Histone H3.3 Mutations Drive Pediatric Glioblastoma through Upregulation of MYCN." Cancer Discov.

Bonora, G., K. Plath and M. Denholtz (2014). "A mechanistic link between gene regulation and genome architecture in mammalian development." Curr Opin Genet Dev **27C**: 92-101.

Brandts, J. F. and L. N. Lin (1990). "Study of strong to ultratight protein interactions using differential scanning calorimetry." Biochemistry **29**(29): 6927-6940.

Bressi, J. C., A. J. Jennings, R. Skene, Y. Wu, R. Melkus, R. De Jong, S. O'Connell, C. E. Grimshaw, M. Navre and A. R. Gangloff (2010). "Exploration of the HDAC2 foot pocket: Synthesis and SAR of substituted N-(2-aminophenyl)benzamides." Bioorg Med Chem Lett **20**(10): 3142-3145.

Cao, J. and Q. Yan (2012). "Histone ubiquitination and deubiquitination in transcription, DNA damage response, and cancer." Front Oncol **2**: 26.

Cavellan, E., P. Asp, P. Percipalle and A. K. Farrants (2006). "The WSTF-SNF2h chromatin remodeling complex interacts with several nuclear proteins in transcription." J Biol Chem **281**(24): 16264-16271.

Chapuy, B., M. R. McKeown, C. Y. Lin, S. Monti, M. G. Roemer, J. Qi, P. B. Rahl, H. H. Sun, K. T. Yeda, J. G. Doench, E. Reichert, A. L. Kung, S. J. Rodig, R. A. Young, M. A. Shipp and J. E. Bradner (2013). "Discovery and characterization of super-enhancer-associated dependencies in diffuse large B cell lymphoma." Cancer Cell **24**(6): 777-790.

Chen, R., J. H. Yik, Q. J. Lew and S. H. Chao (2014). "Brd4 and HEXIM1: multiple roles in P-TEFb regulation and cancer." Biomed Res Int **2014**: 232870.

Cheng, Y. and W. H. Prusoff (1973). "Relationship between the inhibition constant (K1) and the concentration of inhibitor which causes 50 per cent inhibition (I50) of an enzymatic reaction." Biochem Pharmacol **22**(23): 3099-3108.

Cheng, Z., Y. Gong, Y. Ma, K. Lu, X. Lu, L. A. Pierce, R. C. Thompson, S. Muller, S. Knapp and J. Wang (2013). "Inhibition of BET bromodomain targets genetically diverse glioblastoma." Clin Cancer Res **19**(7): 1748-1759.

Chiang, C. M. (2009). "Brd4 engagement from chromatin targeting to transcriptional regulation: selective contact with acetylated histone H3 and H4." F1000 Biol Rep **1**: 98.

Choudhuri, S. (2011). "From Waddington's epigenetic landscape to small noncoding RNA: some important milestones in the history of epigenetics research." Toxicol Mech Methods **21**(4): 252-274.

Chung, C. W. and J. Witherington (2011). "Progress in the discovery of small-molecule inhibitors of bromodomain--histone interactions." J Biomol Screen **16**(10): 1170-1185.

Ciceri, P., S. Muller, A. O'Mahony, O. Fedorov, P. Filippakopoulos, J. P. Hunt, E. A. Lasater, G. Pallares, S. Picaud, C. Wells, S. Martin, L. M. Wodicka, N. P. Shah, D. K. Treiber and S. Knapp (2014). "Dual kinase-bromodomain inhibitors for rationally designed polypharmacology." Nat Chem Biol **10**(4): 305-312.

Conway O'Brien, E., S. Prideaux and T. Chevassut (2014). "The epigenetic landscape of acute myeloid leukemia." Adv Hematol **2014**: 103175.

Costa, F. F. (2005). "Non-coding RNAs: new players in eukaryotic biology." Gene **357**(2): 83-94.

Costa, F. F. (2007). "Non-coding RNAs: lost in translation?" Gene **386**(1-2): 1-10.

Crawford, N. P., J. Alsarraj, L. Lukes, R. C. Walker, J. S. Officewala, H. H. Yang, M. P. Lee, K. Ozato and K. W. Hunter (2008). "Bromodomain 4 activation predicts breast cancer survival." Proc Natl Acad Sci U S A **105**(17): 6380-6385.

Dang, C. V. (2012). "MYC on the path to cancer." Cell **149**(1): 22-35.

Dardenne, E., S. Pierredon, K. Driouch, L. Gratadou, M. Lacroix-Triki, M. P. Espinoza, E. Zonta, S. Germann, H. Mortada, J. P. Villemin, M. Dutertre, R. Lidereau, S. Vagner and D. Auboeuf (2012). "Splicing switch of an epigenetic regulator by RNA helicases promotes tumor-cell invasiveness." Nat Struct Mol Biol **19**(11): 1139-1146.

Dawson, M. A., R. K. Prinjha, A. Dittmann, G. Giotopoulos, M. Bantscheff, W. I. Chan, S. C. Robson, C. W. Chung, C. Hopf, M. M. Savitski, C. Huthmacher, E. Gudgin, D. Lugo, S. Beinke, T. D. Chapman, E. J. Roberts, P. E. Soden, K. R. Auger, O. Mirguet, K. Doehner, R. Delwel, A. K. Burnett, P. Jeffrey, G. Drewes, K. Lee, B. J. Huntly and T. Kouzarides (2011). "Inhibition of BET recruitment to chromatin as an effective treatment for MLL-fusion leukaemia." Nature **478**(7370): 529-533.

Delmore, J. E., G. C. Issa, M. E. Lemieux, P. B. Rahl, J. Shi, H. M. Jacobs, E. Kastritis, T. Gilpatrick, R. M. Paranal, J. Qi, M. Chesi, A. C. Schinzel, M. R. McKeown, T. P. Heffernan, C. R. Vakoc, P. L. Bergsagel, I. M. Ghobrial, P. G. Richardson, R. A. Young, W. C. Hahn, K. C. Anderson, A. L. Kung, J. E. Bradner and C. S. Mitsiades (2011). "BET bromodomain inhibition as a therapeutic strategy to target c-Myc." Cell **146**(6): 904-917.

Demont, E. H., P. Bamborough, C. W. Chung, P. D. Craggs, D. Fallon, L. J. Gordon, P. Grandi, C. I. Hobbs, J. Hussain, E. J. Jones, A. Le Gall, A. M. Michon, D. J. Mitchell, R. K. Prinjha, A. D. Roberts, R. J. Sheppard and R. J. Watson (2014). "1,3-Dimethyl Benzimidazolones Are Potent, Selective Inhibitors of the BRPF1 Bromodomain." ACS Med Chem Lett **5**(11): 1190-1195.

Denis, G. V., M. E. McComb, D. V. Faller, A. Sinha, P. B. Romesser and C. E. Costello (2006). "Identification of transcription complexes that contain the double bromodomain protein Brd2 and chromatin remodeling machines." J Proteome Res **5**(3): 502-511.

DePrimo, S. E., M. Diehn, J. B. Nelson, R. E. Reiter, J. Matese, M. Fero, R. Tibshirani, P. O. Brown and J. D. Brooks (2002). "Transcriptional programs activated by exposure of human prostate cancer cells to androgen." Genome Biol **3**(7): RESEARCH0032.

Devaiah, B. N., B. A. Lewis, N. Cherman, M. C. Hewitt, B. K. Albrecht, P. G. Robey, K. Ozato, R. J. Sims, 3rd and D. S. Singer (2012). "BRD4 is an atypical kinase that phosphorylates Serine2 of the RNA Polymerase II carboxy-terminal domain." Proc Natl Acad Sci U S A **109**(18): 6927-6932.

Devaiah, B. N. and D. S. Singer (2013). "Two faces of brd4: mitotic bookmark and transcriptional lynchpin." Transcription **4**(1): 13-17.

Dey, A., F. Chitsaz, A. Abbasi, T. Misteli and K. Ozato (2003). "The double bromodomain protein Brd4 binds to acetylated chromatin during interphase and mitosis." Proc Natl Acad Sci U S A **100**(15): 8758-8763.

Dey, A., J. Ellenberg, A. Farina, A. E. Coleman, T. Maruyama, S. Sciortino, J. Lippincott-Schwartz and K. Ozato (2000). "A bromodomain protein, MCAP, associates with mitotic chromosomes and affects G(2)-to-M transition." Mol Cell Biol **20**(17): 6537-6549.

Dhalluin, C., J. E. Carlson, L. Zeng, C. He, A. K. Aggarwal and M. M. Zhou (1999). "Structure and ligand of a histone acetyltransferase bromodomain." Nature **399**(6735): 491-496.

Dhar, S., A. Thota and M. R. Rao (2012). "Insights into role of bromodomain, testis-specific (Brdt) in acetylated histone H4-dependent chromatin remodeling in mammalian spermiogenesis." J Biol Chem **287**(9): 6387-6405.

Diribarne, G. and O. Bensaude (2009). "7SK RNA, a non-coding RNA regulating P-TEFb, a general transcription factor." RNA Biol **6**(2): 122-128.

Draker, R., M. K. Ng, E. Sarcinella, V. Ignatchenko, T. Kislinger and P. Cheung (2012). "A combination of H2A.Z and H4 acetylation recruits Brd2 to chromatin during transcriptional activation." PLoS Genet **8**(11): e1003047.

Ember, S. W., J. Y. Zhu, S. H. Olesen, M. P. Martin, A. Becker, N. Berndt, G. I. Georg and E. Schonbrunn (2014). "Acetyl-lysine Binding Site of Bromodomain-Containing Protein 4 (BRD4) Interacts with Diverse Kinase Inhibitors." ACS Chem Biol.

Estojak, J., R. Brent and E. A. Golemis (1995). "Correlation of two-hybrid affinity data with in vitro measurements." Mol Cell Biol **15**(10): 5820-5829.

Feldman, J. L., K. E. Dittenhafer-Reed and J. M. Denu (2012). "Sirtuin catalysis and regulation." J Biol Chem **287**(51): 42419-42427.

Feng, Q., Z. Zhang, M. J. Shea, C. J. Creighton, C. Coarfa, S. G. Hilsenbeck, R. Lanz, B. He, L. Wang, X. Fu, A. Nardone, Y. Song, J. Bradner, N. Mitsiades, C. S. Mitsiades, C. K. Osborne, R. Schiff and B. W. O'Malley (2014). "An epigenomic approach to therapy for tamoxifen-resistant breast cancer." Cell Res **24**(7): 809-819.

Filippakopoulos, P. and S. Knapp (2012). "The bromodomain interaction module." FEBS Lett.

Filippakopoulos, P. and S. Knapp (2014). "Targeting bromodomains: epigenetic readers of lysine acetylation." Nat Rev Drug Discov **13**(5): 337-356.

Filippakopoulos, P., S. Picaud, M. Mangos, T. Keates, J. P. Lambert, D. Barsyte-Lovejoy, I. Felletar, R. Volkmer, S. Muller, T. Pawson, A. C. Gingras, C. H. Arrowsmith and S. Knapp (2012). "Histone recognition and large-scale structural analysis of the human bromodomain family." Cell **149**(1): 214-231.

Filippakopoulos, P., J. Qi, S. Picaud, Y. Shen, W. B. Smith, O. Fedorov, E. M. Morse, T. Keates, T. T. Hickman, I. Felletar, M. Philpott, S. Munro, M. R. McKeown, Y. Wang, A. L. Christie, N. West, M. J. Cameron, B. Schwartz, T. D. Heightman, N. La Thangue, C. A. French, O. Wiest, A. L. Kung, S. Knapp and J. E. Bradner (2010). "Selective inhibition of BET bromodomains." Nature **468**(7327): 1067-1073.

Flemming, W. (1882). Zellsubstanz, Kern und Zelltheilung

Florence, B. and D. V. Faller (2001). "You bet-cha: a novel family of transcriptional regulators." Front Biosci **6**: D1008-1018.

Floyd, S. R., M. E. Pacold, Q. Huang, S. M. Clarke, F. C. Lam, I. G. Cannell, B. D. Bryson, J. Rameseder, M. J. Lee, E. J. Blake, A. Fydrych, R. Ho, B. A. Greenberger, G. C. Chen, A. Maffa, A. M. Del Rosario, D. E. Root, A. E. Carpenter, W. C. Hahn, D. M. Sabatini, C. C. Chen, F. M. White, J. E. Bradner and M. B. Yaffe (2013). "The bromodomain protein Brd4 insulates chromatin from DNA damage signalling." Nature **498**(7453): 246-250.

Fredly, H., B. T. Gjertsen and O. Bruserud (2013). "Histone deacetylase inhibition in the treatment of acute myeloid leukemia: the effects of valproic acid on leukemic cells, and the clinical and experimental evidence for combining valproic acid with other antileukemic agents." Clin Epigenetics **5**(1): 12.

French, C. A. (2010). "Demystified molecular pathology of NUT midline carcinomas." J Clin Pathol **63**(6): 492-496.

French, C. A. (2012). "Pathogenesis of NUT midline carcinoma." Annu Rev Pathol **7**: 247-265.

French, C. A. (2013). "The importance of diagnosing NUT midline carcinoma." Head Neck Pathol **7**(1): 11-16.

French, C. A., I. Miyoshi, J. C. Aster, I. Kubonishi, T. G. Kroll, P. Dal Cin, S. O. Vargas, A. R. Perez-Atayde and J. A. Fletcher (2001). "BRD4 bromodomain gene rearrangement in aggressive carcinoma with translocation t(15;19)." Am J Pathol **159**(6): 1987-1992.

French, C. A., I. Miyoshi, I. Kubonishi, H. E. Grier, A. R. Perez-Atayde and J. A. Fletcher (2003). "BRD4-NUT fusion oncogene: a novel mechanism in aggressive carcinoma." Cancer Res **63**(2): 304-307.

Gallagher, S. J., B. Mijatov, D. Gunatilake, K. Gowrishankar, J. Tiffen, W. James, L. Jin, G. Pupo, C. Cullinane, G. A. McArthur, P. J. Tummino, H. Rizos and P. Hersey (2014). "Control of NF-kB activity in human melanoma by bromodomain and extra-terminal protein inhibitor I-BET151." Pigment Cell Melanoma Res.

Gallagher, S. J., B. Mijatov, D. Gunatilake, J. C. Tiffen, K. Gowrishankar, L. Jin, G. M. Pupo, C. Cullinane, R. K. Prinjha, N. Smithers, G. A. McArthur, H. Rizos and P. Hersey (2014). "The Epigenetic Regulator I-BET151 Induces BIM-Dependent Apoptosis and Cell Cycle Arrest of Human Melanoma Cells." J Invest Dermatol.

Gallenkamp, D., K. A. Gelato, B. Haendler and H. Weinmann (2014). "Bromodomains and Their Pharmacological Inhibitors." ChemMedChem **9**: 438–464.

Gamsjaeger, R., S. R. Webb, J. M. Lamonica, A. Billin, G. A. Blobel and J. P. Mackay (2011). "Structural basis and specificity of acetylated transcription factor GATA1 recognition by BET family bromodomain protein Brd3." Mol Cell Biol **31**(13): 2632-2640.

Ganesan, A., L. Nolan, S. J. Crabb and G. Packham (2009). "Epigenetic therapy: histone acetylation, DNA methylation and anti-cancer drug discovery." Curr Cancer Drug Targets **9**(8): 963-981.

Garcia-Gutierrez, P., M. Mundi and M. Garcia-Dominguez (2012). "Association of bromodomain BET proteins to the chromatin requires dimerization through the conserved motif B." J Cell Sci.

Gaucher, J., F. Boussouar, E. Montellier, S. Curtet, T. Buchou, S. Bertrand, P. Hery, S. Jounier, A. Depaux, A. L. Vitte, P. Guardiola, K. Pernet, A. Debernardi, F. Lopez, H. Holota, J. Imbert, D. J. Wolgemuth, M. Gerard, S. Rousseaux and S. Khochbin (2012). "Bromodomain-dependent stage-specific male genome programming by Brdt." EMBO J **31**(19): 3809-3820.

Goldberg, A. D., C. D. Allis and E. Bernstein (2007). "Epigenetics: a landscape takes shape." Cell **128**(4): 635-638.

Gong, F. and K. M. Miller (2013). "Mammalian DNA repair: HATs and HDACs make their mark through histone acetylation." Mutat Res **750**(1-2): 23-30.

Grayson, A. R., E. M. Walsh, M. J. Cameron, J. Godec, T. Ashworth, J. M. Ambrose, A. B. Aserlind, H. Wang, G. I. Evan, M. J. Kluk, J. E. Bradner, J. C. Aster and C. A. French (2014). "MYC, a downstream target of BRD-NUT, is necessary and sufficient for the blockade of differentiation in NUT midline carcinoma." Oncogene **33**(13): 1736-1742.

Greenwald, R. J., J. R. Tumang, A. Sinha, N. Currier, R. D. Cardiff, T. L. Rothstein, D. V. Faller and G. V. Denis (2004). "E mu-BRD2 transgenic mice develop B-cell lymphoma and leukemia." Blood **103**(4): 1475-1484.

Greer, E. L. and Y. Shi (2012). "Histone methylation: a dynamic mark in health, disease and inheritance." Nat Rev Genet **13**(5): 343-357.

Gregory, G. D., C. R. Vakoc, T. Rozovskaia, X. Zheng, S. Patel, T. Nakamura, E. Canaani and G. A. Blobel (2007). "Mammalian ASH1L is a histone methyltransferase that occupies the transcribed region of active genes." Mol Cell Biol **27**(24): 8466-8479.

Gurard-Levin, Z. A. and G. Almouzni (2014). "Histone modifications and a choice of variant: a language that helps the genome express itself." F1000Prime Rep **6**: 76.

Hayami, S., J. D. Kelly, H. S. Cho, M. Yoshimatsu, M. Unoki, T. Tsunoda, H. I. Field, D. E. Neal, H. Yamaue, B. A. Ponder, Y. Nakamura and R. Hamamoto (2011). "Overexpression of LSD1 contributes to human carcinogenesis through chromatin regulation in various cancers." Int J Cancer **128**(3): 574-586.

Haynes, S. R., B. A. Mozer, N. Bhatia-Dey and I. B. Dawid (1989). "The Drosophila fsh locus, a maternal effect homeotic gene, encodes apparent membrane proteins." Dev Biol **134**(1): 246-257.

He, H. and N. Lehming (2003). "Global effects of histone modifications." Brief Funct Genomic Proteomic **2**(3): 234-243.

Henssen, A., T. Thor, A. Odersky, L. Heukamp, N. El-Hindy, A. Beckers, F. Speleman, K. Althoff, S. Schafers, A. Schramm, U. Sure, G. Fleischhack, A. Eggert and J. H. Schulte (2013). "BET bromodomain protein inhibition is a therapeutic option for medulloblastoma." Oncotarget **4**(11): 2080-2095.

Hewings, D. S., T. P. Rooney, L. E. Jennings, D. A. Hay, C. J. Schofield, P. E. Brennan, S. Knapp and S. J. Conway (2012). "Progress in the development and application of small molecule inhibitors of bromodomain-acetyl-lysine interactions." J Med Chem **55**(22): 9393-9413.

Hnilicova, J., S. Hozeifi, E. Stejskalova, E. Duskova, I. Poser, J. Humpolickova, M. Hof and D. Stanek (2013). "The C-terminal domain of Brd2 is important for chromatin interaction and regulation of transcription and alternative splicing." Mol Biol Cell **24**(22): 3557-3568.

Horikoshi, M. (2013). "Histone acetylation: from code to web and router via intrinsically disordered regions." Curr Pharm Des **19**(28): 5019-5042.

Houzelstein, D., S. L. Bullock, D. E. Lynch, E. F. Grigorieva, V. A. Wilson and R. S. Beddington (2002). "Growth and early postimplantation defects in mice deficient for the bromodomain-containing protein Brd4." Mol Cell Biol **22**(11): 3794-3802.

Hu, X., X. Lu, R. Liu, N. Ai, Z. Cao, Y. Li, J. Liu, B. Yu, K. Liu, H. Wang, C. Zhou, Y. Wang, A. Han, F. Ding and R. Chen (2014). "Histone Crosstalk Connects Protein Phosphatase 1alpha (PP1alpha) and Histone Deacetylase (HDAC) Pathways to Regulate the Functional Transition of Bromodomain-containing 4 (Brd4) for Inducible Gene Expression." J Biol Chem.

Huang, B., X. D. Yang, M. M. Zhou, K. Ozato and L. F. Chen (2009). "Brd4 coactivates transcriptional activation of NF-kappaB via specific binding to acetylated RelA." Mol Cell Biol **29**(5): 1375-1387.

Hussong, M., S. T. Borno, M. Kerick, A. Wunderlich, A. Franz, H. Sultmann, B. Timmermann, H. Lehrach, M. Hirsch-Kauffmann and M. R. Schweiger (2014). "The bromodomain protein BRD4 regulates the KEAP1/NRF2-dependent oxidative stress response." Cell Death Dis **5**: e1195.

Ito, T., T. Umehara, K. Sasaki, Y. Nakamura, N. Nishino, T. Terada, M. Shirouzu, B. Padmanabhan, S. Yokoyama, A. Ito and M. Yoshida (2011). "Real-time imaging of histone H4K12-specific acetylation determines the modes of action of histone deacetylase and bromodomain inhibitors." Chem Biol **18**(4): 495-507.

Jacobson, R. H., A. G. Ladurner, D. S. King and R. Tjian (2000). "Structure and function of a human TAFII250 double bromodomain module." Science **288**(5470): 1422-1425.

Jenuwein, T. and C. D. Allis (2001). "Translating the histone code." Science **293**(5532): 1074-1080.

Jin, C., C. Zang, G. Wei, K. Cui, W. Peng, K. Zhao and G. Felsenfeld (2009). "H3.3/H2A.Z double variant-containing nucleosomes mark 'nucleosome-free regions' of active promoters and other regulatory regions." Nat Genet **41**(8): 941-945.

Johnson, C. A. and B. M. Turner (1999). "Histone deacetylases: complex transducers of nuclear signals." Semin Cell Dev Biol **10**(2): 179-188.

Jones, D. T., N. Jager, M. Kool, T. Zichner, B. Hutter, M. Sultan, Y. J. Cho, T. J. Pugh, V. Hovestadt, A. M. Stutz, T. Rausch, H. J. Warnatz, M. Ryzhova, S. Bender, D. Sturm, S. Pleier, H. Cin, E. Pfaff, L. Sieber, A. Wittmann, M. Remke, H. Witt, S. Hutter, T. Tzaridis, J. Weischenfeldt, B. Raeder, M. Avci, V. Amstislavskiy, M. Zapatka, U. D. Weber, Q. Wang, B. Lasitschka, C. C. Bartholomae, M. Schmidt, C. von Kalle, V. Ast, C. Lawerenz, J. Eils, R. Kabbe, V. Benes, P. van Sluis, J. Koster, R. Volckmann, D. Shih, M. J. Betts, R. B. Russell, S. Coco, G. P. Tonini, U. Schuller, V. Hans, N. Graf, Y. J. Kim, C. Monoranu, W. Roggendorf, A. Unterberg, C. Herold-Mende, T. Milde, A. E. Kulozik, A. von Deimling, O. Witt, E. Maass, J. Rossler, M. Ebinger, M. U. Schuhmann, M. C. Fruhwald, M. Hasselblatt, N. Jabado, S. Rutkowski, A. O. von Bueren, D. Williamson, S. C. Clifford, M. G. McCabe, V. P. Collins, S. Wolf, S. Wiemann, H. Lehrach, B. Brors, W. Scheurlen, J. Felsberg, G. Reifenberger, P. A. Northcott, M. D. Taylor, M. Meyerson, S. L. Pomeroy, M. L. Yaspo, J. O. Korbel, A. Korshunov, R. Eils, S. M. Pfister and P. Lichter (2012). "Dissecting the genomic complexity underlying medulloblastoma." Nature **488**(7409): 100-105.

Jung, M., K. A. Gelato, A. Fernandez-Montalvan, S. Siegel and B. Haendler (2015). "Targeting BET bromodomains for cancer treatment." Epigenomics **in press**.

Jung, M., M. Philpott, S. Muller, J. Schulze, V. Badock, U. Eberspacher, D. Moosmayer, B. Bader, N. Schmees, A. Fernandez-Montalvan and B. Haendler (2014). "Affinity Map of BRD4 Interactions with the Histone H4 Tail and the Small Molecule Inhibitor JQ1." J Biol Chem.

Kahl, P., L. Gullotti, L. C. Heukamp, S. Wolf, N. Friedrichs, R. Vorreuther, G. Solleder, P. J. Bastian, J. Ellinger, E. Metzger, R. Schule and R. Buettner (2006). "Androgen receptor coactivators lysine-specific histone demethylase 1 and four and a half LIM domain protein 2 predict risk of prostate cancer recurrence." Cancer Res **66**(23): 11341-11347.

Kanno, T., Y. Kanno, G. LeRoy, E. Campos, H. W. Sun, S. R. Brooks, G. Vahedi, T. D. Heightman, B. A. Garcia, D. Reinberg, U. Siebenlist, J. J. O'Shea and K. Ozato (2014). "BRD4 assists elongation of both coding and enhancer RNAs by interacting with acetylated histones." Nat Struct Mol Biol.

Kanno, T., Y. Kanno, R. M. Siegel, M. K. Jang, M. J. Lenardo and K. Ozato (2004). "Selective recognition of acetylated histones by bromodomain proteins visualized in living cells." Mol Cell **13**(1): 33-43.

Kauffman, E. C., B. D. Robinson, M. J. Downes, L. G. Powell, M. M. Lee, D. S. Scherr, L. J. Gudas and N. P. Mongan (2011). "Role of androgen receptor and associated lysine-demethylase coregulators, LSD1 and JMJD2A, in localized and advanced human bladder cancer." Mol Carcinog **50**(12): 931-944.

Khan, O. and N. B. La Thangue (2012). "HDAC inhibitors in cancer biology: emerging mechanisms and clinical applications." Immunol Cell Biol **90**(1): 85-94.

Khorasanizadeh, S. (2004). "The nucleosome: from genomic organization to genomic regulation." Cell **116**(2): 259-272.

Kleer, C. G., Q. Cao, S. Varambally, R. Shen, I. Ota, S. A. Tomlins, D. Ghosh, R. G. Sewalt, A. P. Otte, D. F. Hayes, M. S. Sabel, D. Livant, S. J. Weiss, M. A. Rubin and A. M. Chinnaiyan (2003). "EZH2 is a marker of aggressive breast cancer and promotes neoplastic transformation of breast epithelial cells." Proc Natl Acad Sci U S A **100**(20): 11606-11611.

Klose, R. J. and Y. Zhang (2007). "Regulation of histone methylation by demethylimination and demethylation." Nat Rev Mol Cell Biol **8**(4): 307-318.

Kornberg, R. D. (1974). "Chromatin structure: a repeating unit of histones and DNA." Science **184**(4139): 868-871.

Korzus, E. (2010). "Manipulating the brain with epigenetics." Nat Neurosci **13**(4): 405-406.

Kwak, H. and J. T. Lis (2013). "Control of transcriptional elongation." Annu Rev Genet **47**: 483-508.

Lamonica, J. M., W. Deng, S. Kadauke, A. E. Campbell, R. Gamsjaeger, H. Wang, Y. Cheng, A. N. Billin, R. C. Hardison, J. P. Mackay and G. A. Blobel (2011). "Bromodomain protein Brd3 associates with acetylated GATA1 to promote its chromatin occupancy at erythroid target genes." Proc Natl Acad Sci U S A **108**(22): E159-168.

Layton, C. J. and H. W. Hellinga (2010). "Thermodynamic analysis of ligand-induced changes in protein thermal unfolding applied to high-throughput determination of ligand affinities with extrinsic fluorescent dyes." Biochemistry **49**(51): 10831-10841.

Lee, J. J., G. F. Murphy and C. G. Lian (2014). "Melanoma epigenetics: novel mechanisms, markers, and medicines." Lab Invest **94**(8): 822-838.

Lee, K. K. and J. L. Workman (2007). "Histone acetyltransferase complexes: one size doesn't fit all." Nat Rev Mol Cell Biol **8**(4): 284-295.

LeRoy, G., B. Rickards and S. J. Flint (2008). "The double bromodomain proteins Brd2 and Brd3 couple histone acetylation to transcription." Mol Cell **30**(1): 51-60.

Li, K. K., C. Luo, D. Wang, H. Jiang and Y. G. Zheng (2012). "Chemical and biochemical approaches in the study of histone methylation and demethylation." Med Res Rev **32**(4): 815-867.

Liu, W., Q. Ma, K. Wong, W. Li, K. Ohgi, J. Zhang, A. K. Aggarwal and M. G. Rosenfeld (2013). "Brd4 and JMJD6-associated anti-pause enhancers in regulation of transcriptional pause release." Cell **155**(7): 1581-1595.

Liu, Y., X. Wang, J. Zhang, H. Huang, B. Ding, J. Wu and Y. Shi (2008). "Structural basis and binding properties of the second bromodomain of Brd4 with acetylated histone tails." Biochemistry **47**(24): 6403-6417.

Lockwood, W. W., K. Zejnullahu, J. E. Bradner and H. Varmus (2012). "Sensitivity of human lung adenocarcinoma cell lines to targeted inhibition of BET epigenetic signaling proteins." Proc Natl Acad Sci U S A **109**(47): 19408-19413.

Loury, R. and P. Sassone-Corsi (2003). "Histone phosphorylation: how to proceed." Methods **31**(1): 40-48.

Loven, J., H. A. Hoke, C. Y. Lin, A. Lau, D. A. Orlando, C. R. Vakoc, J. E. Bradner, T. I. Lee and R. A. Young (2013). "Selective inhibition of tumor oncogenes by disruption of super-enhancers." Cell **153**(2): 320-334.

Loyola, A., T. Bonaldi, D. Roche, A. Imhof and G. Almouzni (2006). "PTMs on H3 variants before chromatin assembly potentiate their final epigenetic state." Mol Cell **24**(2): 309-316.

Malik, S. and S. R. Bhaumik (2010). "Mixed lineage leukemia: histone H3 lysine 4 methyltransferases from yeast to human." FEBS J **277**(8): 1805-1821.

Marmorstein, R. and R. C. Trievel (2009). "Histone modifying enzymes: structures, mechanisms, and specificities." Biochim Biophys Acta **1789**(1): 58-68.

Martinez Molina, D., R. Jafari, M. Ignatushchenko, T. Seki, E. A. Larsson, C. Dan, L. Sreekumar, Y. Cao and P. Nordlund (2013). "Monitoring drug target engagement in cells and tissues using the cellular thermal shift assay." Science **341**(6141): 84-87.

Masica, D. L. and R. Karchin (2013). "Collections of simultaneously altered genes as biomarkers of cancer cell drug response." Cancer Res **73**(6): 1699-1708.

Matulis, D., J. K. Kranz, F. R. Salemme and M. J. Todd (2005). "Thermodynamic stability of carbonic anhydrase: measurements of binding affinity and stoichiometry using ThermoFluor." Biochemistry **44**(13): 5258-5266.

Matzuk, M. M., M. R. McKeown, P. Filippakopoulos, Q. Li, L. Ma, J. E. Agno, M. E. Lemieux, S. Picaud, R. N. Yu, J. Qi, S. Knapp and J. E. Bradner (2012). "Small-molecule inhibition of BRDT for male contraception." Cell **150**(4): 673-684.

Maxmen, A. (2012). "Cancer research: Open ambition." Nature **488**(7410): 148-150.

Mertz, J. A., A. R. Conery, B. M. Bryant, P. Sandy, S. Balasubramanian, D. A. Mele, L. Bergeron and R. J. Sims, 3rd (2011). "Targeting MYC dependence in cancer by inhibiting BET bromodomains." Proc Natl Acad Sci U S A **108**(40): 16669-16674.

Meyer, N. and L. Z. Penn (2008). "Reflecting on 25 years with MYC." Nat Rev Cancer **8**(12): 976-990.

Mochizuki, K., A. Nishiyama, M. K. Jang, A. Dey, A. Ghosh, T. Tamura, H. Natsume, H. Yao and K. Ozato (2008). "The bromodomain protein Brd4 stimulates G1 gene transcription and promotes progression to S phase." J Biol Chem **283**(14): 9040-9048.

Mohrmann, L., K. Langenberg, J. Krijgsveld, A. J. Kal, A. J. Heck and C. P. Verrijzer (2004). "Differential targeting of two distinct SWI/SNF-related Drosophila chromatin-remodeling complexes." Mol Cell Biol **24**(8): 3077-3088.

Moriniere, J., S. Rousseaux, U. Steuerwald, M. Soler-Lopez, S. Curtet, A. L. Vitte, J. Govin, J. Gaucher, K. Sadoul, D. J. Hart, J. Krijgsveld, S. Khochbin, C. W. Muller and C. Petosa (2009). "Cooperative binding of two acetylation marks on a histone tail by a single bromodomain." Nature **461**(7264): 664-668.

Muller, S. and G. Almouzni (2014). "A network of players in H3 histone variant deposition and maintenance at centromeres." Biochim Biophys Acta **1839**(3): 241-250.

Muller, S., P. Filippakopoulos and S. Knapp (2011). "Bromodomains as therapeutic targets." Expert Rev Mol Med **13**: e29.

Musselman, C. A., M. E. Lalonde, J. Cote and T. G. Kutateladze (2012). "Perceiving the epigenetic landscape through histone readers." Nat Struct Mol Biol **19**(12): 1218-1227.

Myers, J. K., C. N. Pace and J. M. Scholtz (1995). "Denaturant m values and heat capacity changes: relation to changes in accessible surface areas of protein unfolding." Protein Sci **4**(10): 2138-2148.

Myung, J. K., C. A. Banuelos, J. G. Fernandez, N. R. Mawji, J. Wang, A. H. Tien, Y. C. Yang, I. Tavakoli, S. Haile, K. Watt, I. J. McEwan, S. Plymate, R. J. Andersen and M. D. Sadar (2013). "An androgen receptor N-terminal domain antagonist for treating prostate cancer." J Clin Invest **123**(7): 2948-2960.

Nagarajan, S., T. Hossan, M. Alawi, Z. Najafova, D. Indenbirken, U. Bedi, H. Taipaleenmaki, I. Ben-Batalla, M. Scheller, S. Loges, S. Knapp, E. Hesse, C. M. Chiang, A. Grundhoff and S. A. Johnsen (2014). "Bromodomain Protein BRD4 Is Required for Estrogen Receptor-Dependent Enhancer Activation and Gene Transcription." Cell Rep **8**(2): 460-469.

Nicodeme, E., K. L. Jeffrey, U. Schaefer, S. Beinke, S. Dewell, C. W. Chung, R. Chandwani, I. Marazzi, P. Wilson, H. Coste, J. White, J. Kirilovsky, C. M. Rice, J. M. Lora, R. K. Prinjha, K. Lee and A. Tarakhovsky (2010). "Suppression of inflammation by a synthetic histone mimic." Nature **468**(7327): 1119-1123.

Owen, D. J., P. Ornaghi, J. C. Yang, N. Lowe, P. R. Evans, P. Ballario, D. Neuhaus, P. Filetici and A. A. Travers (2000). "The structural basis for the recognition of acetylated histone H4 by the bromodomain of histone acetyltransferase gcn5p." EMBO J **19**(22): 6141-6149.

Pastori, C., M. Daniel, C. Penas, C. H. Volmar, A. L. Johnstone, S. P. Brothers, R. M. Graham, B. Allen, J. N. Sarkaria, R. J. Komotar, C. Wahlestedt and N. G. Ayad (2014). "BET bromodomain proteins are required for glioblastoma cell proliferation." Epigenetics **9**(4).

Peters, A. H. and D. Schubeler (2005). "Methylation of histones: playing memory with DNA." Curr Opin Cell Biol **17**(2): 230-238.

Phillips, D. M. and E. W. Johns (1965). "A FRACTIONATION OF THE HISTONES OF GROUP F2A FROM CALF THYMUS." Biochem J **94**: 127-130.

Pillai, R. S., S. N. Bhattacharyya and W. Filipowicz (2007). "Repression of protein synthesis by miRNAs: how many mechanisms?" Trends Cell Biol **17**(3): 118-126.

Pivot-Pajot, C., C. Caron, J. Govin, A. Vion, S. Rousseaux and S. Khochbin (2003). "Acetylation-dependent chromatin reorganization by BRDT, a testis-specific bromodomain-containing protein." Mol Cell Biol **23**(15): 5354-5365.

Plass, C., S. M. Pfister, A. M. Lindroth, O. Bogatyrova, R. Claus and P. Lichter (2013). "Mutations in regulators of the epigenome and their connections to global chromatin patterns in cancer." Nat Rev Genet **14**(11): 765-780.

Prinjha, R. K., J. Witherington and K. Lee (2012). "Place your BETs: the therapeutic potential of bromodomains." Trends Pharmacol Sci **33**(3): 146-153.

Puissant, A., S. M. Frumm, G. Alexe, C. F. Bassil, J. Qi, Y. H. Chanthery, E. A. Nekritz, R. Zeid, W. C. Gustafson, P. Greninger, M. J. Garnett, U. McDermott, C. H. Benes, A. L. Kung, W. A. Weiss, J. E. Bradner and K. Stegmaier (2013). "Targeting MYCN in Neuroblastoma by BET Bromodomain Inhibition." Cancer Discov.

Qi, P. and X. Du (2013). "The long non-coding RNAs, a new cancer diagnostic and therapeutic gold mine." Mod Pathol **26**(2): 155-165.

Quina, A. S., M. Buschbeck and L. Di Croce (2006). "Chromatin structure and epigenetics." Biochem Pharmacol **72**(11): 1563-1569.

Rahman, S., M. E. Sowa, M. Ottinger, J. A. Smith, Y. Shi, J. W. Harper and P. M. Howley (2011). "The Brd4 extraterminal domain confers transcription activation independent of pTEFb by recruiting multiple proteins, including NSD3." Mol Cell Biol **31**(13): 2641-2652.

Rando, O. J. and F. Winston (2012). "Chromatin and transcription in yeast." Genetics **190**(2): 351-387.

Ray, S., Y. Zhao, M. Jamaluddin, C. B. Edeh, C. Lee and A. R. Brasier (2014). "Inducible STAT3 NH2 terminal mono-ubiquitination promotes BRD4 complex formation to regulate apoptosis." Cell Signal **26**(7): 1445-1455.

Rea, S., F. Eisenhaber, D. O'Carroll, B. D. Strahl, Z. W. Sun, M. Schmid, S. Opravil, K. Mechtler, C. P. Ponting, C. D. Allis and T. Jenuwein (2000). "Regulation of chromatin structure by site-specific histone H3 methyltransferases." Nature **406**(6796): 593-599.

Reeves, R., C. M. Gorman and B. Howard (1985). "Minichromosome assembly of non-integrated plasmid DNA transfected into mammalian cells." Nucleic Acids Res **13**(10): 3599-3615.

Reik, W., W. Dean and J. Walter (2001). "Epigenetic reprogramming in mammalian development." Science **293**(5532): 1089-1093.

Reynoird, N., B. E. Schwartz, M. Delvecchio, K. Sadoul, D. Meyers, C. Mukherjee, C. Caron, H. Kimura, S. Rousseaux, P. A. Cole, D. Panne, C. A. French and S. Khochbin (2010). "Oncogenesis by sequestration of CBP/p300 in transcriptionally inactive hyperacetylated chromatin domains." EMBO J **29**(17): 2943-2952.

Ryan, R. J. and B. E. Bernstein (2012). "Molecular biology. Genetic events that shape the cancer epigenome." Science **336**(6088): 1513-1514.

Sahai, V., K. Kumar, L. M. Knab, C. R. Chow, S. S. Raza, D. J. Bentrem, K. Ebine and H. G. Munshi (2014). "BET Bromodomain Inhibitors Block Growth of Pancreatic Cancer Cells in Three-Dimensional Collagen." Mol Cancer Ther **13**(7): 1907-1917.

Sanchez, R., J. Meslamani and M. M. Zhou (2014). "The bromodomain: From epigenome reader to druggable target." Biochim Biophys Acta.

Schaukowitch, K. and T. K. Kim (2014). "Emerging epigenetic mechanisms of long non-coding RNAs." Neuroscience **264**: 25-38.

Schreiber, S. L. and B. E. Bernstein (2002). "Signaling network model of chromatin." Cell **111**(6): 771-778.

Schroder, S., S. Cho, L. Zeng, Q. Zhang, K. Kaehlcke, L. Mak, J. Lau, D. Bisgrove, M. Schnolzer, E. Verdin, M. M. Zhou and M. Ott (2012). "Two-pronged binding with bromodomain-containing protein 4 liberates positive transcription elongation factor b from inactive ribonucleoprotein complexes." J Biol Chem **287**(2): 1090-1099.

Schulze, J., D. Moosmayer, J. Weiske, A. Fernandez-Montalvan, C. Herbst, M. Jung and B. Haendler (2014). "Cell-Based Protein Stabilization Assays for the Detection of Interactions between Small Molecule Inhibitors and BRD4." Journal of Biomolecular Screening **in press**.

Schulze, J., D. Moosmayer, J. Weiske, A. Fernandez-Montalvan, C. Herbst, M. Jung, B. Haendler and B. Bader (2014). "Cell-Based Protein Stabilization Assays for the Detection of Interactions between Small-Molecule Inhibitors and BRD4." J Biomol Screen.

Schwartzentruber, J., A. Korshunov, X. Y. Liu, D. T. Jones, E. Pfaff, K. Jacob, D. Sturm, A. M. Fontebasso, D. A. Quang, M. Tonjes, V. Hovestadt, S. Albrecht, M. Kool, A. Nantel, C. Konermann, A. Lindroth, N. Jager, T. Rausch, M. Ryzhova, J. O. Korbel, T. Hielscher, P. Hauser, M. Garami, A. Klekner, L. Bognar, M. Ebinger, M. U. Schuhmann, W. Scheurlen, A. Pekrun, M. C. Fruhwald, W. Roggendorf, C. Kramm, M. Durken, J. Atkinson, P. Lepage, A. Montpetit, M. Zakrzewska, K. Zakrzewski, P. P. Liberski, Z. Dong, P. Siegel, A. E. Kulozik, M. Zapatka, A. Guha, D. Malkin, J. Felsberg, G. Reifenberger, A. von Deimling, K. Ichimura, V. P. Collins, H. Witt, T. Milde, O. Witt, C. Zhang, P. Castelo-Branco, P. Lichter, D. Faury, U. Tabori, C. Plass, J. Majewski, S. M. Pfister and N. Jabado (2012). "Driver mutations in histone H3.3 and chromatin remodelling genes in paediatric glioblastoma." Nature **482**(7384): 226-231.

Segura, M. F., B. Fontanals-Cirera, A. Gaziel-Sovran, M. V. Guijarro, D. Hanniford, G. Zhang, P. Gonzalez-Gomez, M. Morante, L. Jubierre, W. Zhang, F. Darvishian, M. Ohlmeyer, I. Osman, M. M. Zhou and E. Hernando (2013). "BRD4 sustains proliferation and represents a new target for epigenetic therapy in melanoma." Cancer Res **73**(20): 6264-6276.

Shang, E., H. D. Nickerson, D. Wen, X. Wang and D. J. Wolgemuth (2007). "The first bromodomain of Brdt, a testis-specific member of the BET sub-family of double-bromodomain-containing proteins, is essential for male germ cell differentiation." Development **134**(19): 3507-3515.

Shang, E., X. Wang, D. Wen, D. A. Greenberg and D. J. Wolgemuth (2009). "Double bromodomain-containing gene Brd2 is essential for embryonic development in mouse." Dev Dyn **238**(4): 908-917.

Shen, C. and C. R. Vakoc (2015). "Gain-of-function mutation of chromatin regulators as a tumorigenic mechanism and an opportunity for therapeutic intervention." Curr Opin Oncol **27**(1): 57-63.

Shi, J., Y. Wang, L. Zeng, Y. Wu, J. Deng, Q. Zhang, Y. Lin, J. Li, T. Kang, M. Tao, E. Rusinova, G. Zhang, C. Wang, H. Zhu, J. Yao, Y. X. Zeng, B. M. Evers, M. M. Zhou and B. P. Zhou (2014). "Disrupting the interaction of BRD4 with diacetylated Twist suppresses tumorigenesis in basal-like breast cancer." Cancer Cell **25**(2): 210-225.

Shiio, Y. and R. N. Eisenman (2003). "Histone sumoylation is associated with transcriptional repression." Proc Natl Acad Sci U S A **100**(23): 13225-13230.

Shilatifard, A. (2006). "Chromatin modifications by methylation and ubiquitination: implications in the regulation of gene expression." Annu Rev Biochem **75**: 243-269.

Shimamura, T., Z. Chen, M. Soucheray, J. Carretero, E. Kikuchi, J. H. Tchaicha, Y. Gao, K. A. Cheng, T. J. Cohoon, J. Qi, E. Akbay, A. C. Kimmelman, A. L. Kung, J. E. Bradner and K. K. Wong (2013). "Efficacy of BET bromodomain inhibition in Kras-mutant non-small cell lung cancer." Clin Cancer Res **19**(22): 6183-6192.

Sierra, J. R., V. Cepero and S. Giordano (2010). "Molecular mechanisms of acquired resistance to tyrosine kinase targeted therapy." Mol Cancer **9**: 75.

Simo-Riudalbas, L. and M. Esteller (2014). "Targeting the histone orthography of cancer: drugs for writers, erasers and readers." Br J Pharmacol.

Smith, S. G., R. Sanchez and M. M. Zhou (2014). "Privileged diazepine compounds and their emergence as bromodomain inhibitors." Chem Biol **21**(5): 573-583.

Sneeringer, C. J., M. P. Scott, K. W. Kuntz, S. K. Knutson, R. M. Pollock, V. M. Richon and R. A. Copeland (2010). "Coordinated activities of wild-type plus mutant EZH2 drive tumor-associated hypertrimethylation of lysine 27 on histone H3 (H3K27) in human B-cell lymphomas." Proc Natl Acad Sci U S A **107**(49): 20980-20985.

Steiner, S., A. Magno, D. Huang and A. Caflisch (2013). "Does bromodomain flexibility influence histone recognition?" FEBS Lett **587**(14): 2158-2163.

Strahl, B. D. and C. D. Allis (2000). "The language of covalent histone modifications." Nature **403**(6765): 41-45.

Sun, H., J. Liu, J. Zhang, W. Shen, H. Huang, C. Xu, H. Dai, J. Wu and Y. Shi (2007). "Solution structure of BRD7 bromodomain and its interaction with acetylated peptides from histone H3 and H4." Biochem Biophys Res Commun **358**(2): 435-441.

Swaminathan, J., E. M. Baxter and V. G. Corces (2005). "The role of histone H2Av variant replacement and histone H4 acetylation in the establishment of Drosophila heterochromatin." Genes Dev **19**(1): 65-76.

Tahiliani, M., K. P. Koh, Y. Shen, W. A. Pastor, H. Bandukwala, Y. Brudno, S. Agarwal, L. M. Iyer, D. R. Liu, L. Aravind and A. Rao (2009). "Conversion of 5-methylcytosine to 5-hydroxymethylcytosine in mammalian DNA by MLL partner TET1." Science **324**(5929): 930-935.

Takawa, M., K. Masuda, M. Kunizaki, Y. Daigo, K. Takagi, Y. Iwai, H. S. Cho, G. Toyokawa, Y. Yamane, K. Maejima, H. I. Field, T. Kobayashi, T. Akasu, M. Sugiyama, E. Tsuchiya, Y. Atomi, B. A. Ponder, Y. Nakamura and R. Hamamoto (2011). "Validation of the histone methyltransferase EZH2 as a therapeutic target for various types of human cancer and as a prognostic marker." Cancer Sci **102**(7): 1298-1305.

Tamkun, J. W., R. Deuring, M. P. Scott, M. Kissinger, A. M. Pattatucci, T. C. Kaufman and J. A. Kennison (1992). "brahma: a regulator of Drosophila homeotic genes structurally related to the yeast transcriptional activator SNF2/SWI2." Cell **68**(3): 561-572.

Tolani, B., R. Gopalakrishnan, V. Punj, H. Matta and P. M. Chaudhary (2013). "Targeting Myc in KSHV-associated primary effusion lymphoma with BET bromodomain inhibitors." Oncogene.

Trotter, K. W. and T. K. Archer (2008). "The BRG1 transcriptional coregulator." Nucl Recept Signal **6**: e004.

Turner, B. M. (2002). "Cellular memory and the histone code." Cell **111**(3): 285-291.

Umehara, T., Y. Nakamura, M. K. Jang, K. Nakano, A. Tanaka, K. Ozato, B. Padmanabhan and S. Yokoyama (2010). "Structural basis for acetylated histone H4 recognition by the human BRD2 bromodomain." J Biol Chem **285**(10): 7610-7618.

van Otterdijk, S. D., J. C. Mathers and G. Strathdee (2013). "Do age-related changes in DNA methylation play a role in the development of age-related diseases?" Biochem Soc Trans **41**(3): 803-807.

Venturini, L., J. You, M. Stadler, R. Galien, V. Lallemand, M. H. Koken, M. G. Mattei, A. Ganser, P. Chambon, R. Losson and H. de The (1999). "TIF1gamma, a novel member of the transcriptional intermediary factor 1 family." Oncogene **18**(5): 1209-1217.

Vidler, L. R., N. Brown, S. Knapp and S. Hoelder (2012). "Druggability Analysis and Structural Classification of Bromodomain Acetyl-lysine Binding Sites." J Med Chem.

Volle, C. and Y. Dalal (2014). "Histone variants: the tricksters of the chromatin world." Curr Opin Genet Dev **25**: 8-14,138.

Vollmuth, F., W. Blankenfeldt and M. Geyer (2009). "Structures of the dual bromodomains of the P-TEFb-activating protein Brd4 at atomic resolution." J Biol Chem **284**(52): 36547-36556.

Waddington, C. (1942). "Canalization of development and the inheritance of acquired characters." Nature **150**: 563-565.

Waddington, C. H. (1957). The Strategy of the Genes.

Wang, F., H. Liu, W. P. Blanton, A. Belkina, N. K. Lebrasseur and G. V. Denis (2010). "Brd2 disruption in mice causes severe obesity without Type 2 diabetes." Biochem J **425**(1): 71-83.

Wang, R., Q. Li, C. M. Helfer, J. Jiao and J. You (2012). "The bromodomain protein Brd4 associated with acetylated chromatin is important for maintenance of higher-order chromatin structure." J Biol Chem.

Wapinski, O. and H. Y. Chang (2011). "Long noncoding RNAs and human disease." Trends Cell Biol **21**(6): 354-361.

Watson, J. D. and F. H. Crick (1953). "The structure of DNA." Cold Spring Harb Symp Quant Biol **18**: 123-131.

Weber, C. M. and S. Henikoff (2014). "Histone variants: dynamic punctuation in transcription." Genes Dev **28**(7): 672-682.

Wells, R. A., B. Leber, N. Y. Zhu and J. M. Storring (2014). "Optimizing outcomes with azacitidine: recommendations from Canadian centres of excellence." Curr Oncol **21**(1): 44-50.

Wu, S. Y., A. Y. Lee, H. T. Lai, H. Zhang and C. M. Chiang (2013). "Phospho Switch Triggers Brd4 Chromatin Binding and Activator Recruitment for Gene-Specific Targeting." Mol Cell.

Wyce, A., Y. Degenhardt, Y. Bai, B. Le, S. Korenchuk, M. C. Crouthame, C. F. McHugh, R. Vessella, C. L. Creasy, P. J. Tummino and O. Barbash (2013). "Inhibition of BET bromodomain proteins as a therapeutic approach in prostate cancer." Oncotarget **4**(12): 2419-2429.

Xu, Y., M. K. Ayrapetov, C. Xu, O. Gursoy-Yuzugullu, Y. Hu and B. D. Price (2012). "Histone H2A.Z controls a critical chromatin remodeling step required for DNA double-strand break repair." Mol Cell **48**(5): 723-733.

Yan, M. S., C. C. Matouk and P. A. Marsden (2010). "Epigenetics of the vascular endothelium." J Appl Physiol (1985) **109**(3): 916-926.

Yan, X. J., J. Xu, Z. H. Gu, C. M. Pan, G. Lu, Y. Shen, J. Y. Shi, Y. M. Zhu, L. Tang, X. W. Zhang, W. X. Liang, J. Q. Mi, H. D. Song, K. Q. Li, Z. Chen and S. J. Chen (2011). "Exome sequencing identifies somatic mutations of DNA methyltransferase gene DNMT3A in acute monocytic leukemia." Nat Genet **43**(4): 309-315.

Yang, X. J., V. V. Ogryzko, J. Nishikawa, B. H. Howard and Y. Nakatani (1996). "A p300/CBP-associated factor that competes with the adenoviral oncoprotein E1A." Nature **382**(6589): 319-324.

Yang, X. J. and E. Seto (2008). "The Rpd3/Hda1 family of lysine deacetylases: from bacteria and yeast to mice and men." Nat Rev Mol Cell Biol **9**(3): 206-218.

Yang, Z., N. He and Q. Zhou (2008). "Brd4 recruits P-TEFb to chromosomes at late mitosis to promote G1 gene expression and cell cycle progression." Mol Cell Biol **28**(3): 967-976.

Yavuz, E. N., O. Ozdemir, S. Catal, N. Bebek, U. Ozbek and B. Baykan (2012). "Bromodomain-containing protein 2 gene in photosensitive epilepsy." Seizure **21**(8): 646-648.

Yoshida, M., M. Kijima, M. Akita and T. Beppu (1990). "Potent and specific inhibition of mammalian histone deacetylase both in vivo and in vitro by trichostatin A." J Biol Chem **265**(28): 17174-17179.

You, J., Q. Li, C. Wu, J. Kim, M. Ottinger and P. M. Howley (2009). "Regulation of aurora B expression by the bromodomain protein Brd4." Mol Cell Biol **29**(18): 5094-5103.

Yuen, B. T. and P. S. Knoepfler (2013). "Histone H3.3 mutations: a variant path to cancer." Cancer Cell **24**(5): 567-574.

Yun, C. H., K. E. Mengwasser, A. V. Toms, M. S. Woo, H. Greulich, K. K. Wong, M. Meyerson and M. J. Eck (2008). "The T790M mutation in EGFR kinase causes drug resistance by increasing the affinity for ATP." Proc Natl Acad Sci U S A **105**(6): 2070-2075.

Yun, M., J. Wu, J. L. Workman and B. Li (2011). "Readers of histone modifications." Cell Res **21**(4): 564-578.

Zeng, L. and M. M. Zhou (2002). "Bromodomain: an acetyl-lysine binding domain." FEBS Lett **513**(1): 124-128.

Zhang, G., R. Liu, Y. Zhong, A. N. Plotnikov, W. Zhang, L. Zeng, E. Rusinova, G. Gerona-Nevarro, N. Moshkina, J. Joshua, P. Y. Chuang, M. Ohlmeyer, J. C. He and M. M. Zhou (2012). "Down-

regulation of NF-kappaB transcriptional activity in HIV-associated kidney disease by BRD4 inhibition." J Biol Chem **287**(34): 28840-28851.

Zhang, J., P. L. Yang and N. S. Gray (2009). "Targeting cancer with small molecule kinase inhibitors." Nat Rev Cancer **9**(1): 28-39.

Zhang, W., C. Prakash, C. Sum, Y. Gong, Y. Li, J. J. Kwok, N. Thiessen, S. Pettersson, S. J. Jones, S. Knapp, H. Yang and K. C. Chin (2012). "Bromodomain-containing Protein 4 (BRD4) Regulates RNA Polymerase II Serine 2 Phosphorylation in Human CD4+ T Cells." J Biol Chem **287**(51): 43137-43155.

Zhao, R., T. Nakamura, Y. Fu, Z. Lazar and D. L. Spector (2011). "Gene bookmarking accelerates the kinetics of post-mitotic transcriptional re-activation." Nat Cell Biol **13**(11): 1295-1304.

Zhou, Q. and J. H. Yik (2006). "The Yin and Yang of P-TEFb regulation: implications for human immunodeficiency virus gene expression and global control of cell growth and differentiation." Microbiol Mol Biol Rev **70**(3): 646-659.

Zou, Z., B. Huang, X. Wu, H. Zhang, J. Qi, J. Bradner, S. Nair and L. F. Chen (2013). "Brd4 maintains constitutively active NF-kappaB in cancer cells by binding to acetylated RelA." Oncogene.

Zuber, J., J. Shi, E. Wang, A. R. Rappaport, H. Herrmann, E. A. Sison, D. Magoon, J. Qi, K. Blatt, M. Wunderlich, M. J. Taylor, C. Johns, A. Chicas, J. C. Mulloy, S. C. Kogan, P. Brown, P. Valent, J. E. Bradner, S. W. Lowe and C. R. Vakoc (2011). "RNAi screen identifies Brd4 as a therapeutic target in acute myeloid leukaemia." Nature **478**(7370): 524-528.

Publications

Publications in journals

Jung, M., Philpott, M., Muller, S., Schulze, J., Badock, V., Eberspacher, U., Moosmayer, D., Bader, B., Schmees, N., Fernandez-Montalvan, A., and Haendler, B. (2014). "Affinity Map of BRD4 Interactions with the Histone H4 Tail and the Small Molecule Inhibitor JQ1." J Biol Chem.

Schulze, J., Moosmayer, D., Weiske, J., Fernandez-Montalvan, A., Herbst, C., **Jung, M.**, Haendler, B., and Bader, B. (2014). "Cell-Based Protein Stabilization Assays for the Detection of Interactions between Small Molecule Inhibitors and BRD4." Journal of Biomolecular Screening. *In press.*

Jung, M., Gelato, K.A, Fernandez-Montalvan, A., Siegel, S., and Haendler, B. (2015) "Targeting BET bromodomains for cancer treatment". Epigenomics. *In press.*

Conference poster presentations

Jung, M., Haendler, B., Fernandez-Montalvan, A. "Generation of BRD4 mutants and analysis of their interaction with small molecule inhibitors" first poster price, Bayer Young Scientist poster session 2012, Bayer Pharma AG, Berlin, Germany.

Jung, M., Haendler, B., Fernandez-Montalvan, A. "Structural determinants for histone and inhibitor recognition by BRD4: Towards improved drug design strategies" Bayer Science & Education Foundation Alumni Meeting 2013, Ewerk, Berlin.

Jung, M., Haendler, B., Fernandez-Montalvan, A. "Structural determinants for histone and inhibitor recognition by BRD4" Gordon Research Conference on Cancer Genetics & Epigenetics 2013, Lucca, Italy.

Jung, M., Haendler, B., Fernandez-Montalvan, A. "Structural determinants for histone and inhibitor recognition by BRD4" Bayer Young Scientist poster session 2013, Bayer Pharma AG, Berlin, Germany.

Curriculum Vitae

For reasons of data protection,
the curriculum vitae is not included in the online version

Abbreviations

%	Percent
°C	Degree celsius
A	Alanine
ac	Acetyl
AR	Androgen receptor
ARE	Androgen response element
ATCC	American Type Culture Collection
ATP	Adenosine triphosphate
BD1	Bromodomain 1
BD2	Bromodomain 2
BET	Bromodomain and extra-terminal domain protein
BG	Background
bp	Base pairs
BRD4	Bromodomain-containing protein 4
BRDT	Bromodomain testis-specific protein
BRET	Bioluminescence Resonance Energy Transfer
BRPF1	Bromodomain and PHD finger containing protein family
BSA	Bovine serum albumin
c-Myc	V-myc myelocytomatosis viral oncogene homolog
cDNA	Complementary DNA
ChIP	Chromatin immunoprecipitation
CRPC	Castration-resistant prostate cancer
CTD	Carboxy-terminal domain
D	Aspartic acid
Da	Dalton
DLBCL	Diffuse large B-cell lymphoma
DMEM	Dulbecco's Modied Eagle's Medium
DMSO	Dimethyl sulfoxide
DNA	Deoxyribonucleic acid
DNMT	DNA methyltransferase
dNTP	Deoxyribonucleotide
DOT1L	DOT1-like
DPBS	Dulbecco’s Phosphate-Buffered Saline
DPBS	Dulbecco's phosphate buered saline
DSMZ	Deutsche Sammlung von Mikroorganismen und Zellkulturen
E	Glutamic acid
E.coli	*Escherichia coli*
ER	Estrogen receptor
ET	Extra terminal domain
EZH2	Enhancer of zeste homolog 2
F	Phenylalanine
FBS	Fetal bovine serum
FDA	Food and drug administration

Fig.	Figure
FP	Fluorescence polarization
FRAP	Fluorescence recovery after photobleaching
G	Glycine
GFP	Green fluorescent protein
GPCRs	G-protein-coupled receptors
H	Histidine
h	Hour
H4K5(ac)	Histone H4 lysine 5 acetylation
HATs	Histone acetylases
HDAC	Histone deacetylase
HDM	Histone demethylase
HMT	Histone methyltransferase
hu	Human
I	Isoleucine
ITC	Isothermal titration calorimetry
JARID	Jumonji AT-rich interactive domain
Jmj	Jumonji
JMJD	Jumonji domain-containing protein
K	Lysine
KDM	Lysine demethylase
KLK	Kallikrein
l	Liter
LB	Luria Bertani
LC-MS	Liquid chromatography mass spectrometry
lncRNA	Long noncoding RNA
LSD	Lysine-specific demethylase
LSD-1	Flavin-dependent monoamine oxidase lysine-specific demethylase
Luc	Luciferase
M	Methionine
M	Molar
me	Methyl
MEM	Modified Eagle's Medium
MLL	Mixed-lineage leukemia proteins
MM	Multiple myeloma
mRNA	Messenger RNA
nl, µl, ml,	Nano, micro, milli liter
NLS	Nuclear localization signal
nm	Nanometer
NMC	NUT (nuclear protein in testis) midline carcinoma
NMR	Nuclear magnetic resonance
NTD	N-terminal domain
P	Proline
PAGE	Polyacrylamide gel electrophoresis

PBS	Dulbecco's phosphate-buffered saline
PCR	Polymerase chain reaction
PFA	Paraformaldehyde
Pg, ng, µg, mg, g	Pico, nano, micro, milli, gram
PHD	Plant homeo domain
PID	P-TEFb interacting domain
Pol	Polymerase
PRMT	Protein arginine methyltransferase
P-TEFb	Positive transcription elongation factor b
PTMs	Posttranslational modifications
qPCR	Quantitative PCR
R	Arginine
RNA	Ribonucleic acid
Rpm	Revolutions per minute
RU	Response units
RT	Room temperature
RT-PCR	Reverse transcriptase-PCR
s, min, h	Second, minute, hour
SAH	S-adenosyl-L-homocysteine
SAM	S-adenosyl-methionine
SAR	Structure-activity relationship
SDS	Sodium dodecyle sulfate
siRNA	Small interfering RNA
SPR	Surface Plasmon Resonance
TAMRA	Tetramethylrhodamine
TR-FRET	Time-resolved fluorescence resonance energy transfer
TSA	Thermal Shift Assay
UV	Ultraviolet
V	Valine
W	Tryptophan
WT	Wild type
Y	Tyrosine